

NPS ARCHIVE

1968

YESKE, L.

THE CORRELATION OF OCEANIC PARAMETERS WITH LIGHT
ATTENUATION IN MONTEREY BAY, CALIFORNIA

by

Lanny Alan Yeske
and
Richard Dean Waer

Gaylord
PAMPHLET BINDER
Syracuse, N. Y.
Stackton, Calif.

UNITED STATES NAVAL POSTGRADUATE SCHOOL



THESIS

THE CORRELATION OF OCEANIC PARAMETERS WITH LIGHT
ATTENUATION IN MONTEREY BAY, CALIFORNIA

by

Lanny Alan Yeske

and

Richard Dean Waer

December 1968

*This document has been approved for public re-
lease and sale; its distribution is unlimited.*

THE CORRELATION OF OCEANIC PARAMETERS WITH LIGHT
ATTENUATION IN MONTEREY BAY, CALIFORNIA

by

Lanny Alan Yeske
Lieutenant, United States Navy
B.S., University of Nebraska, 1960

and

Richard Dean Waer
Lieutenant, United States Navy
B.S., Naval Academy, 1961

Submitted in partial fulfillment of the
requirements for the degree of

MASTER OF SCIENCE IN OCEANOGRAPHY

from the

NAVAL POSTGRADUATE SCHOOL
December 1968

908
YESKE, A

ABSTRACT

An investigation of the correlation of oceanic parameters with light attenuation in Monterey Bay, California, was conducted during July and August 1968. Measurements of beam transmittance, salinity, temperature, density, and particulate matter, related in time and depth, were obtained during four cruises. Nearly 400 water samples were taken from two stations at depths between 0 and 85 m.

Temperature showed the greatest correlation with beam transmittance. Isopycnals and beam transmittance contours showed a similar good correlation. Although salinity correlations were not clearly defined, isolated salinity pockets often appeared to be associated with transmissivity perturbations. A nearly linear relationship between values of particulate count and beam transmittance was observed. Particle sizes were found to decrease with increased depths. Approximately 96 percent of the particles affecting beam transmittance were less than 13 μ in diameter. Beam transmittance isolines generally oscillate with a tidal cycle period, the minimum values usually occurring at low tide. A possible correlation between lunar period, tidal ranges, and turbidity layers was indicated.

TABLE OF CONTENTS

	Page
I. INTRODUCTION	9
1.1 <u>Background</u>	9
1.2 <u>Previous Investigations</u>	10
1.3 <u>Purpose of the Present Research</u>	12
1.4 <u>Oceanographic Climatology</u>	13
II. EQUIPMENT DESCRIPTION	15
2.1 <u>Beam Transmissometer</u>	15
2.2 <u>Coulter Counter</u>	17
2.3 <u>Hytech Salinometer</u>	20
III. EXPERIMENTAL PROCEDURES	22
3.1 <u>Station Selection</u>	22
3.2 <u>Sample Collection and Beam Transmittance Measure-</u> <u>ments</u>	22
IV. ANALYSIS OF DATA	33
4.1 <u>Introduction</u>	33
4.2 <u>Beam Transmittance Measurements</u>	34
4.2.1 Cruise 1 (26-27 July 1968)	34
4.2.2 Cruise 2 (17 August 1968)	35
4.2.3 Cruise 3 (23 August 1968)	35
4.2.4 Cruise 4 (30-31 August 1968)	43
4.3 <u>The Correlation of Tidal Cycle with Beam</u> <u>Transmittance</u>	43
4.4 <u>The Correlation of Salinity with Beam</u> <u>Transmittance</u>	44
4.5 <u>The Correlation of Temperature with Beam</u> <u>Transmittance</u>	52

LIST OF FIGURES

Figure		Page
1	Beam Transmittance Meter Diagram	16
2	Transmissivity versus Wavelength for the Wratten 61 Filter	18
3	Coulter Counter Diagram	19
4	Chart of Monterey Bay, California	23
5-11	Time-Depth Sampling Locations	26-32
12-18	Time-Depth Contours of Beam Transmittance in Relation to Tidal Cycle	36-42
19-25	Time-Depth Contours of Beam Transmittance in Relation to Salinity	45-51
26-32	Time-Depth Contours of Beam Transmittance in Relation to Temperature	53-59
33-39	Time-Depth Contours of Beam Transmittance in Relation to Density	61-67
40-43	Time-Depth Contours of Beam Transmittance in Relation to Coulter Count	69-72
44-62	Depth Profiles of Temperature, Density, Salinity, and Transmittance	75-93
63	Linear Least-Squares Fit for Beam Transmittance vs. Particle Count at Coulter Threshold 0	94
64	Linear Least-Squares Fit for Beam Transmittance vs. Particle Count at Coulter Thresholds 10, 20, and 30	95
65	Photographs of Particulate Samples and 6-14 μ Latex Spheres	96
66	Relative Pulse Height for 6-14 μ Latex Spheres	97

ACKNOWLEDGEMENTS

Many people have assisted the authors in this research. We wish to express our appreciation to Dr. Robert E. Morrison for his assistance in initially planning the project. The technical advice of Professor Warren W. Denner in physical oceanography, Dr. Eugene C. Haderlie in biological oceanography, and Dr. Charles F. Rowell in chemical oceanography, during the preparation and sampling portions is greatly appreciated. To Professor Stevens P. Tucker, our faculty thesis advisor, the authors wish to express their profound gratitude. Without his continued support and assistance, a project of this dimension could not have been completed. For the Coulter Counter use and technical assistance we wish to express our appreciation to Dr. John H. Phillips, Director of Hopkins Marine Station, Stanford University, and to Mr. William Hinds, Laboratory Technician. We are greatly indebted to Mr. Theodore J. Petzold, Senior Engineer of the Visibility Laboratory at Scripps Institution of Oceanography, for his instruction concerning the beam transmissometer. The work and cooperation of CWO James O. White, U. S. Navy, and the crew of the Naval Postgraduate School Hydrographic Research vessel were outstanding and are deeply appreciated. We wish to express our sincere thanks to Mr. Norman Walker, Leading Model Maker of the Naval Postgraduate School Machine Facility, for his cooperation and assistance in fabricating essential cruise equipment. To our neglected wives, Gay Waer and Jacqueline Yeske, a great deal of credit is due. Their continued encouragement, moral support, typing, and editing was exemplary.

CHAPTER 1

INTRODUCTION

1.1 Background

Most of the optical properties of seawater can be investigated by measuring all aspects of the flux distribution of a highly collimated beam of monochromatic light as it passes through the water (7).^{*} One of these aspects is flux loss per unit length of path.

The flux loss, or attenuation, is an inherent optical property of seawater and is equal to the sum of two independent losses, scattering and absorption. Unlike the atmosphere, which is primarily a scattering medium, the ocean is a medium in which both scattering and absorption play significant roles.

Scattering, or the deviation of individual photons from their original path, consists of two different components, that produced by the water itself, and that produced by suspended particles (10). Scattering is a function of the refractive index of the particles relative to the water and the ratio of particle diameter to wavelength.

Absorption is the result of light energy conversion into such forms as thermal kinetic energy and chemical potential energy. Seawater is a highly selective absorbing medium and, as a result, acts as a narrow-band filter with a transmissivity peak in the blue-green region.

(*) Numbers in parentheses refer to the listing in the Bibliography.

1.2 Previous Investigations

Optical oceanography became an increasingly important aspect of physical oceanography when Petterson in 1934 developed a forerunner of the modern beam transmissometer (10). The beam transmissometer is an instrument used to measure the ratio of the transmitted radiant flux to the incident radiant flux for a beam the diameter of which is small compared to its length. Numerous investigations have been made to determine the complex relationships existing between beam transmittance, temperature, tides, internal waves, particulate matter, and other parameters.

Bumpus and Clarke (4) attributed turbidity to suspended particulate matter and noted that turbidity generally decreases as the distance from land and the depth of water increases. Emery (8) suggested that in the waters off Southern California upwelling, and hence the increase in plankton-supporting nutrients, has a significant effect on water transparency. Burt (5) concluded that a large portion of the particulate matter causing attenuation is less than 2μ in diameter.

Ball and LaFond (1) observed that water turbidity is mainly due to concentrations of plankton and detritus. They also noted that maximum turbidity often lies in the thermocline, and that relationships exist between turbidity and tidal cycle, temperature, and internal waves.

Barham, Wilton, and Sullivan (2) noted that "macroplankton" have little effect on light transmission while dinoflagellates of size range between 14 and 218μ are the most significant of the light-attenuating organisms off Mission Beach, California, in the summer.

Oser, Berger, and Franc (12) observed current dependent fluctuations in transmissivity.

Jerlov (9) noted that there is a correlation between particle distribution and salinity and that this relationship changes due to turbulent fluctuations in the ocean. He also found, through relations computed from the Mie theory and scattering experiments, that particle sizes of the order of 10μ are primarily responsible for scattering in seawater.

Joseph (11) observed a correlation between density distribution and beam transmittance in the upper 20 m of the ocean.

It has been suggested that transparency characteristics of sea water can be used as a means for optical classification of water masses (10). Jerlov concluded that the presence of "yellow substance" can be treated as a characteristic property of a water mass. Yellow substance is formed from free carbohydrates and free amino acids resulting in carbohydrate-humic acids or melanoidines which are yellow in color and fairly stable in seawater. This phenomenon occurs when organic matter decomposes and is most prevalent in regions of high productivity. It is assumed to be the primary cause for light absorption in the ocean. Jerlov has developed three different classifications of ocean water types based upon irradiance measurements at various wavelengths.

Later investigations by Jerlov (10) led him to conclude that particles composed of calcium carbonate and silica cause high scattering, while green algae, composed primarily of cellulose, produce minimum scattering.

Although these and other investigations have contributed greatly to optical applications in oceanographic research, the correlation of several oceanic parameters such as salinity, density, tidal cycle, and lunar period with beam transmittance have not been clearly defined.

This is in part due to the fact that nearly all of the previous research efforts have concentrated on only one or two of the factors possibly relating to beam transmittance. While attempts have been made to relate each parameter individually to beam transmittance at some time or another, the authors are unaware of any prior investigation which has considered the correlation of a comprehensive set of oceanic parameters related in time, space, and depth.

1.3 Purpose of the Present Research

The purpose of this research was to investigate and determine which physical, dynamic, and biological oceanographic parameters are most closely correlated with light attenuation in Monterey Bay, California.

To achieve these goals, the following specific parameters were measured or observed:

1. beam transmittance
2. salinity
3. temperature
4. depth
5. density
6. tidal cycle
7. lunar period
8. particulate matter
9. internal waves

This research differs from previous investigations in several aspects. As previously mentioned, it was an attempt to interrelate simultaneously many parameters to beam transmittance. Beam transmittance, salinity, temperature, depth, density, and particulate matter

measurements were taken concurrently. The duration and spacing of cruises were planned to provide information concerning the tidal cycle and the lunar period. Internal wave or seiche effects were probably present in the sampling data.

Since most research investigations have been conducted in shallow coastal water or very deep oceanic water, two stations were selected which had different bathymetry and oceanic conditions in order to provide more representative information.

Prior studies have indicated the thermocline as the area of most interest. For this reason sampling was usually concentrated at two meter intervals within the thermocline.

A Coulter Counter (described in section 2.2) was used to analyze the particulate matter. This method of analysis has several advantages over a microscopic technique, in that greater accuracy can be achieved through elimination of operator fatigue; data reduction can be simplified; and counting speed can be greatly increased. A major disadvantage of the Coulter Counter is that particle sizes are determined by relative pulse heights, and thus an absolute measure of particle diameter is not obtained.

1.4 Oceanographic Climatology

Monterey Bay is characterized by three seasonal oceanographic periods as described by Skogsberg (14). The period of upwelling generally begins in February and terminates in late August. The oceanic period then sets in. Skogsberg observed upwelling in Monterey Bay from 1929-1933 at points located between the stations utilized for this study.

Because this investigation was conducted in July and August, rising temperatures and a decreased supply of nutrients were anticipated. A reduction in upwelling with a resultant decrease in surface salinity was also expected. Welch (16) discusses the presence of two characteristic salinity minima in Monterey Bay during the oceanic period.

According to Raines (13), sub-tidal oscillations of amplitude 0.1 to 0.5 ft occur in Monterey Bay. He concluded that long period oscillations in Monterey Bay have mean periods in the range of 19 to 39 minutes. These long period waves vary in duration from a few hours to several days and are most prevalent in July between 1200 and 1600 hours.

Wilson (18) found a 50 to 70 minute period seiche to be characteristic in Table Bay, Cape Town, South Africa, which has a configuration and an oceanic exposure remarkably similar to Monterey Bay. Although Table Bay is smaller and shallower than Monterey Bay, both are significantly affected by long-period surges. Wilson (17) concludes that the surges in Monterey Bay are probably the result of long-period waves from the open ocean rather than surf-beats generated locally by swells.

CHAPTER 2

EQUIPMENT DESCRIPTION

2.1 Beam Transmissometer

A Marine Advisors Model C-2 beam transmissometer was used throughout this investigation (Fig. 1). This instrument weighs approximately 80 pounds in air and has an overall length of about 5 ft. It has a self-contained light source (L) and can therefore be used during day or night with an accuracy of about three percent. Its maximum depth limit is 300 m.

The projector of the beam transmissometer consists of a General Electric type 1759 4-amp incandescent lamp (L), an International Rectifier DP-2 selenium photovoltaic reference cell (R), and a system of lenses (C) to collimate the light beam. Collimation provides a high ratio of path length to beam diameter, which is desirable in order to reduce scattering within the beam.

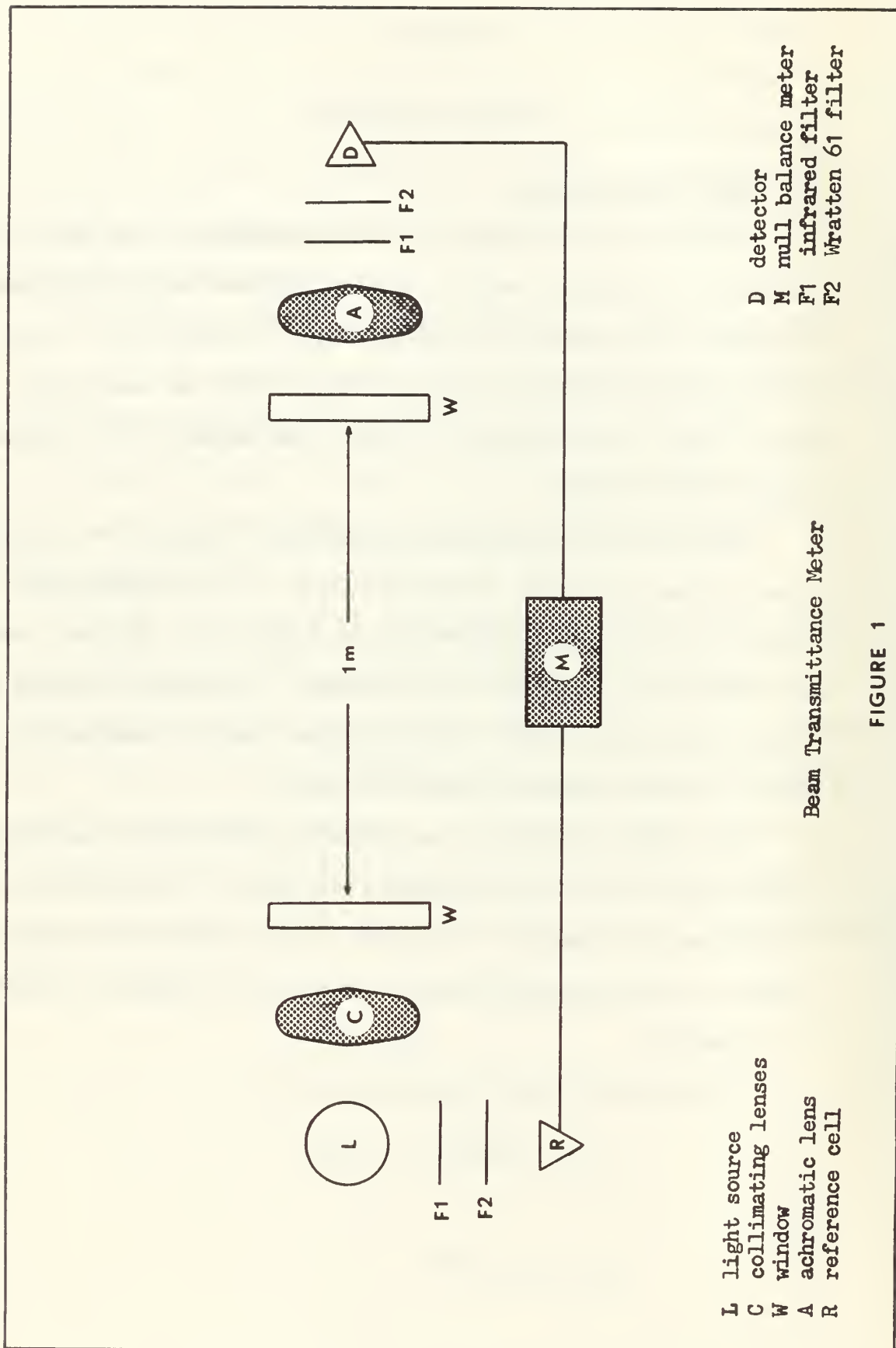
The detector consists of an acromatic lens (A) and a second DP-2 photovoltaic cell (D) which measures the amount of flux received through a one-meter path length. The outputs of the two cells are compared by means of a null-balancing meter (M) to provide a reading of transmittance, T, in percent.

If exponential decay is assumed, then

$$I = I_0 e^{-(a+b)r} = I_0 e^{-cr}$$

or,

$$I/I_0 = T = e^{-cr}$$



L light source
 C collimating lenses
 W window
 A achromatic lens
 R reference cell

D detector
 M mull balance meter
 F1 infrared filter
 F2 Wratten 61 filter

Beam Transmittance Meter

FIGURE 1

where I = flux measured at the receiver end
 I_0 = flux measured at the projector end
 c = total beam attenuation coefficient
 a = absorption coefficient
 b = scattering coefficient

For this instrument r equals one meter, and the beam attenuation coefficient is given by

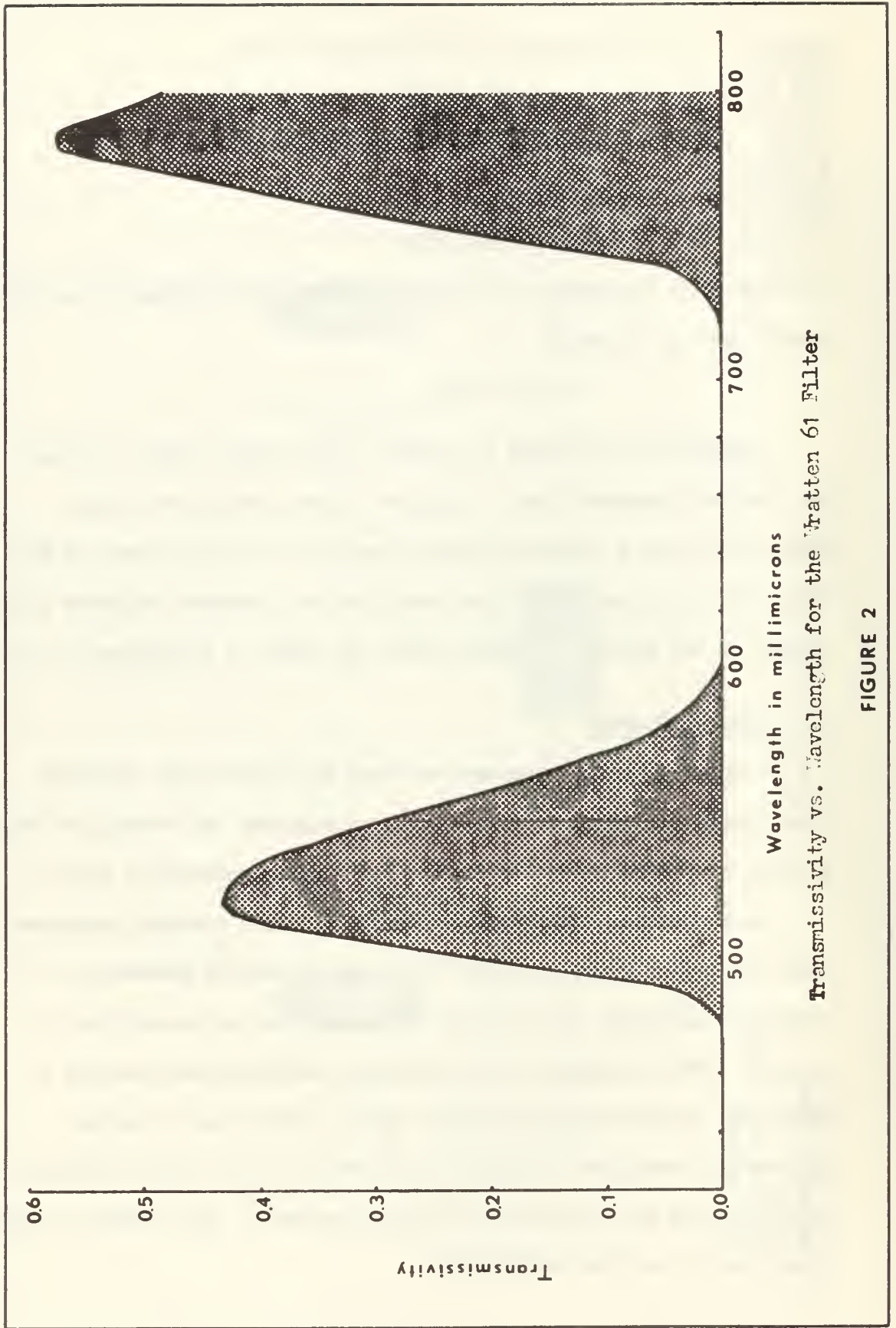
$$c = \ln (I/I_0)$$

Eastman Kodak Wratten 61 gelatin filters were used to reduce the optical bandwidth and to minimize coastal water absorption. This filter has a maximum transmittance at 533.8 m μ as seen in Fig. 2. Schott BG-18 filters were also installed to eliminate infrared light passed by the Wratten 61 filter when the meter is calibrated in air.

2.2 Coulter Counter

A Model A Coulter Counter was used for particulate analysis. This instrument (Fig. 3) is designed to register the number and relative size of suspended particles in an electrically conductive fluid.

As the sample containing particles is drawn through aperture tube (A) having a 100 μ orifice (O), the resistance between two platinum electrodes (E) immersed on either side of the orifice is altered. This produces a short-duration voltage pulse, having a magnitude proportional to particle size. The series of pulses produced by particles passing through the orifice is then electronically scaled and counted by a digital register. The seawater sample itself serves as the electrolyte.



Transmissivity vs. Wavelength for the Wratten 61 Filter

FIGURE 2

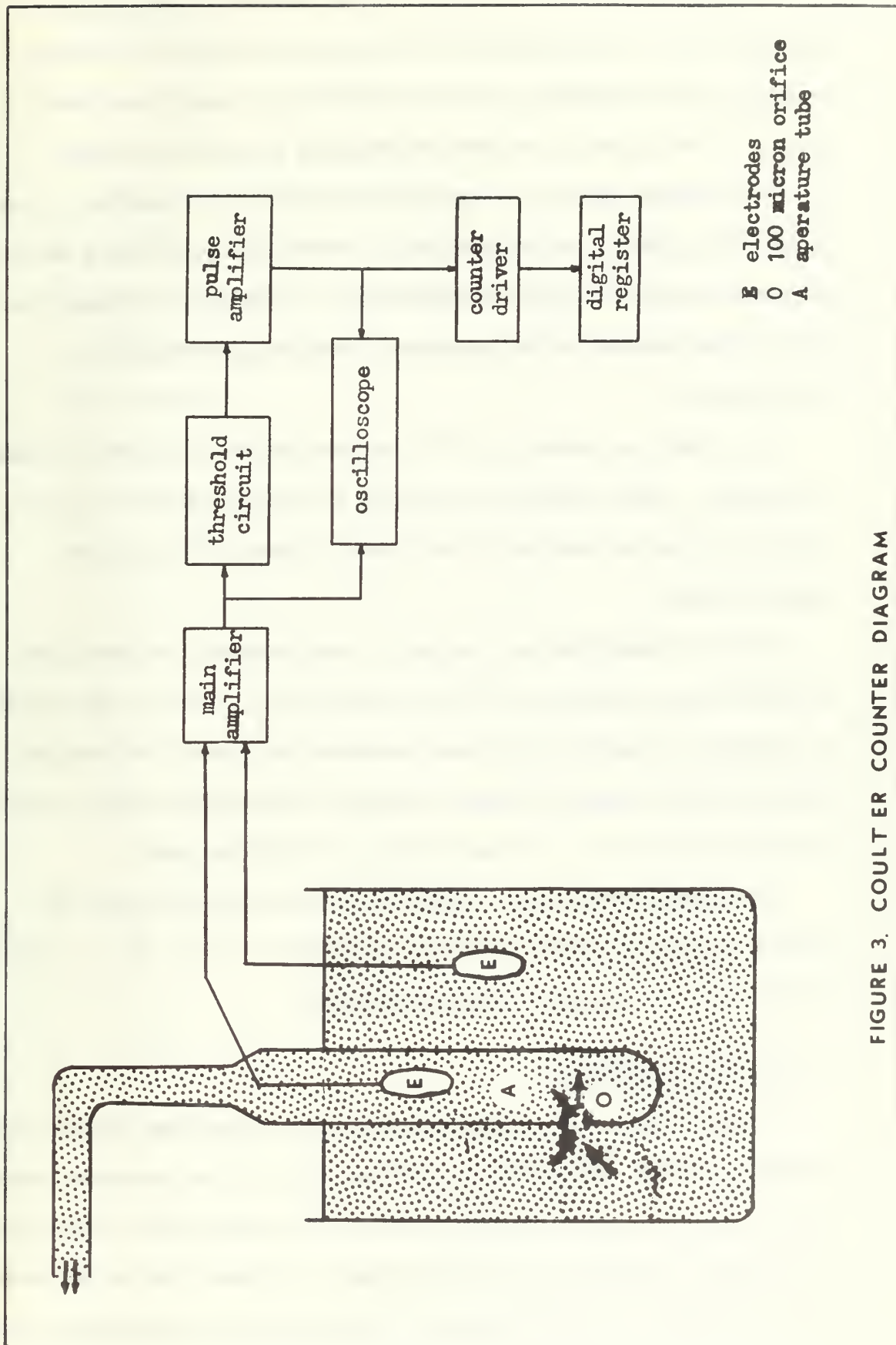


FIGURE 3. COULTER COUNTER DIAGRAM

Sample flow-rate is controlled by an external vacuum pump. Volume control is accomplished with a mercury manometer. As the mercury column advances, it makes contact with "start" and "stop" probes in the manometer, which activate the electronic counter.

The voltage pulses are amplified and fed to a threshold circuit having an adjustable threshold level. For a given threshold setting between 0 and 100, a pulse is counted if it reaches or exceeds that level. The relative pulse height can also be observed on an oscilloscope.

For counts in excess of 10^4 a correction for coincident passages is required. This correction accounts for the probability of count loss due to one or more particles passing through the orifice simultaneously.

Prior to analyzing the samples it was necessary to establish the proper gain setting on the pulse amplifier. This was accomplished by analyzing a sample of filtered seawater containing Dow Chemical Company styrene divinyl-benzene copolymer latex spheres which ranged in size from 6 to 14 μ . A gain setting of four was used.

From each Nansen bottle sample a two milliliter portion was counted at each of eleven different thresholds (0, 10, 20, ..., 100) to determine the relative size distribution.

2.3 Hytech Salinometer

A Hytech Model 6220 portable laboratory salinometer manufactured by Bissett-Berman was used to measure salinity of the seawater samples. This conductivity-type instrument utilizes an inductively coupled sensor to establish a conductivity ratio between an unknown sample and Normal Water prepared by the Hydrographical Laboratories in Copenhagen, Denmark.

A null-balance meter is employed to obtain a conductivity ratio reading. This value is then used in conjunction with tables to obtain salinity in parts per thousand (ppt) which must be corrected for meter drift and temperature changes.

The salinity measurement range is 0 to 51 ppt with an accuracy of ± 0.003 ppt. Temperature is measured from 0°C to 40°C to an accuracy of $\pm 0.05^{\circ}\text{C}$. For temperature differences not exceeding $+ 3.0^{\circ}\text{C}$ between sample and standard, temperature compensation is fully automatic.

CHAPTER 3

EXPERIMENTAL PROCEDURES

3.1 Station Selection

Two stations, Bravo and Delta, were selected on the basis of differences between them in salinity, temperature, density, and depth, as well as their geographical location in order to permit accurate radar navigation and reduce station to station transit time.

Figure 4 shows the position of each station. Station Bravo is located in approximately 102 m of water at latitude $36^{\circ}41.8'$ N longitude $121^{\circ}57.2'$ W and is the site of a California Cooperative Oceanic Fisheries Investigation (CALCOFI) station. Salinity, temperature and density data have been taken at this station weekly for the past several years. Station Delta is situated in approximately 1737 m at latitude $36^{\circ}42.0'$ N longitude $122^{\circ}02.1'$ W and is the location used by Bassett and Furninger (3) to determine the vertical variation of light scattering in Monterey Bay.

Prior to each series of observations the research vessel was maneuvered to minimize the navigational error. It is estimated the maximum error at stations Bravo and Delta was restricted to ± 500 and ± 1000 m, respectively.

3.2 Sample Collection and Beam Transmittance Measurements

Five cruises, separated by periods of one week and of 25 hr duration each, were initially planned to investigate the correlation of tidal cycle and lunar period with beam transmittance. Four were completed, with a three-week interval occurring between Cruises 1 and 2.

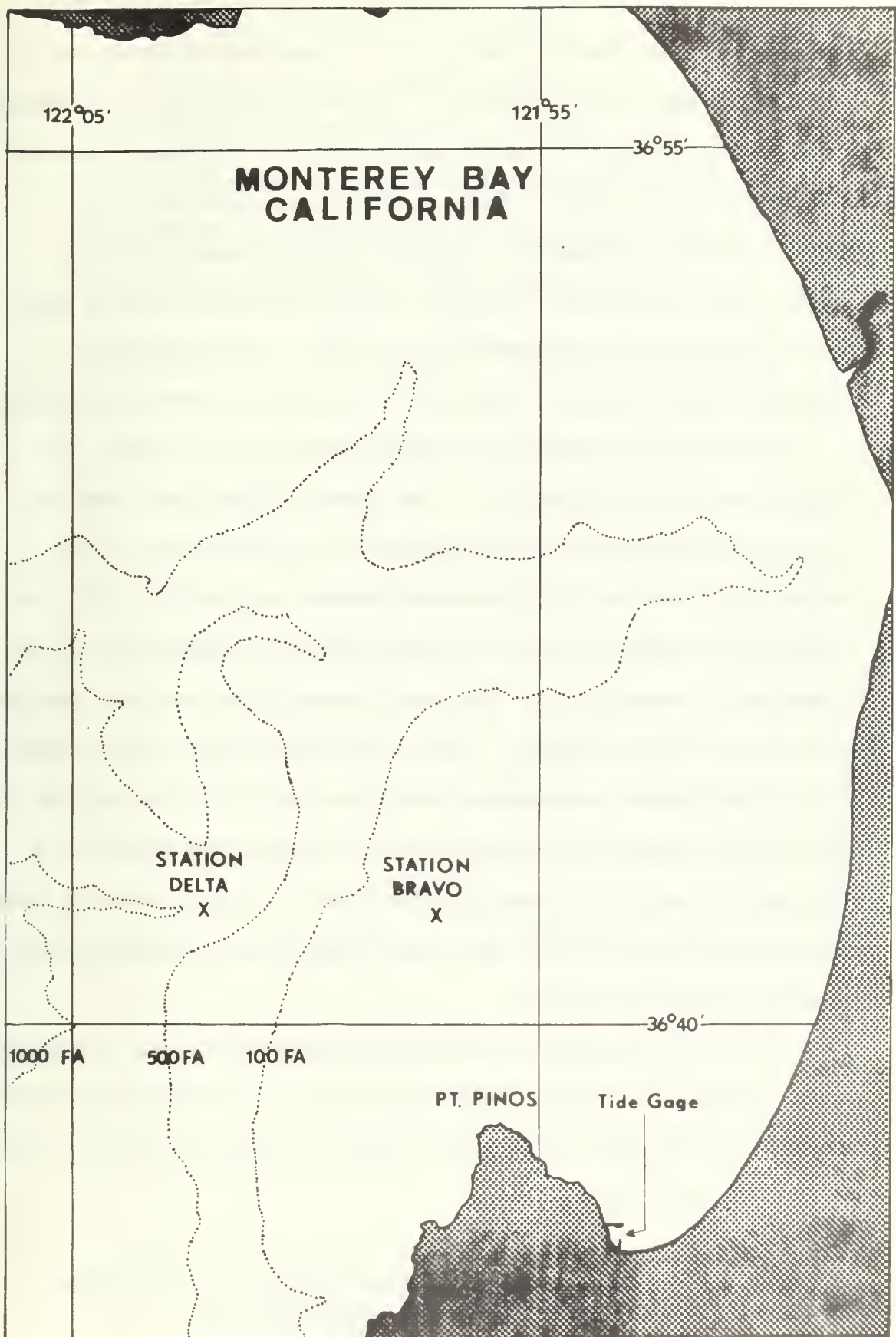


FIGURE 4

Cruise 1 was conducted entirely at Station Bravo to maximize the frequency of observations (Fig. 5). Seas were extremely calm and no problems were encountered. Thirteen hydro-casts were completed.

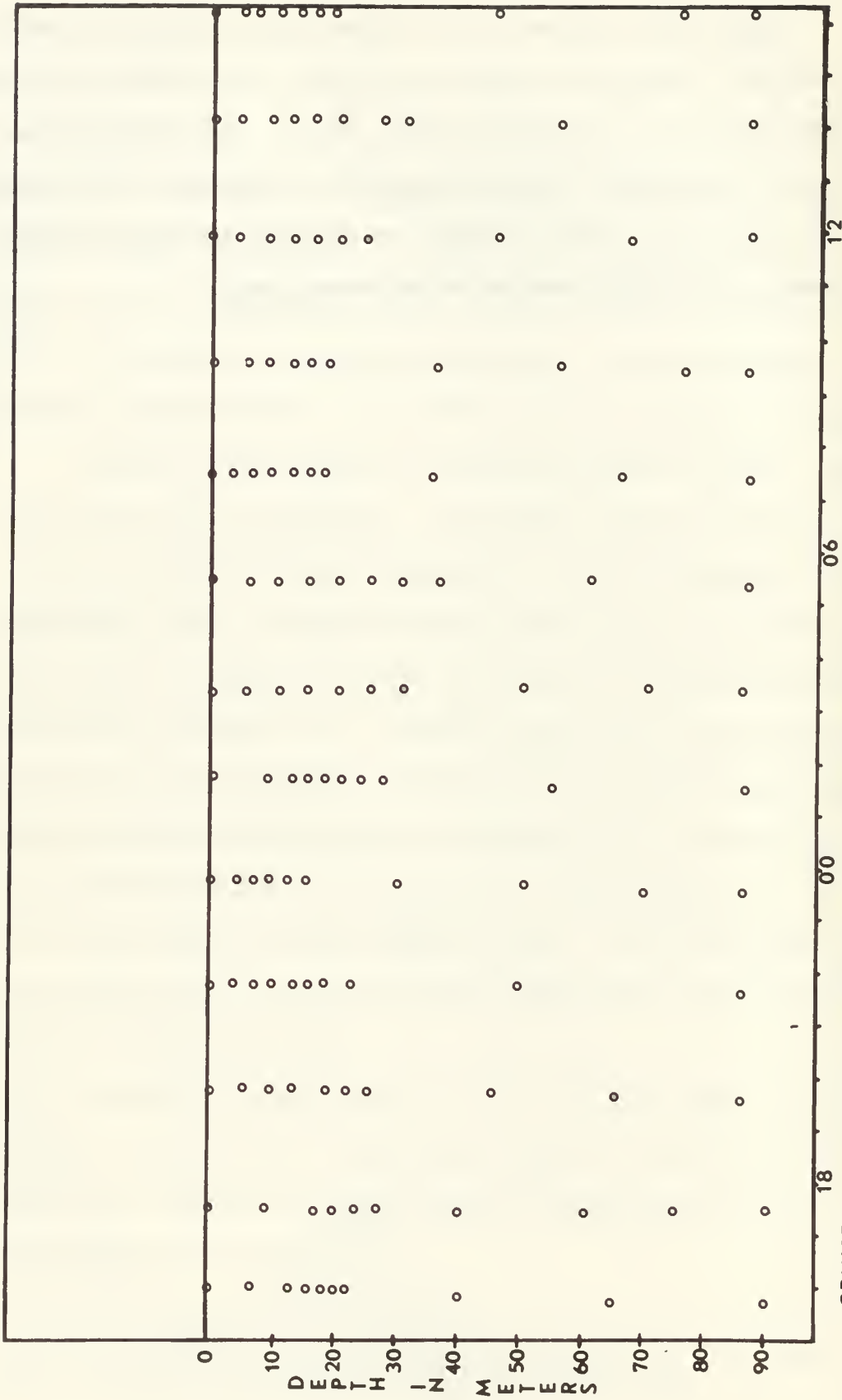
During Cruises 2, 3, and 4 casts were made alternately between stations Bravo and Delta. Times and depths of observations are shown in Figs. 6 through 11. Cruise 2 was terminated after six casts owing to high seas. Cruise 3 was concluded after seven casts due to high seas and equipment malfunctions. Few difficulties occurred during Cruise 4, and twelve casts were achieved in calm seas.

Each cast was preceded by a bathythermograph (BT) drop. BT traces are shown in Appendix I. Ten Nansen bottles, each with one or two protected reversing thermometers, were then placed on the hydrographic wire at depths selected between zero and 85 m with the main bottle concentration in the thermocline as determined from the immediately preceding BT. The beam transmittance meter was attached to the end of the hydrowire. After the Nansen bottles were tripped, beam transmittance measurements were taken enroute to the surface at the previous Nansen bottle depths and at intermediate points if a noticeable change in transmittance occurred. The time interval between the messenger drop and the last beam transmittance measurement did not usually exceed ten minutes.

The cast retrieved, salinity and particulate samples were drawn from the Nansen bottles. Particulate samples, taken only at station Bravo, were preserved in brown quart beer bottles with 25 ml of Lugol's iodine solution* (19, p. 99).

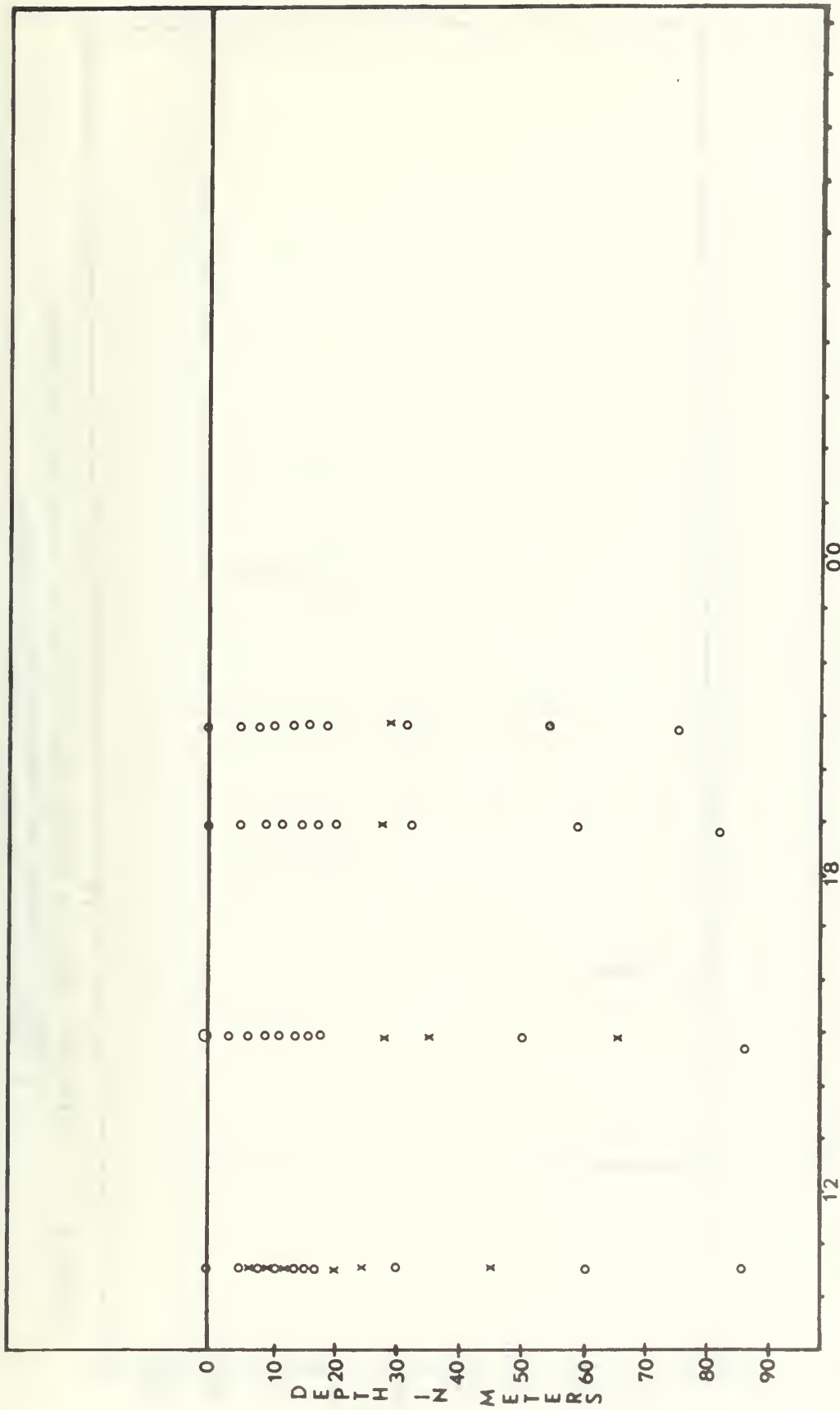
(*) The formula for Lugol's iodine solution is: 1 g iodine and 3 g potassium iodide per 300 cm³ distilled water.

Tidal level readings were recorded on the Standard Automatic Tide Gage (described in reference 15, pp. 7-15) located on Municipal Wharf Number Two in Monterey Harbor (Fig.4). Tide gage readings were not adjusted to the station positions because of the relatively short distances involved between the gage and stations Bravo and Delta, six and nine nautical miles respectively.

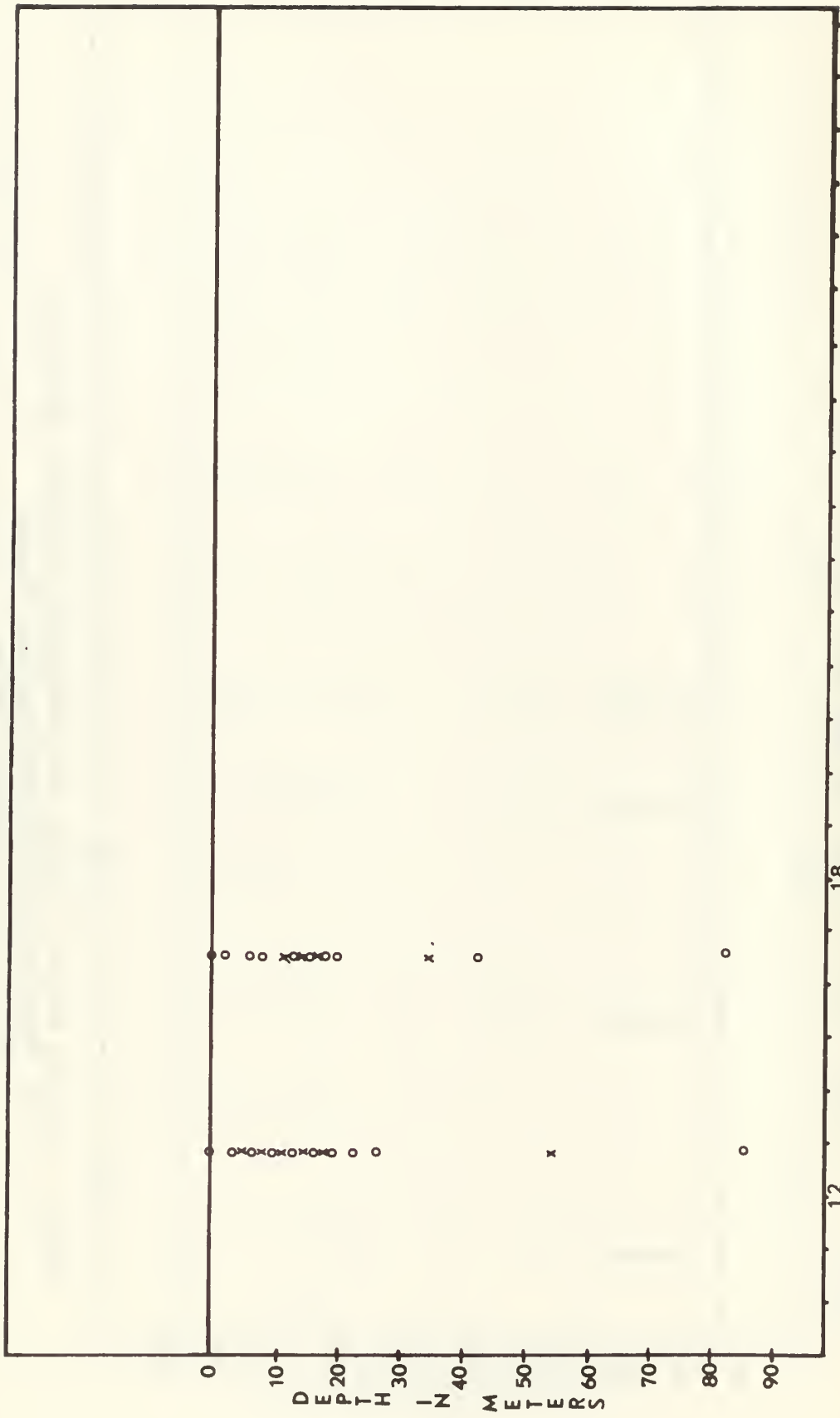


CRUISE 1 STATION BRAVO 26-27 JULY 1968 TIME-DEPTH SAMPLING LOCATIONS
 o Nansen Placement and Beam Transmittance Readings

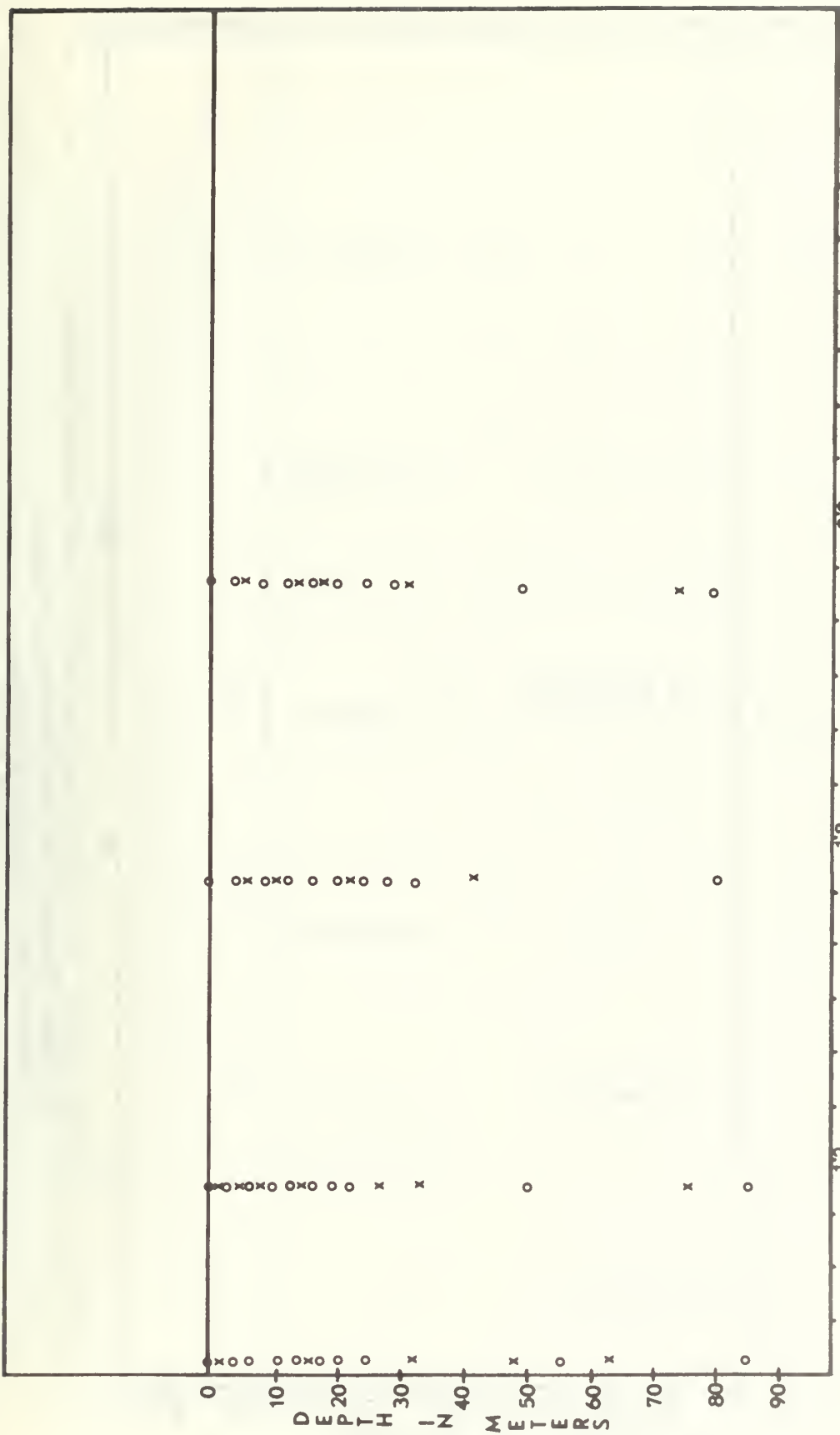
FIGURE 5



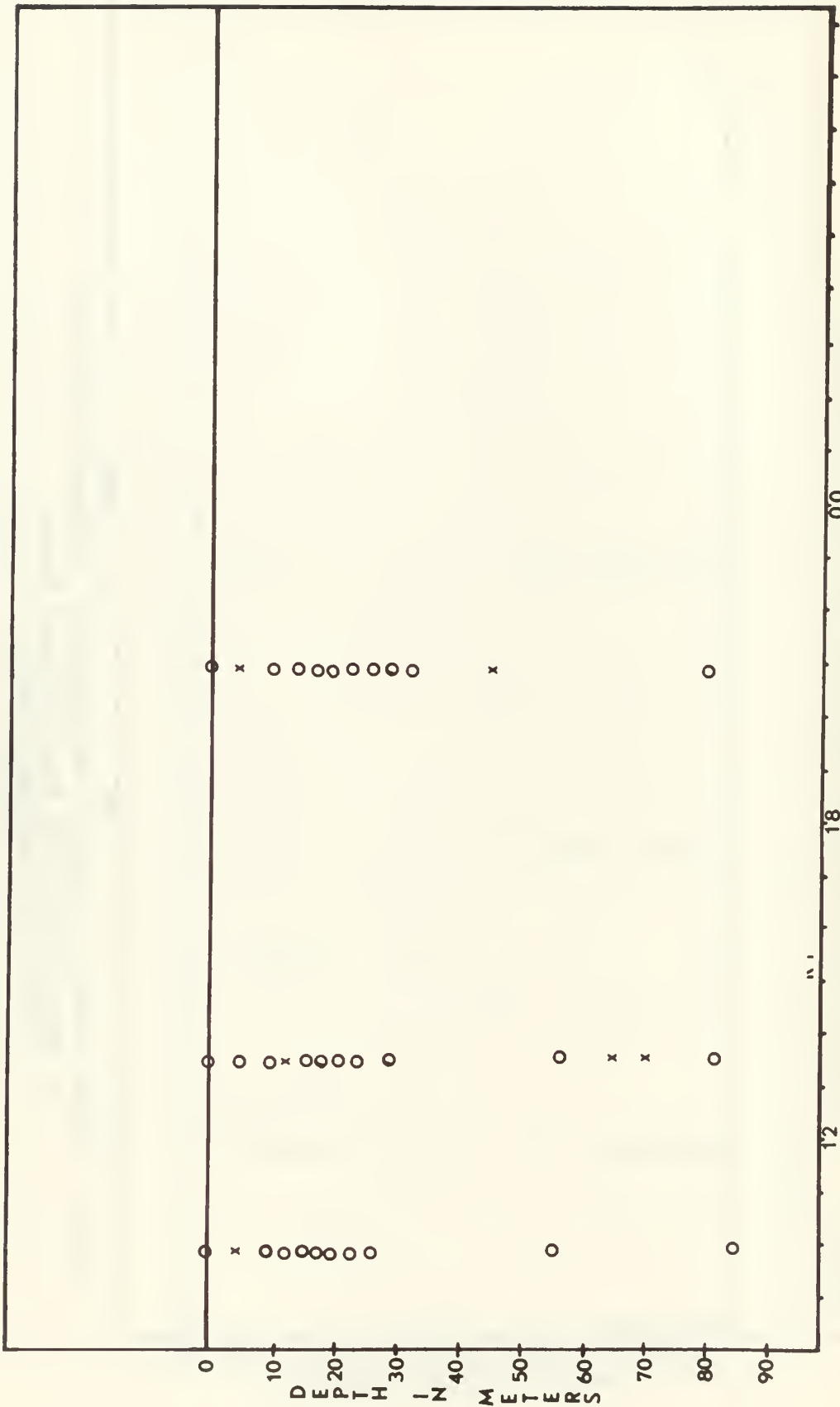
CRUISE 2 STATION BRAVO 17 AUGUST 1968 TIME-DEPTH SAMPLING LOCATIONS
 o Nansen Placement and Beam Transmittance Readings
 x Additional Beam Transmittance Readings
 FIGURE 6



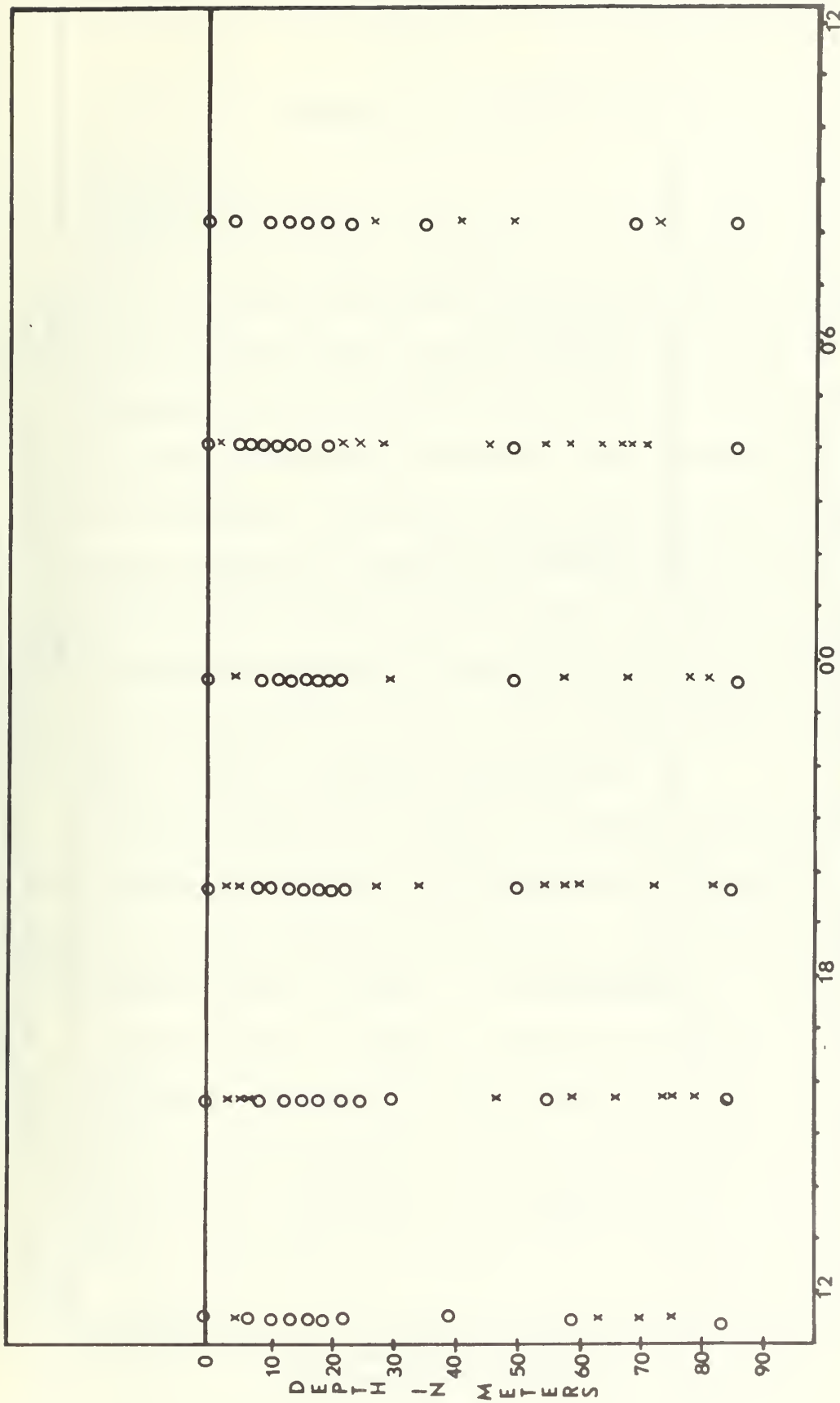
CRUISE 2 STATION DELTA 17 AUGUST 1968 TIME-DEPTH SAMPLING LOCATIONS
 o Nansen Placement and Beam Transmittance Readings
 x Additional Beam Transmittance Readings
 FIGURE 7



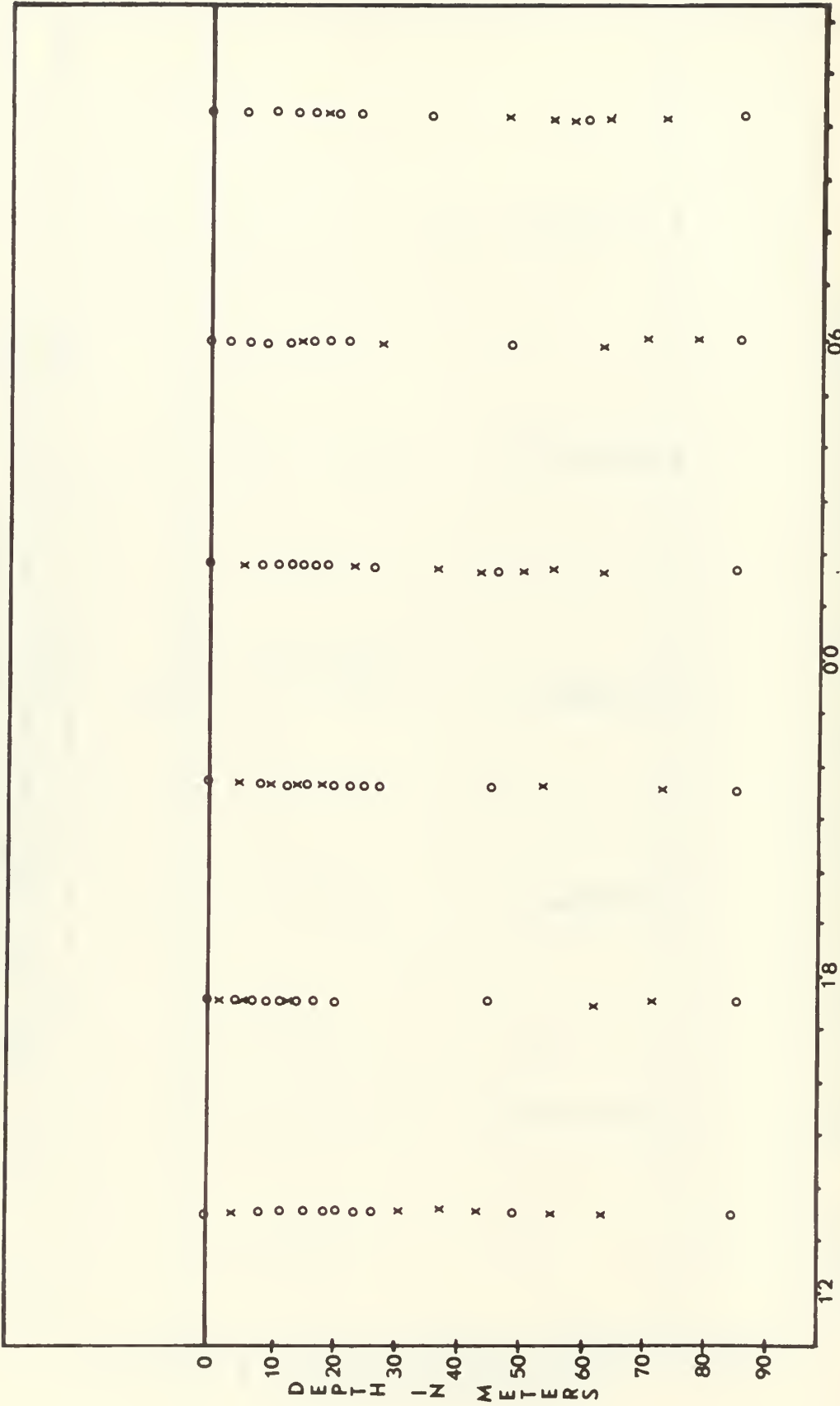
CRUISE 3 STATION BRAVO 23 AUGUST 1968 TIME-DEPTH SAMPLING LOCATIONS
 o Nansen Placement and Beam Transmittance Readings
 x Additional Beam Transmittance Readings
 FIGURE 8



CRUISE 3 STATION DELTA 23 AUGUST 1968 TIME-DEPTH SAMPLING LOCATIONS
 o Nansen Placement and Beam Transmittance Readings
 x Additional Beam Transmittance Readings
 FIGURE 9



CRUISE 4 STATION BRAVO 30-31 AUGUST 1968 TIME-DEPTH SAMPLING LOCATIONS
 o Nansen Placement and Beam Transmittance Readings
 x Additional Beam Transmittance Readings
 FIGURE 10



CRUISE 4 STATION DELTA 30-31 AUGUST 1968 TIME-DEPTH SAMPLING LOCATIONS
 o Nansen Placement and Beam Transmittance Readings
 x Additional Beam Transmittance Readings
 FIGURE 11

CHAPTER 4

ANALYSIS OF DATA

4.1 Introduction

Because several oceanic parameters were investigated, each parameter is discussed separately with respect to beam transmittance in order to indicate clearly specific relations and trends.

Contours of beam transmittance were plotted on time-depth charts as shown in figures 12 through 18. Ten percent intervals were used throughout, except where shorter intervals were required to increase definition. A 20 percent contour implies very turbid water, whereas an 80 percent isoline suggests relatively clear water. Beam transmittance values were linearly interpolated between actual points of measurement. The tidal level above mean lower low water is shown at the top of these figures.

Salinity, temperature, density, and particle count contours were also plotted on time-depth charts using linear interpolation. These contours were then separately transferred to their corresponding beam transmittance charts. Figures 19 through 43 present these overlays.

An IBM 360 Model 67 (Duplex) computer was utilized to facilitate data reduction. Appendix II presents the program used to correct protected reversing thermometer readings, while Appendix III contains the program used to determine in situ density and to plot profiles of salinity, temperature, and density against depth (Figs. 44 through 62). In Appendix IV is the program used to determine the best least square linear fit for the beam transmittance measurements as a function of Coulter particle counts at various counter thresholds (Figs. 63 and 64).

Table 1 in Appendix V, contains the tabulated values of depth, time, temperature, salinity, density, beam transmittance, and total Coulter Count. Table 2 presents the Coulter particle count in relation to time, depth, and relative pulse height. Table 3 shows the relationship between lunar phases and sampling periods.

4.2 Beam Transmittance Measurements

The results of the beam transmittance measurements, separated into the four periods of observation, are presented in the following subsections.

4.2.1 Cruise 1 (26-27 July 1968)

The 25 hr series of measurements made during Cruise 1 (Fig. 12) revealed a sharp transmissivity gradient at a depth of approximately 20 m, which prevailed throughout this sampling period. A turbidity layer, i.e., a layer of minimum beam transmission, was not present. Below about 20 m characteristic transmittance patches were observed. An area of very low transmittance was present between the sea surface and a depth of 10 m at the beginning of this series. This region continued to persist in time and depth throughout all four cruises at station Bravo.

Low values of transmissivity were observed at both low tides. The following high tide in each case resulted in increased transmissivity values. Oscillation of the beam transmittance contours after 0400 hours was generally of the same period as the tidal cycle although 180 degrees out of phase. The four-hour period oscillations occurring at 15 m between 1500 and 0000 hours are possibly the result of seiches or

internal waves. These oscillations are discussed in further detail in sections 4.4 and 4.9.

It should be noted that beam transmittance values for this cruise were much lower than subsequent observations. During this cruise an extremely large amount of particulate matter was visually observed near the surface, in addition to a large amount measured by the Coulter Counter, indicating a probable plankton bloom. This phenomenon was not observed on ensuing cruises.

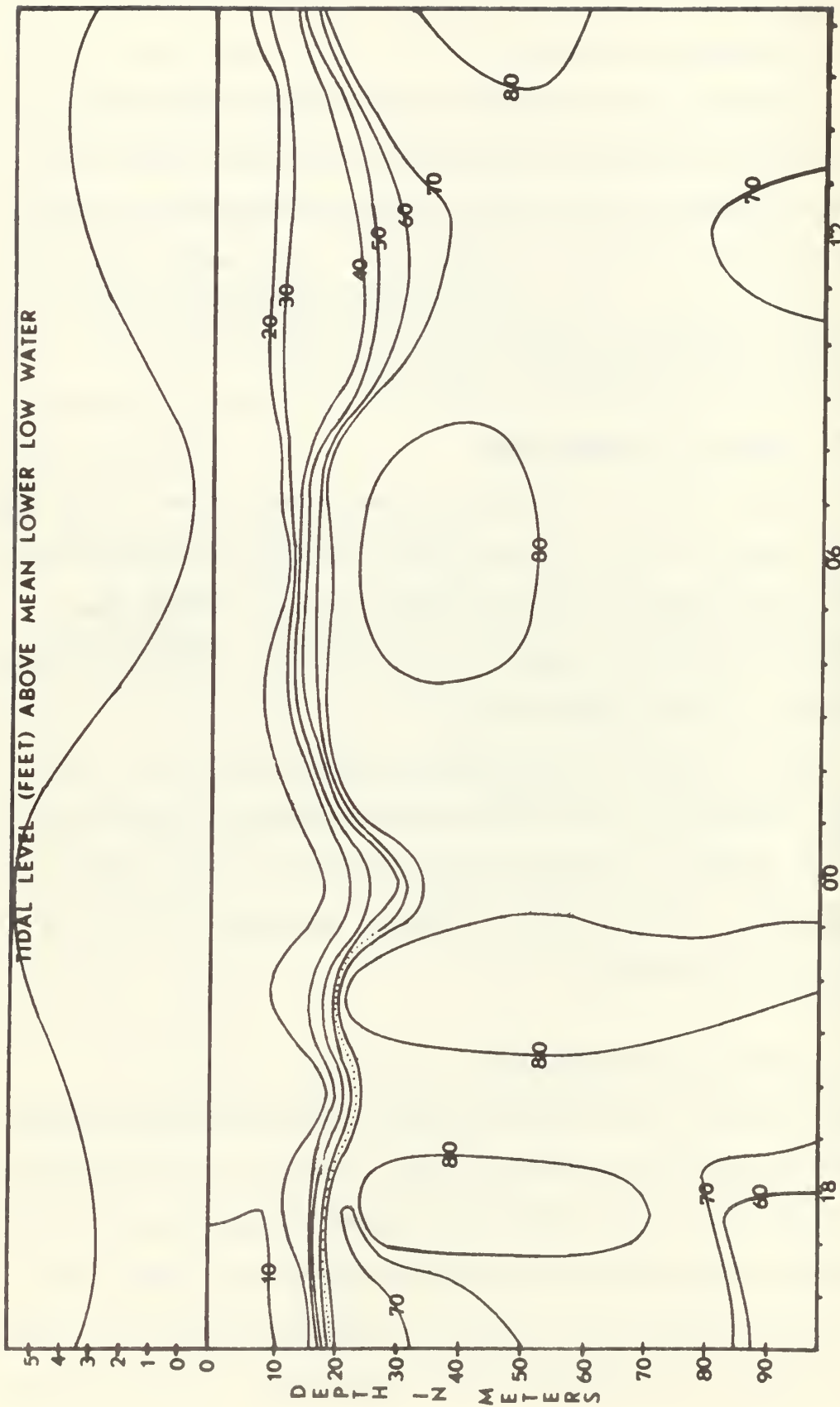
4.2.2 Cruise 2 (17 August 1968)

The 10 hr series of observations made during Cruise 2 (Figs. 13 and 14) shows the effect of high seas in reducing the transmissivity stratification which was present during Cruise 1, although some turbidity patches still appear at station Bravo. A turbidity layer is present at station Delta at 10 m.

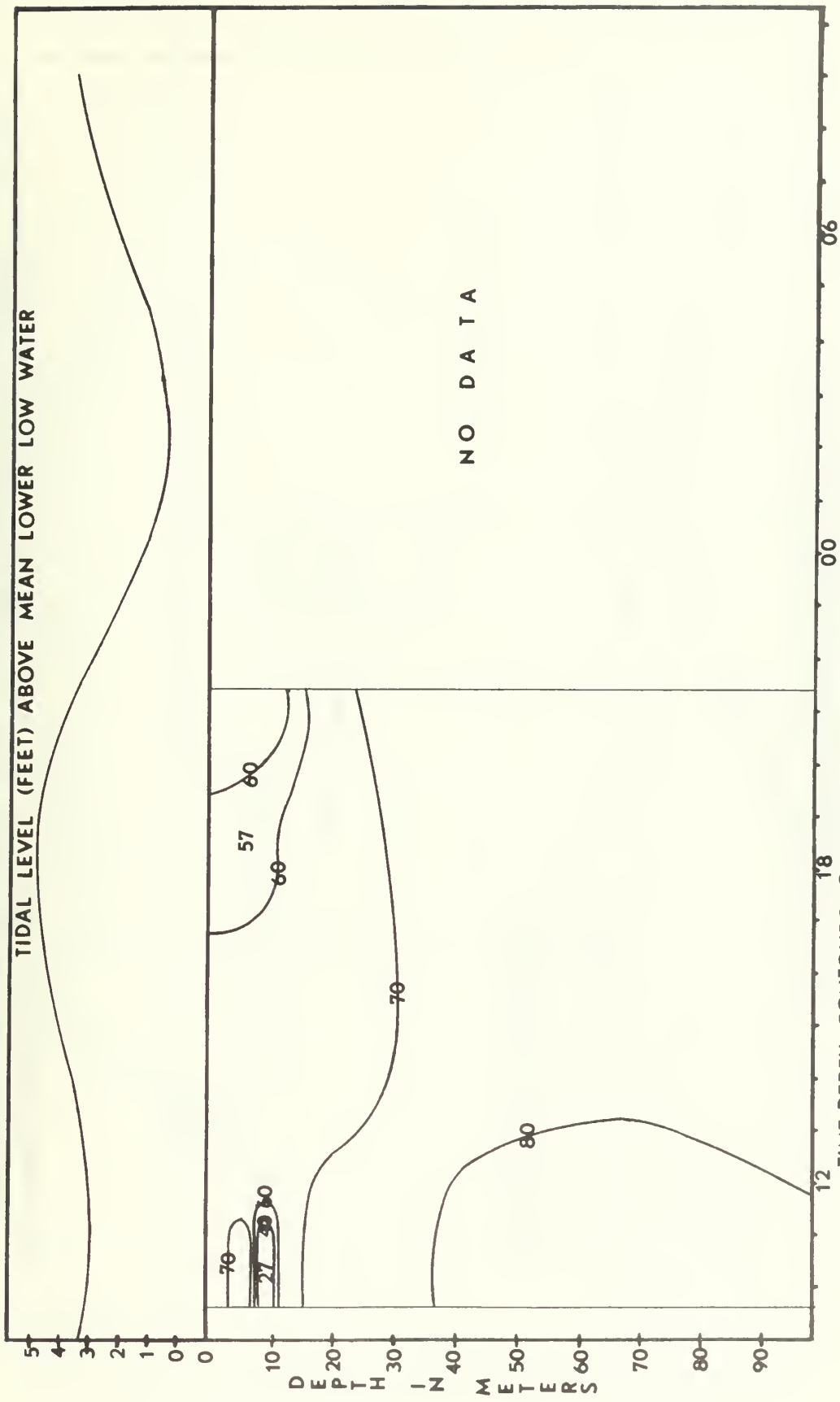
Figure 13 shows a transmittance minimum present at low tide. Higher transmissivity values occur with the following high tide. A possible in-phase relationship between the tidal cycle and beam transmittance is seen in Fig. 14 although the record is too short for accurate verification.

4.2.3 Cruise 3 (23 August 1968)

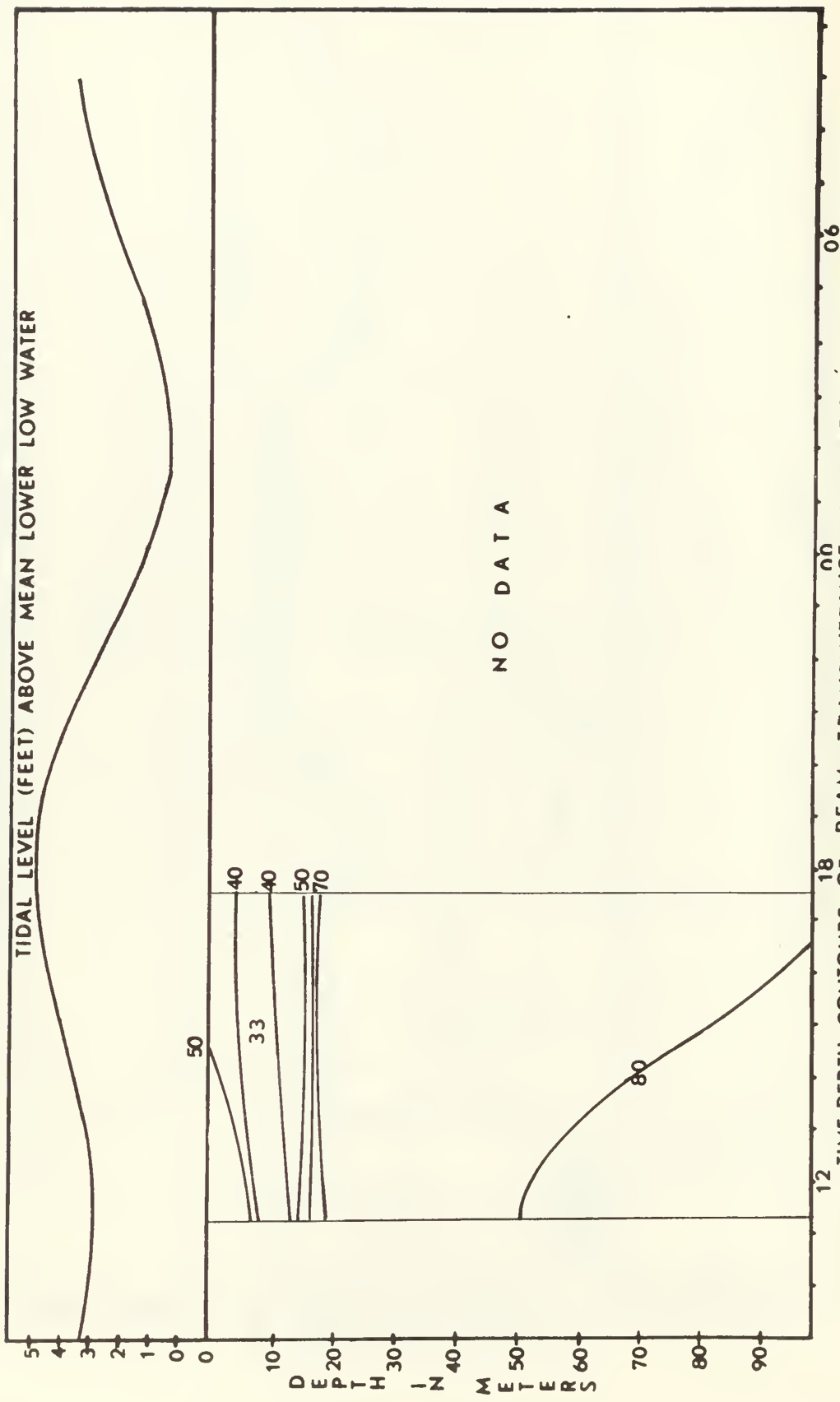
A generally similar profile of beam transmittance was observed at both stations during Cruise 3 (Figs. 15 and 16). A turbidity layer was not present. Beam transmittance minima of approximately 40 percent at 1800 hours for both stations coincide with the low tide. The succeeding high tide again results in increased transmissivity values. The 20 percent transmissivity minimum seen in Fig. 15 occurs during



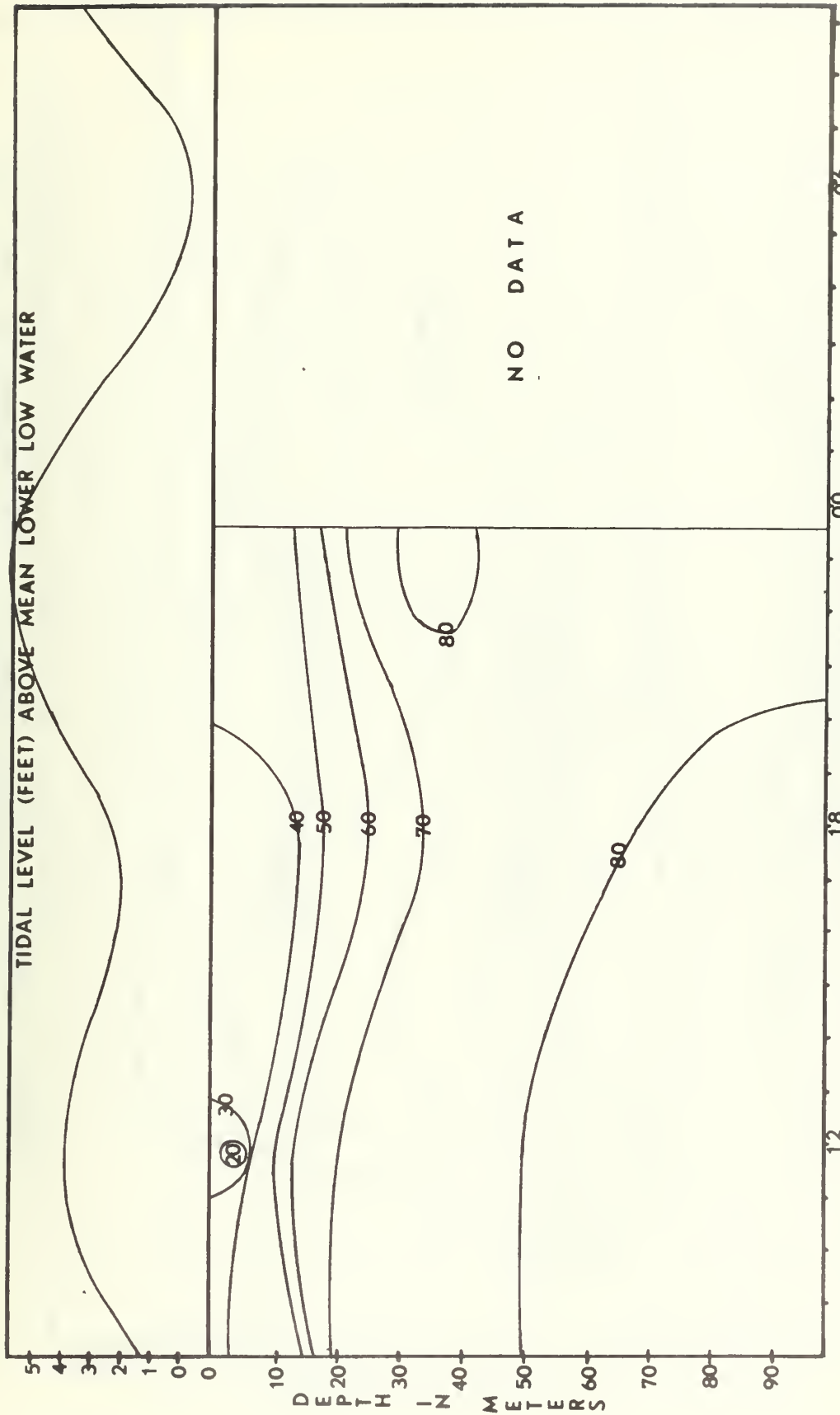
STATION BRAVO 26-27 JULY 1968
 FIGURE 12



STATION BRAVO 17 AUGUST 1968
 FIGURE 13



12 18 06
 TIME-DEPTH CONTOURS OF BEAM TRANSMITTANCE IN RELATION TO TIDAL CYCLE
 STATION DELTA 17 AUGUST 1968
 FIGURE 14



TIME-DEPTH CONTOURS OF BEAM TRANSMITTANCE IN RELATION TO TIDAL CYCLE
 STATION BRAVO 23 AUGUST 1968
 FIGURE 15

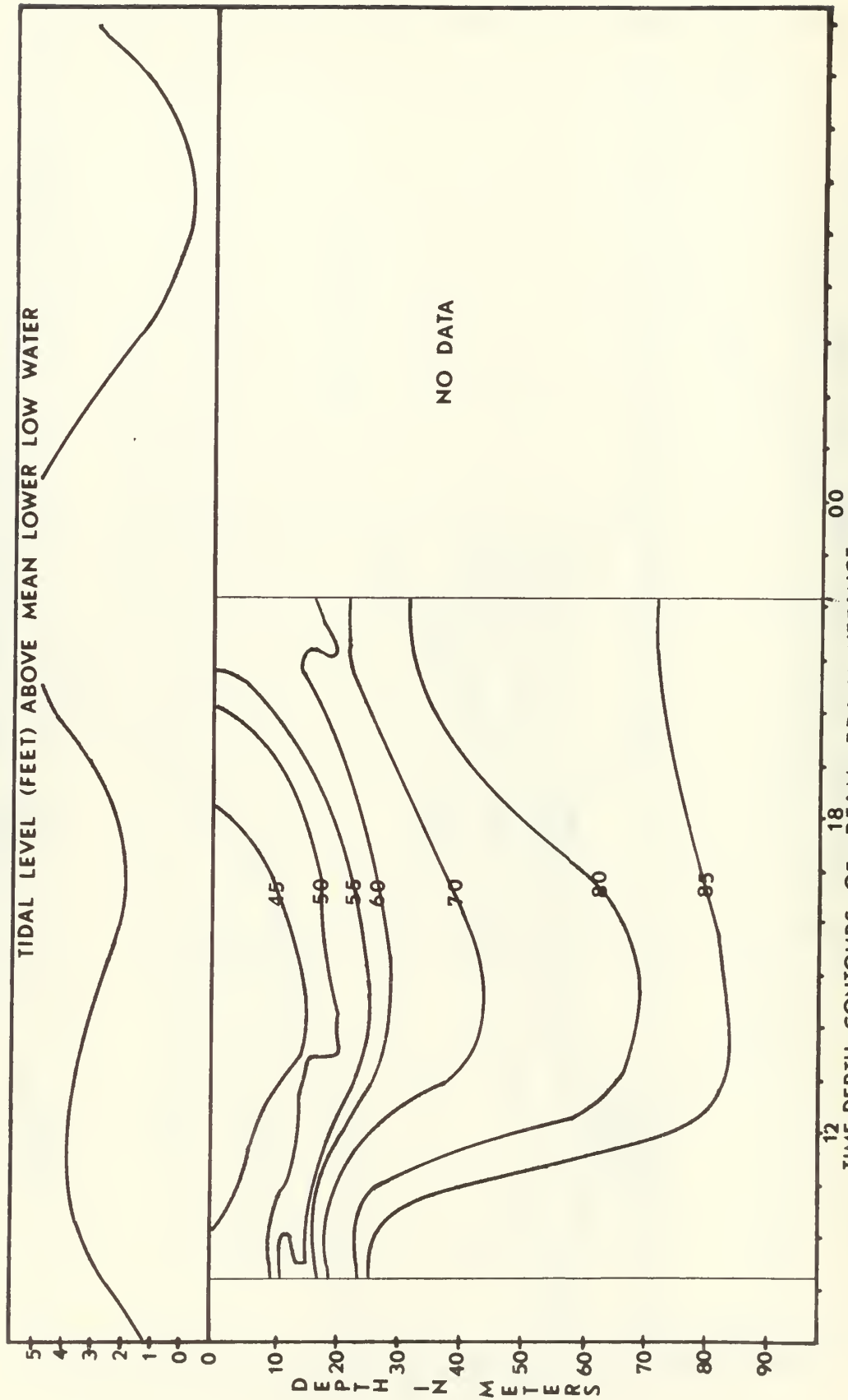


FIGURE 16

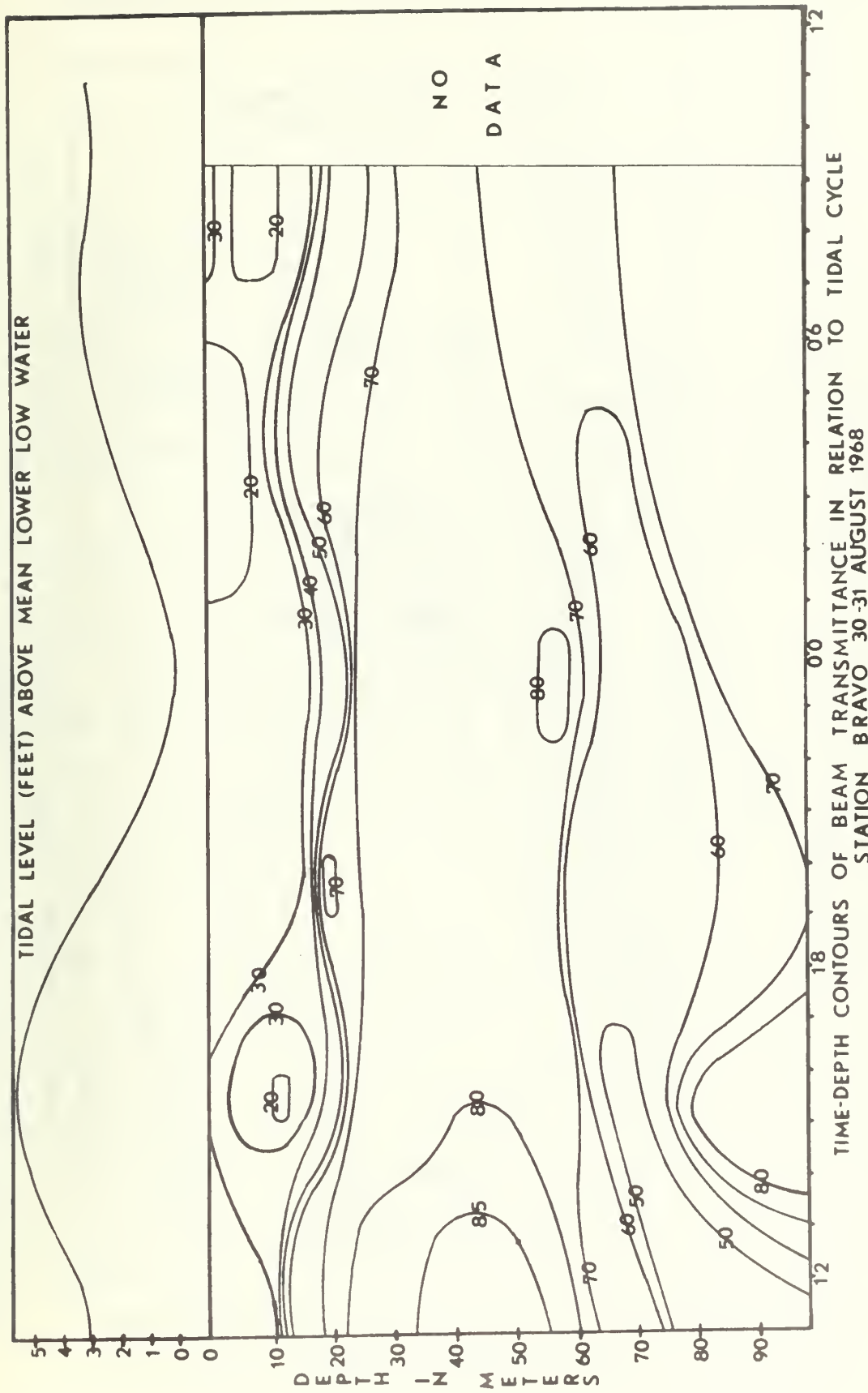
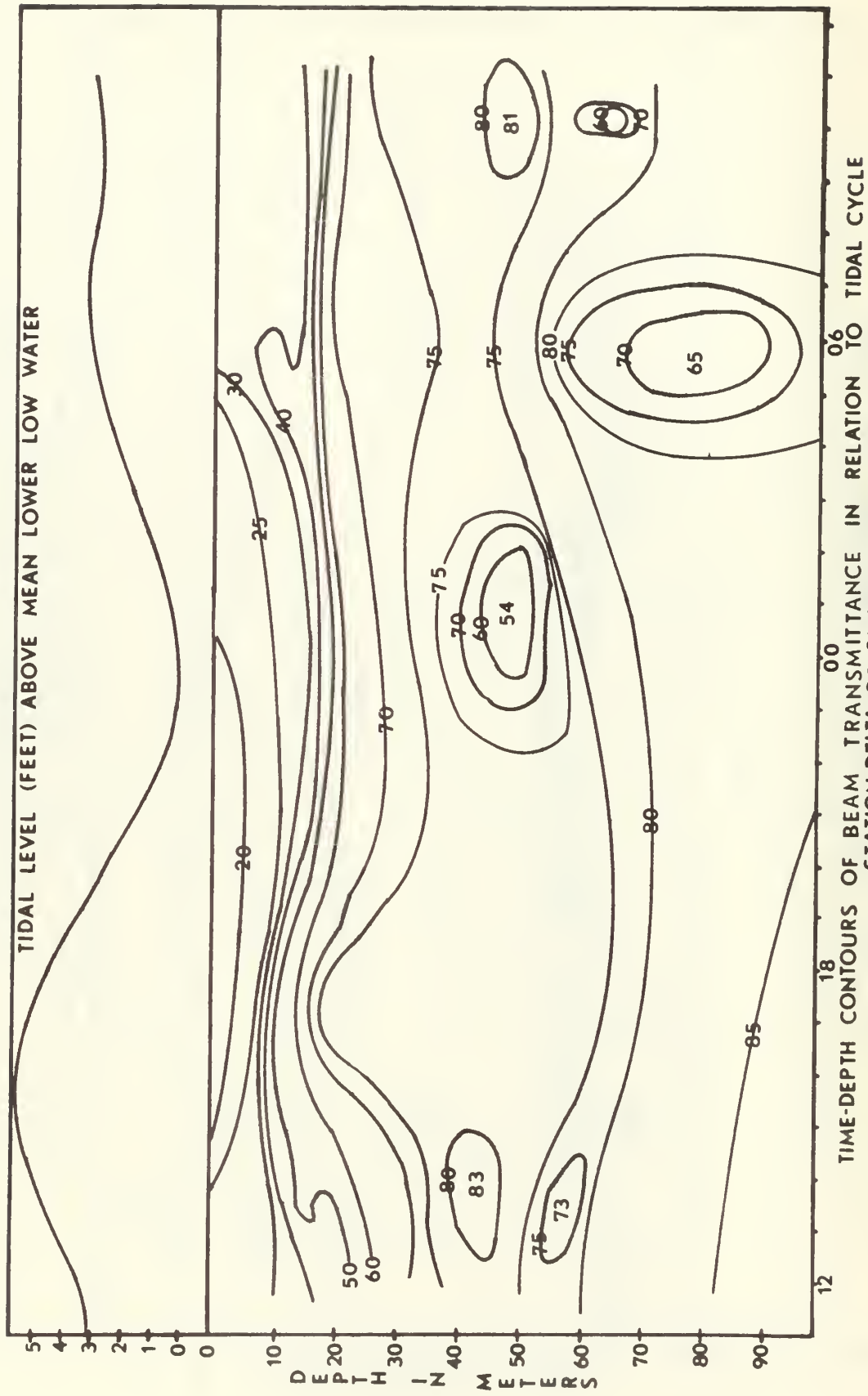


FIGURE 17



STATION DELTA 30-31 AUGUST 1968
FIGURE 18

the lowest of the two high tidal levels. This minimum corresponds approximately with those shown in Figs. 12 and 13, which occurred at the same depth and hour of the day.

Each station depicts an oscillation of beam transmittance contours having the same period as the tidal cycle and very nearly in phase.

4.2.4 Cruise 4 (30-31 August 1968)

The 23 hr series of measurements obtained during Cruise 4 was characterized by the presence of two turbidity layers.

Figure 17 shows a slight intermittent layer at 10 m and a continuous, more pronounced, layer occurring at 70 m. This latter layer was also present at station Delta (Fig. 18).

The trend of minimum transmittance associated with low tide was again observed at 0000 hours. As noted in section 4.2.3, we again see a transmissivity minimum occurring during high tide.

Beam transmittance contours at both stations show an approximate tidal cycle oscillation.

4.3 The Correlation of Tidal Cycle with Beam Transmittance

Beam transmittance contours as discussed in section 4.2, generally show oscillations of a tidal period although phase relations are not consistent. In most cases the water column is most turbid at low tide with clearing accompanying the following high tide. Station Delta, farthest from coastal influences, depicts these features much more clearly than does the nearshore station.

A possible correlation between tidal level, depth of maximum transmittance gradient, and depth where transmittance initially increases most rapidly was investigated. No meaningful relationship was found.

4.4 The Correlation of Salinity with Beam Transmittance

Salinity correlations with beam transmittance during the four periods of measurement varied from excellent to poor.

Cruise 1 contours (Fig. 19) show a slight similarity after 0600 hours in the halocline. The three salinity pockets at 10 m suggest a strong influence on the transmittance isolines and possibly account for the four-hour oscillations occurring between 1500 hours and 0000 hours.

Figure 20 shows a fair comparison between salinity and transmittance especially in regions of minimum transmittance. Station Delta contours (Fig. 21) are nearly the same above 10 meters.

The 23 August station Bravo series before 1900 hours (Fig. 22) presents a fair correlation between isolines to a depth of 20 m. Figure 23 shows an excellent comparison between salinity and transmittance throughout the sampling period in both time and depth. The coincidence in time and depth of three salinity pockets with three beam transmittance discontinuities is remarkable.

The Cruise 4 results (Figs. 24 and 25) show poor correlation between salinity and transmissivity, although a slight following of isohalines exists with the 70 m turbidity layer at station Bravo. The correspondence of two relatively high salinity pockets with two areas of minimum transmittance (Fig. 25) below 40 m at station Delta was observed.

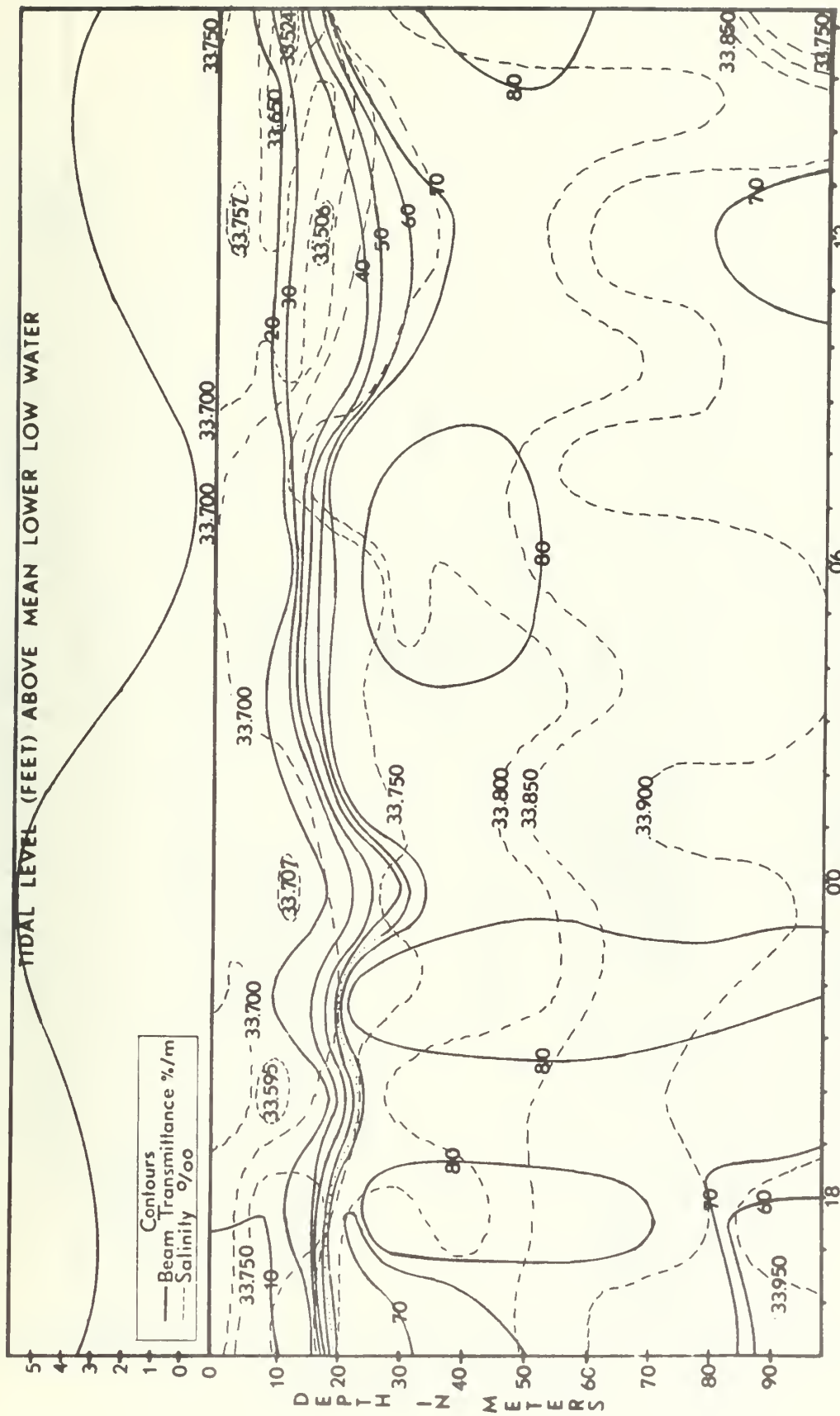
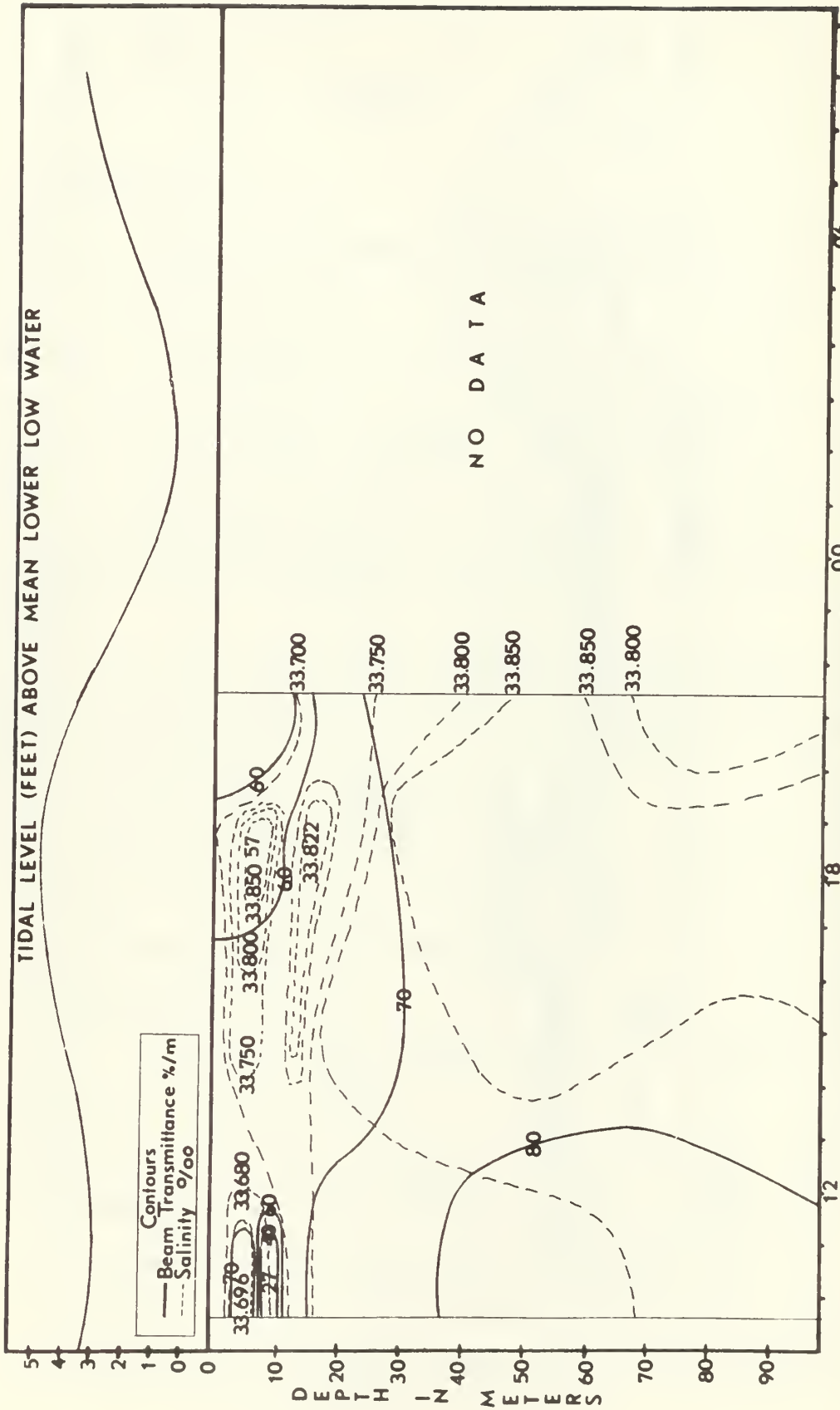
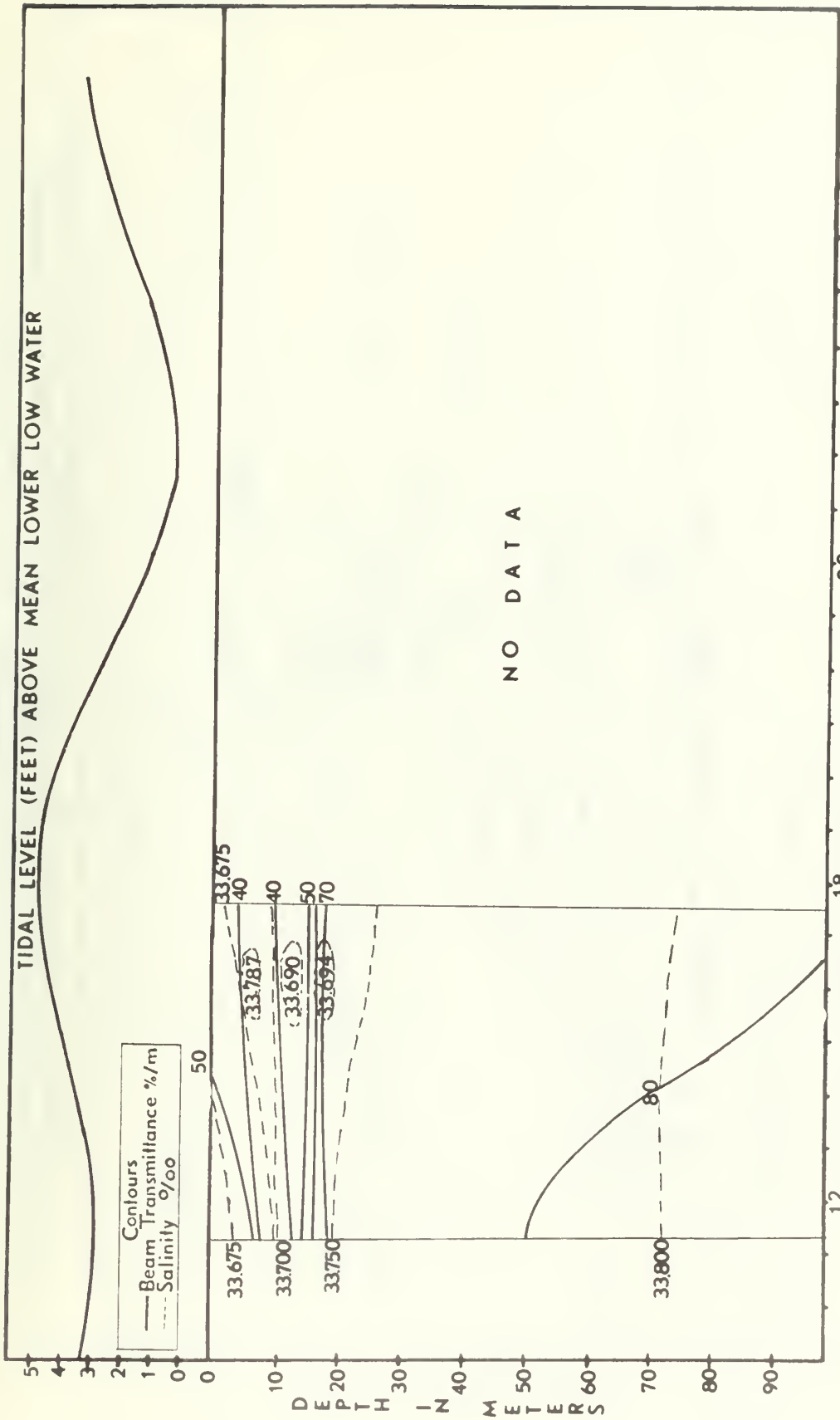


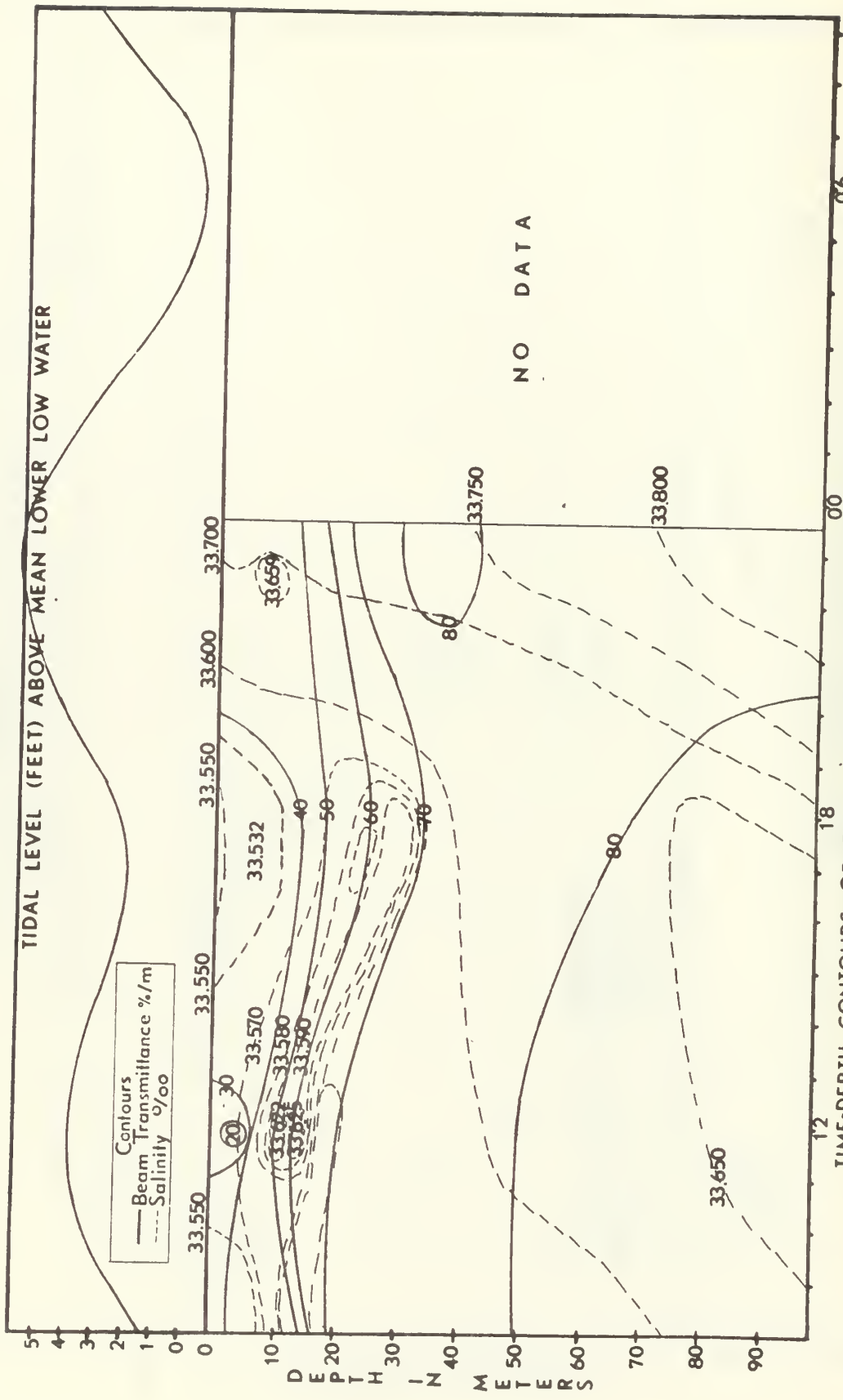
FIGURE 19



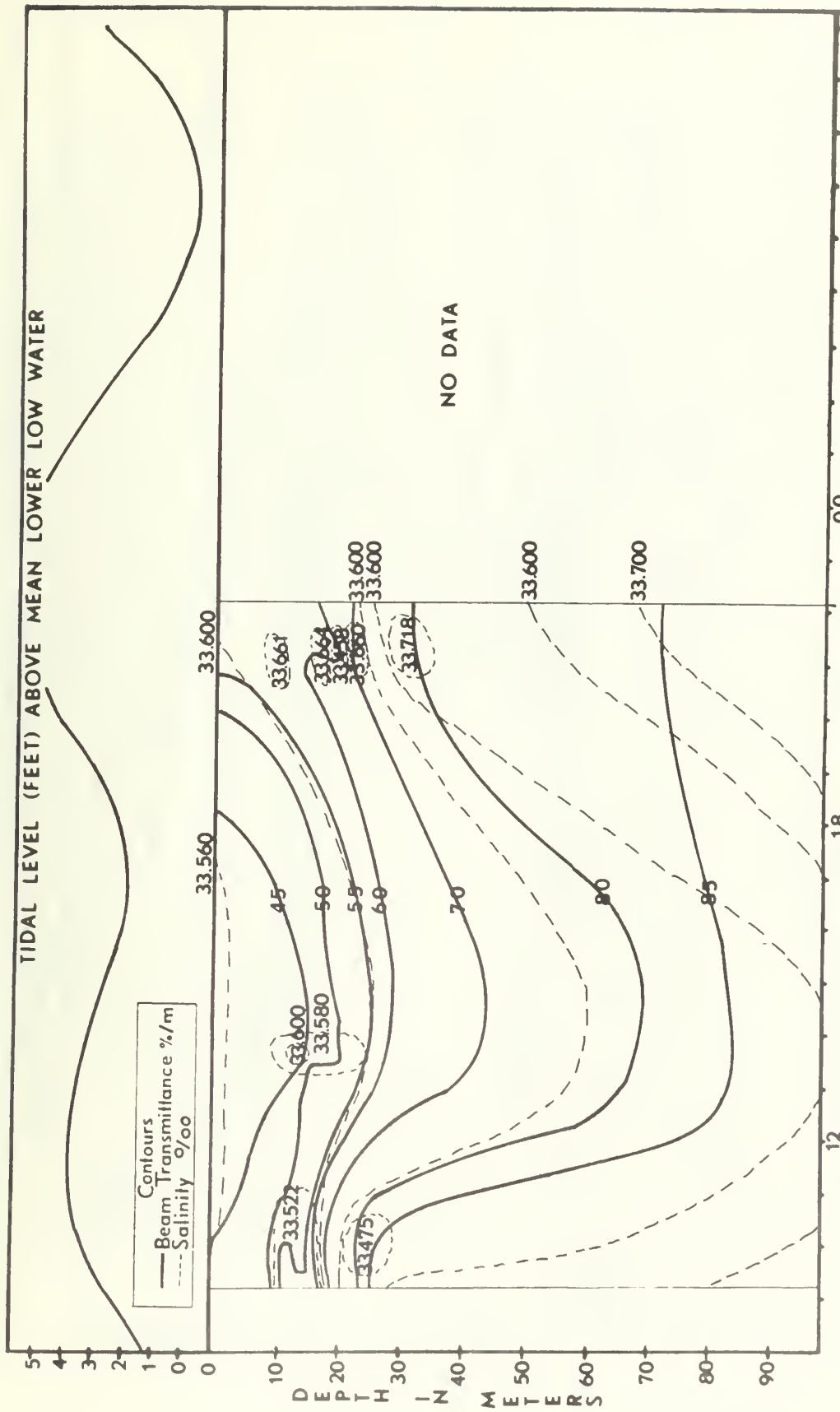
TIME-DEPTH CONTOURS OF BEAM TRANSMITTANCE IN RELATION TO SALINITY
 STATION BRAVO 17 AUGUST 1968
 FIGURE 20



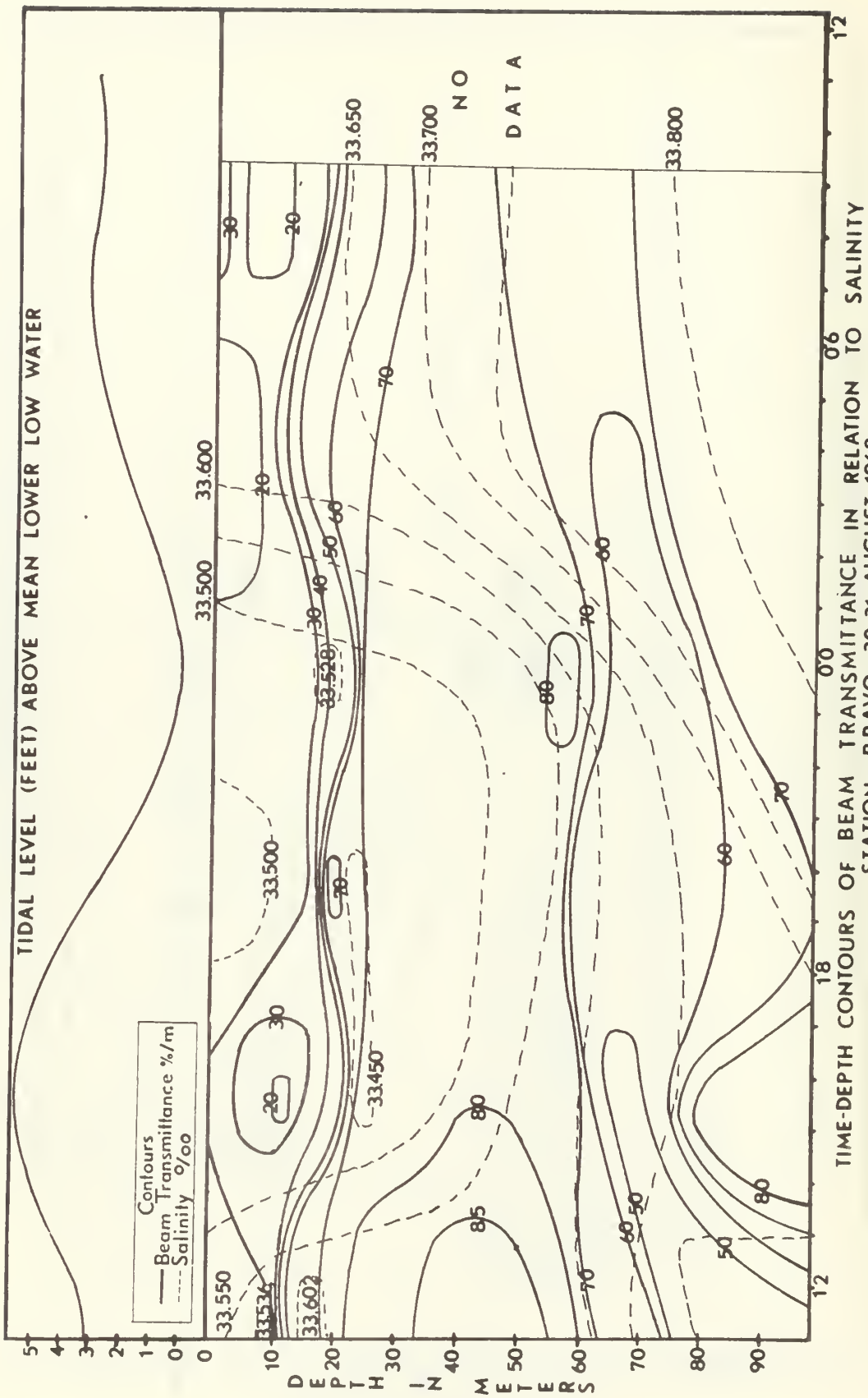
STATION DELTA 17 AUGUST 1968
 FIGURE 21



TIME-DEPTH CONTOURS OF BEAM TRANSMITTANCE IN RELATION TO SALINITY STATION BRAVO 23 AUGUST 1968
 FIGURE 22



TIME-DEPTH CONTOURS OF BEAM TRANSMITTANCE IN RELATION TO SALINITY
STATION DELTA 23 AUGUST 1968
FIGURE 23



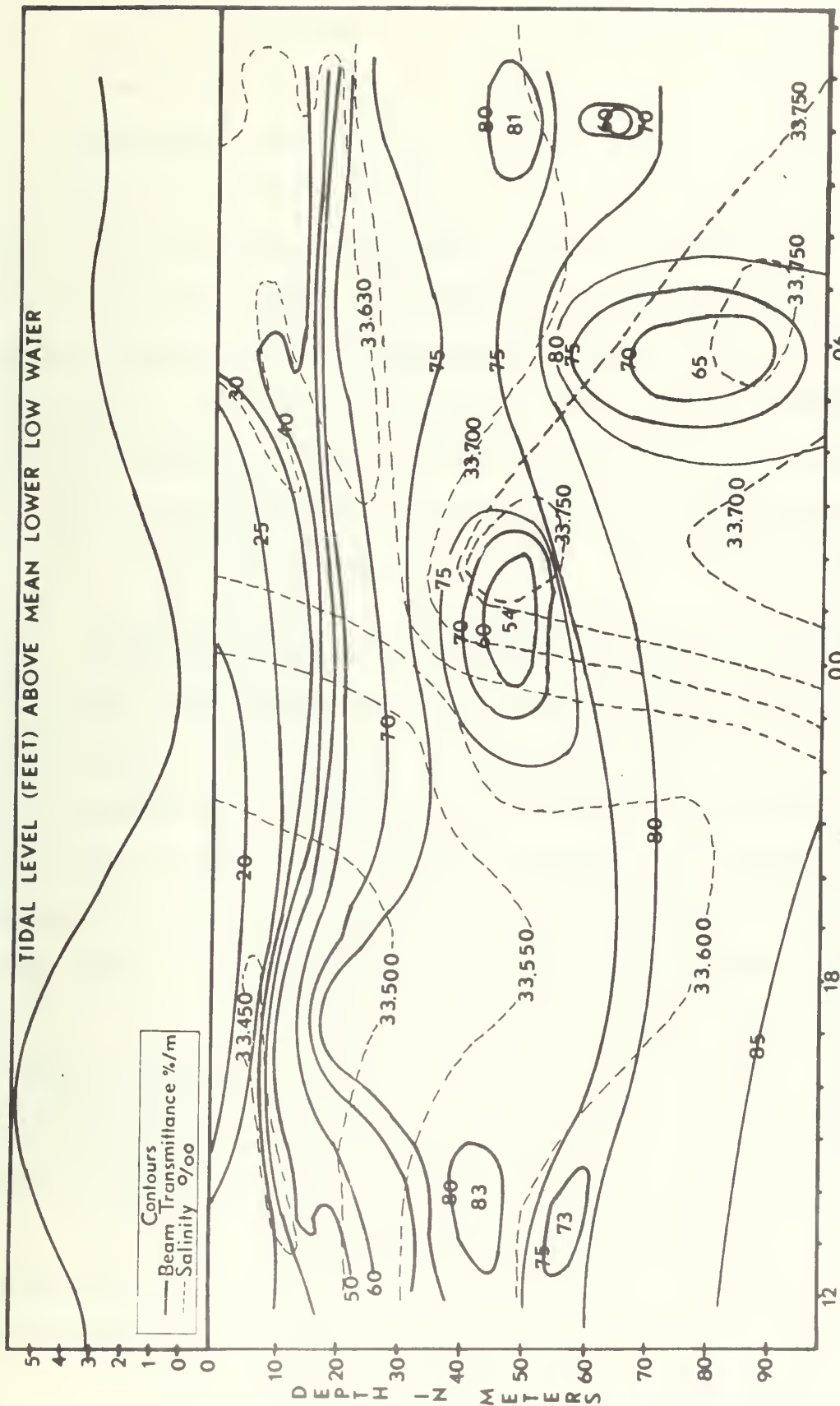


FIGURE 25

Salinity profiles (Figs. 44 through 62) commonly reveal the presence of two salinity minima at average depths of 10 and 19 m. This condition is typical of the area climatology discussed in section 1.4. The average depth of maximum beam transmittance gradient was located at a depth of 16 m between the two minima.

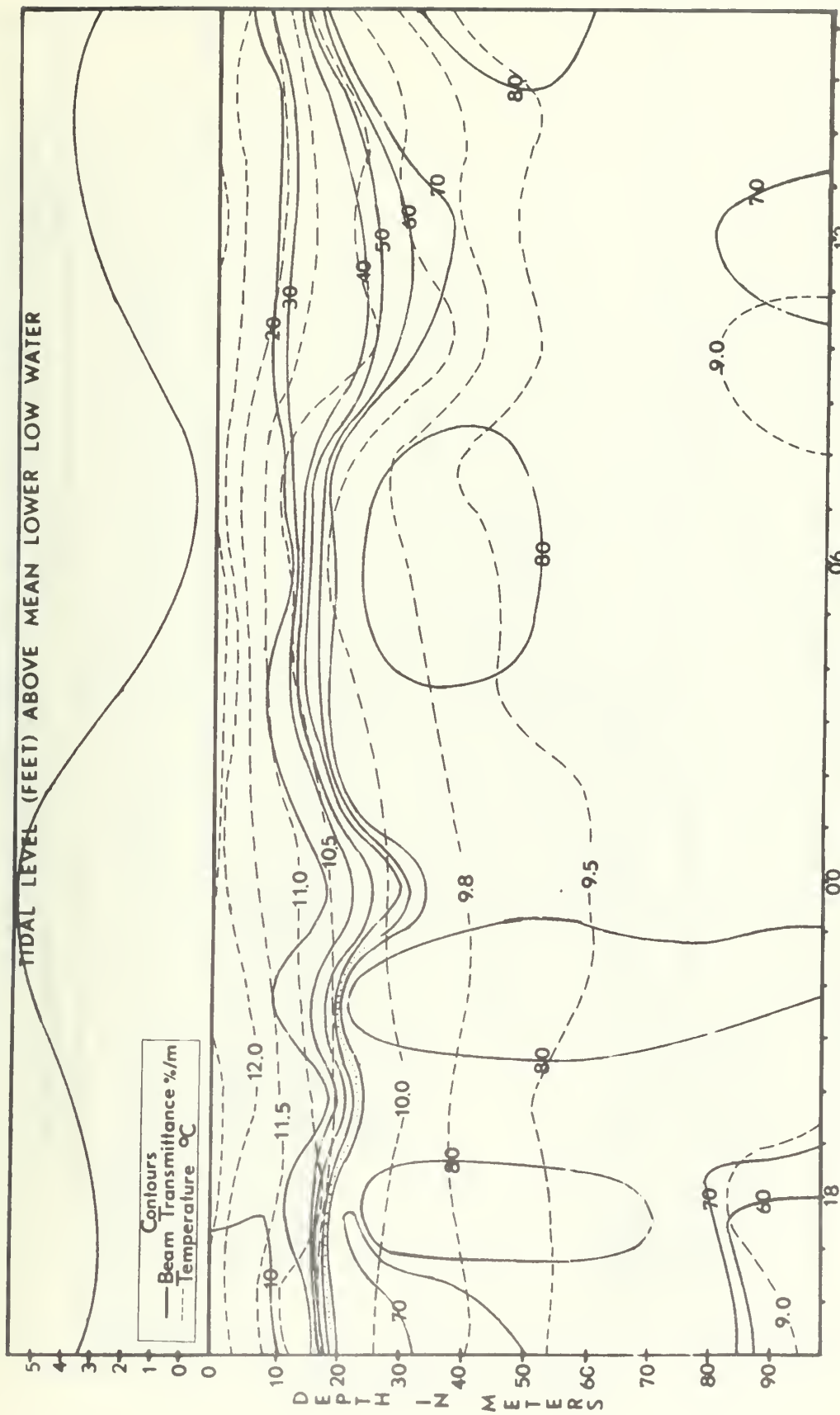
An interesting possible correlation is indicated below 40 m in the salinity and beam transmittance profiles. For example Fig. 47 shows increased salinity gradients corresponding to decreased transmittance gradients. The reverse is also true. Temperature and density gradients appear to be negligible. This salinity and beam transmittance relationship prevails in over 80 percent of the profiles (42 instances), where a salinity gradient change occurs.

4.5 The Correlation of Temperature with Beam Transmittance

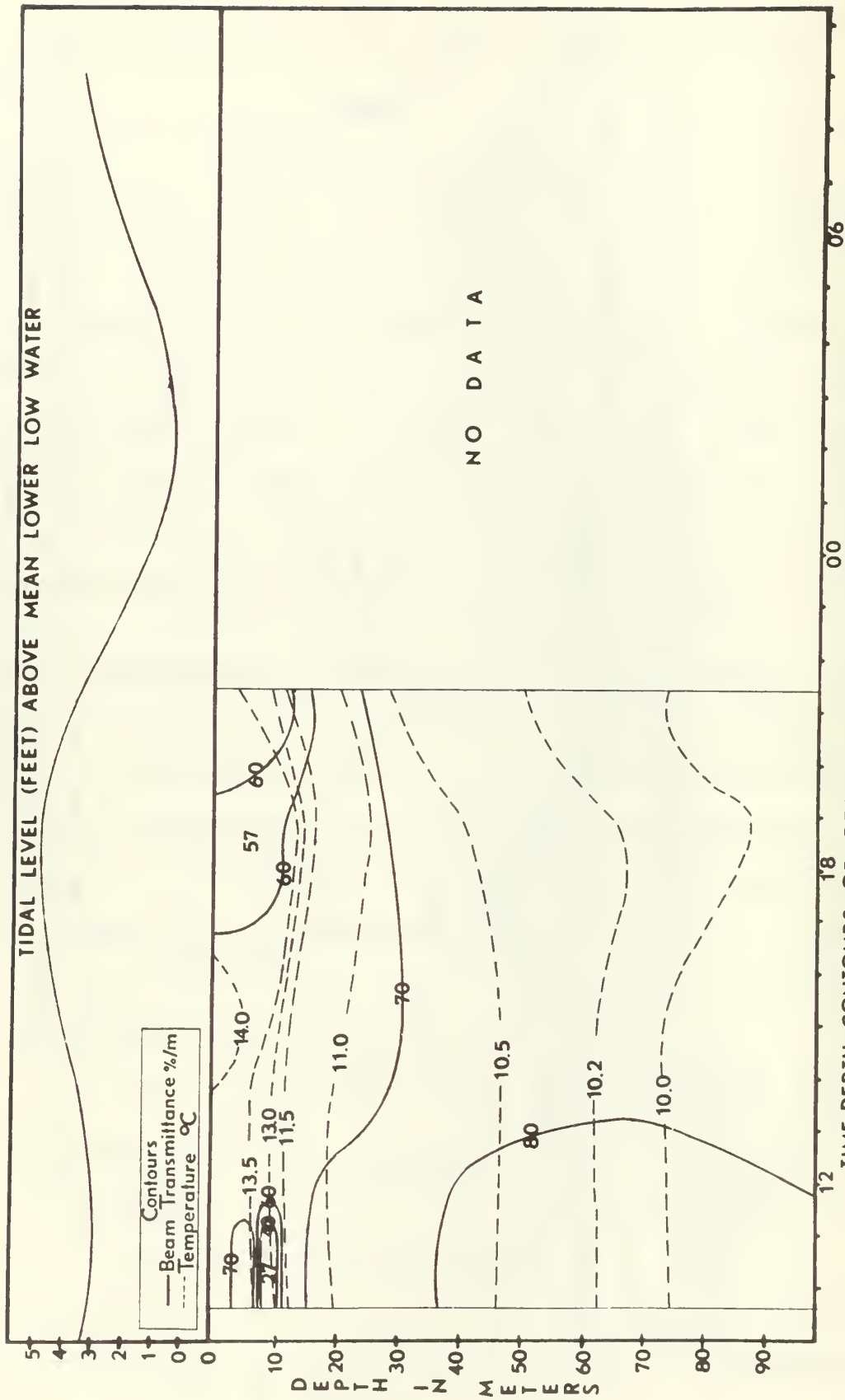
The time-depth plots of beam transmittance, tidal cycle and temperature (Figs. 26 through 32), show a generally excellent correlation between isotherms and isolines of beam transmittance. The undulations in the isotherms vary from being nearly in phase with the tidal cycle (Figs. 31 and 32) to almost 180 degrees out of phase (Fig. 27). These variations may be due to internal waves or other turbulent disturbances (discussed in section 4.9).

In general the maximum gradient in beam transmittance occurs in the lower half of the thermocline. The depth of the thermocline varies between 8 and 16 m, and appears to be deeper at or near low tide during the last two cruises (Figs. 29 through 32).

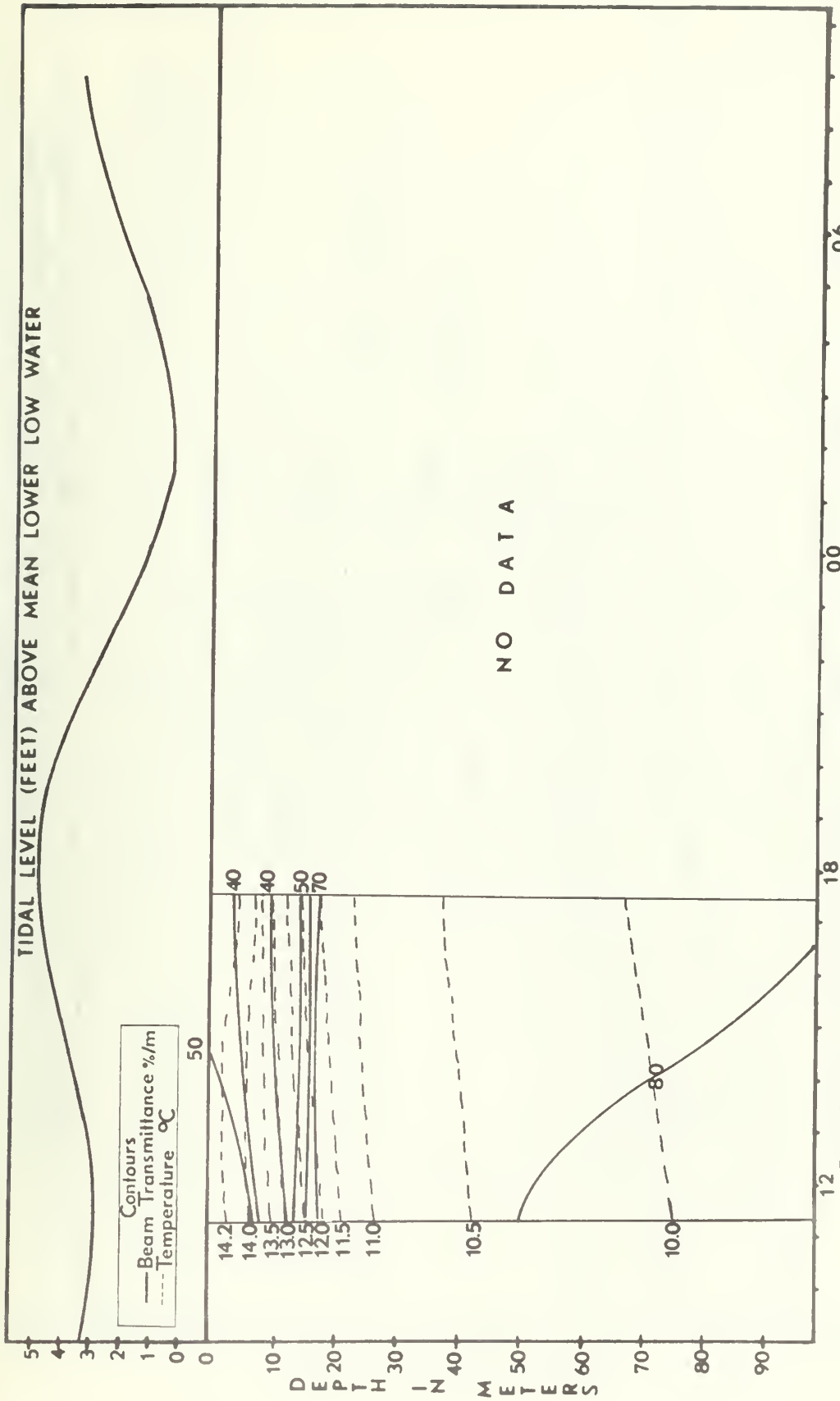
The range in temperature during the total period of observation was 6.45°C , from a low of 8.91°C to a high of 15.36°C . Despite heavy



TIME-DEPTH CONTOURS OF BEAM TRANSMITTANCE IN RELATION TO TEMPERATURE
 STATION BRAVO 26-27 JULY 1968
 FIGURE 26



TIME-DEPTH CONTOURS OF BEAM TRANSMITTANCE. IN RELATION TO TEMPERATURE
 STATION BRAVO 17 AUGUST 1968
 FIGURE 27



STATION DELTA 17 AUGUST 1968
 FIGURE 28

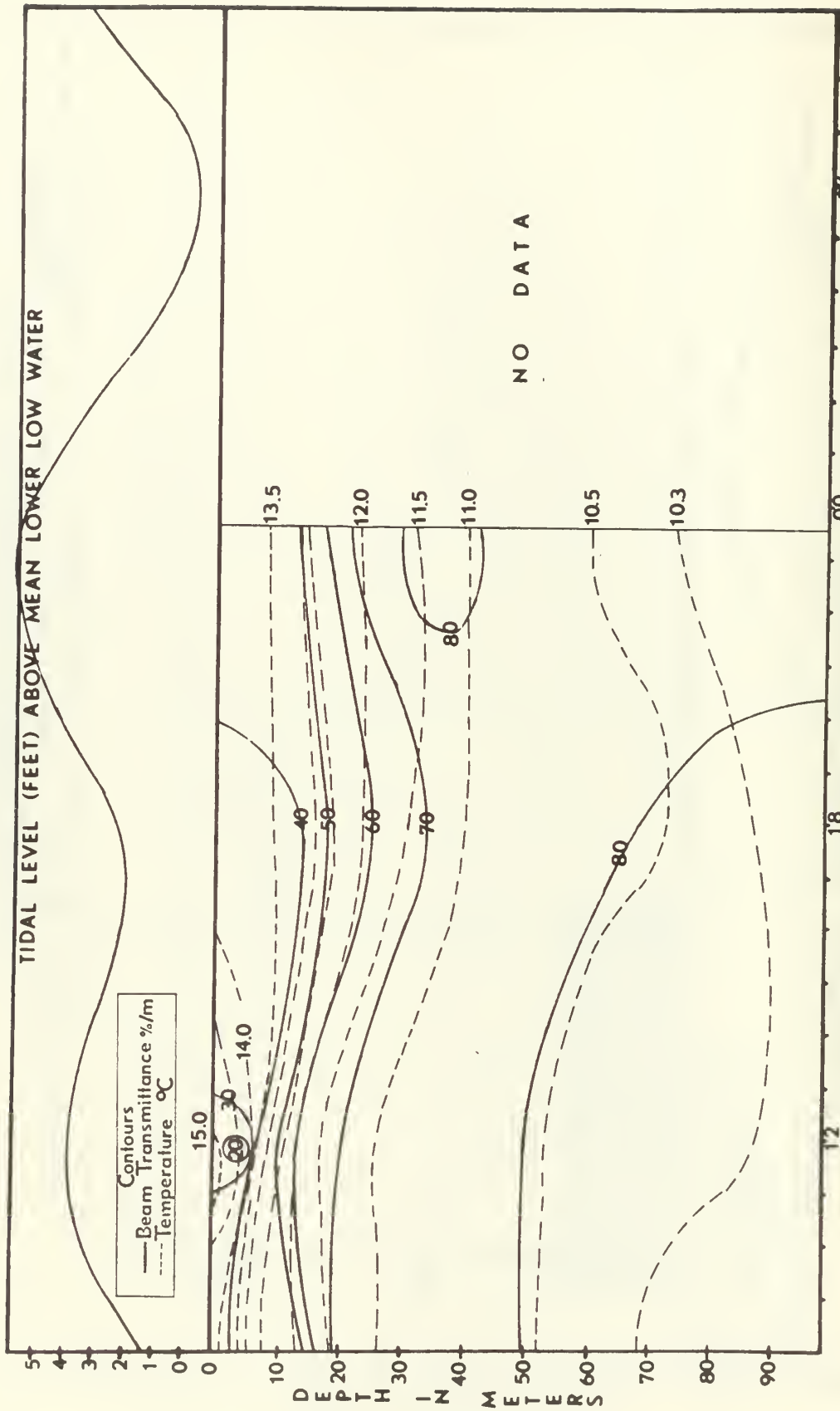
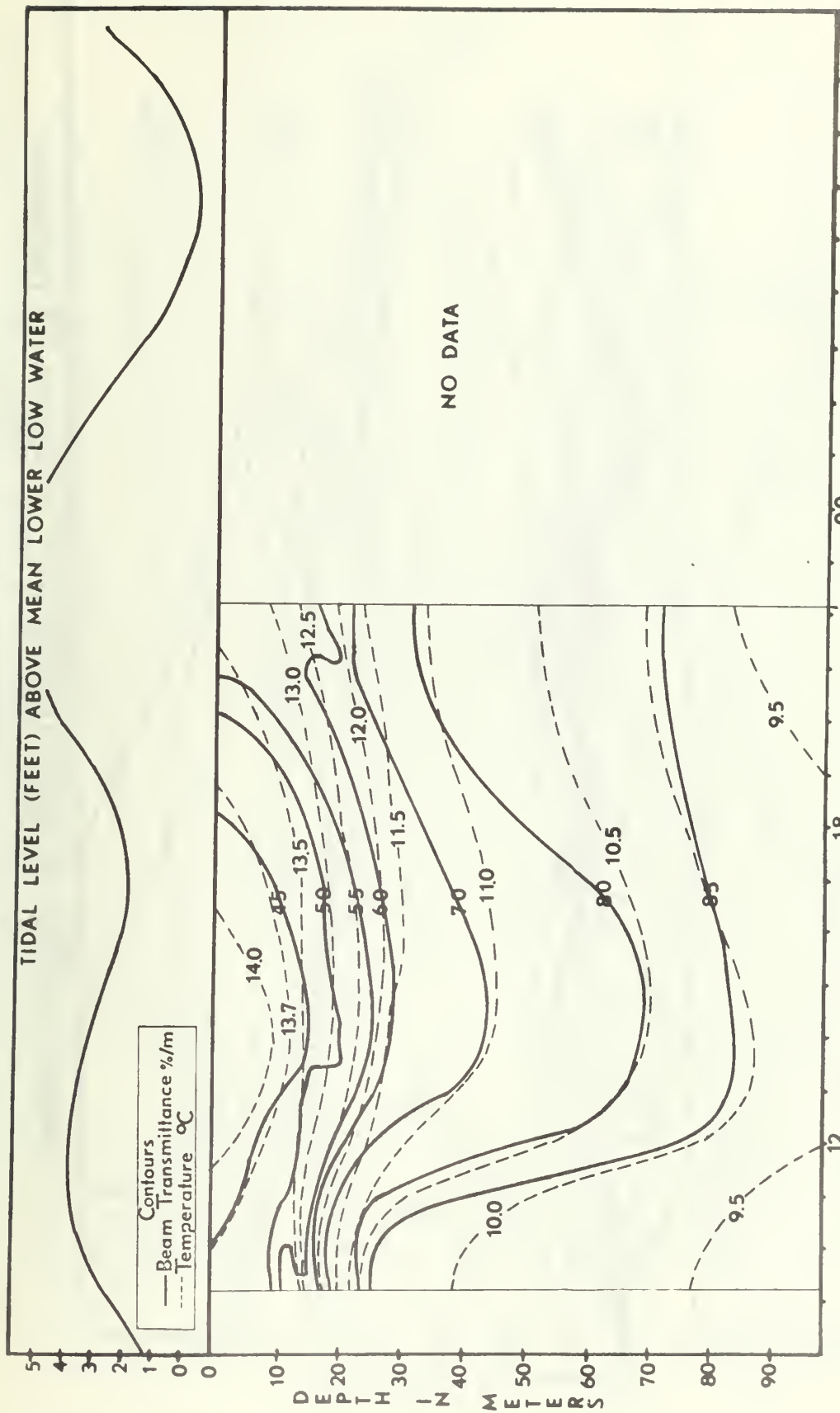
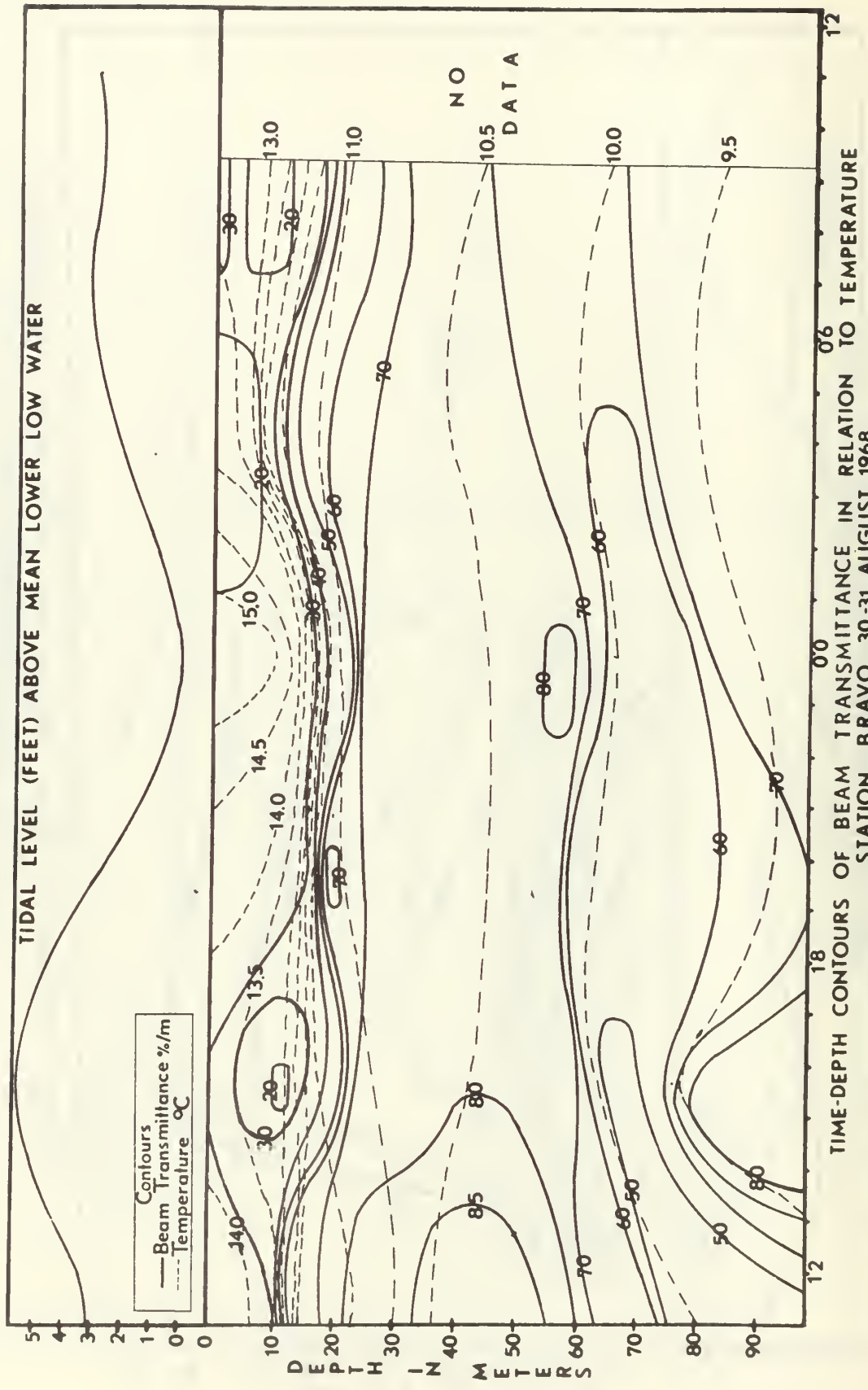
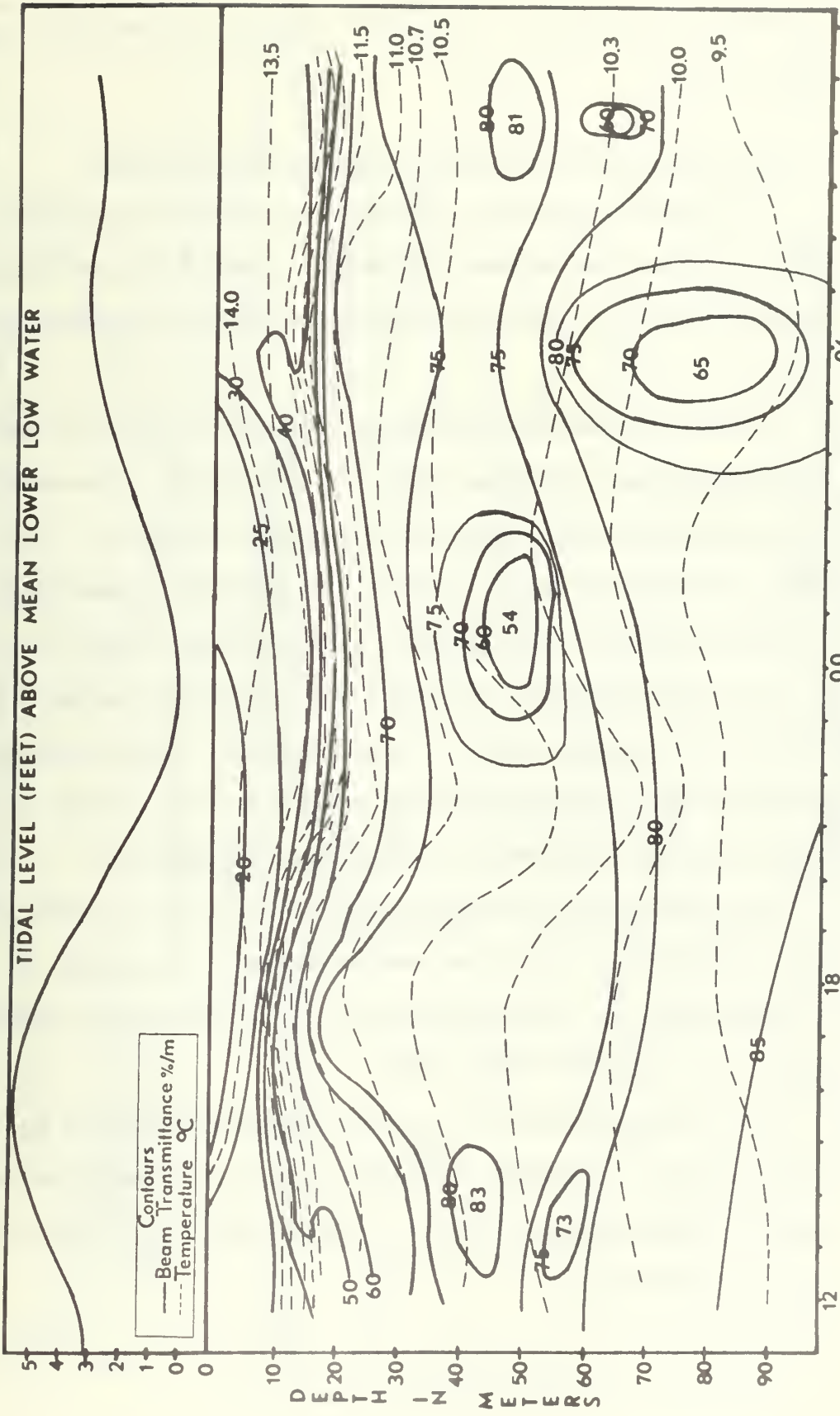


FIGURE 29



TIME-DEPTH CONTOURS OF BEAM TRANSMITTANCE IN RELATION TO TEMPERATURE
 STATION DELTA 23 AUGUST 1968
 FIGURE 30





TIME-DEPTH CONTOURS OF BEAM TRANSMITTANCE IN RELATION TO TEMPERATURE
 STATION DELTA 30-31 AUGUST 1968
 FIGURE 32

weather during two of the four cruises, the presence of mixed layers was the exception rather than the rule, indicating a stable water column.

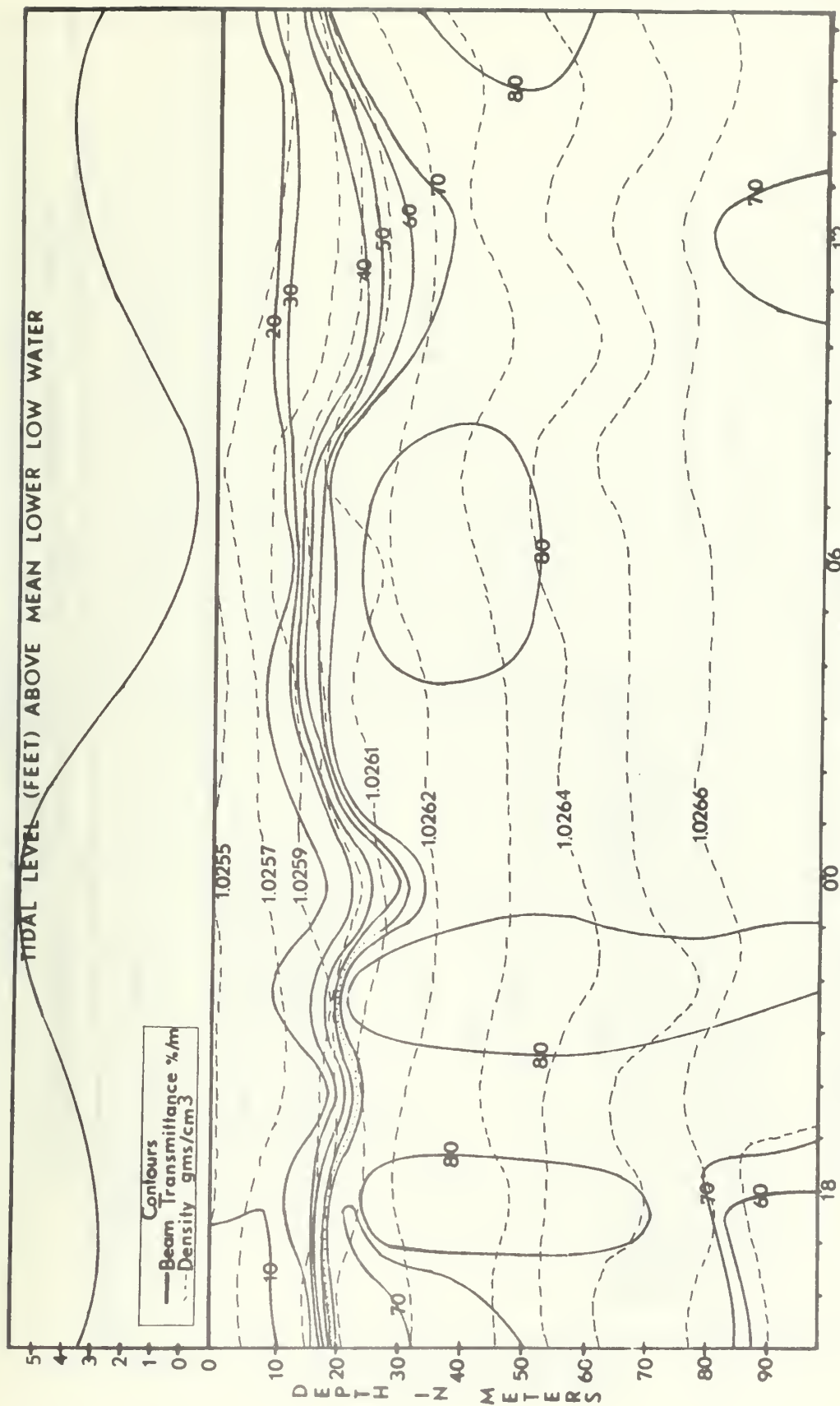
4.6 The Correlation of Density with Beam Transmittance

The similarity between isotherms and isopycnals shows that temperature has the greatest influence in controlling the density structure, which in turn significantly affects the propagation of light.

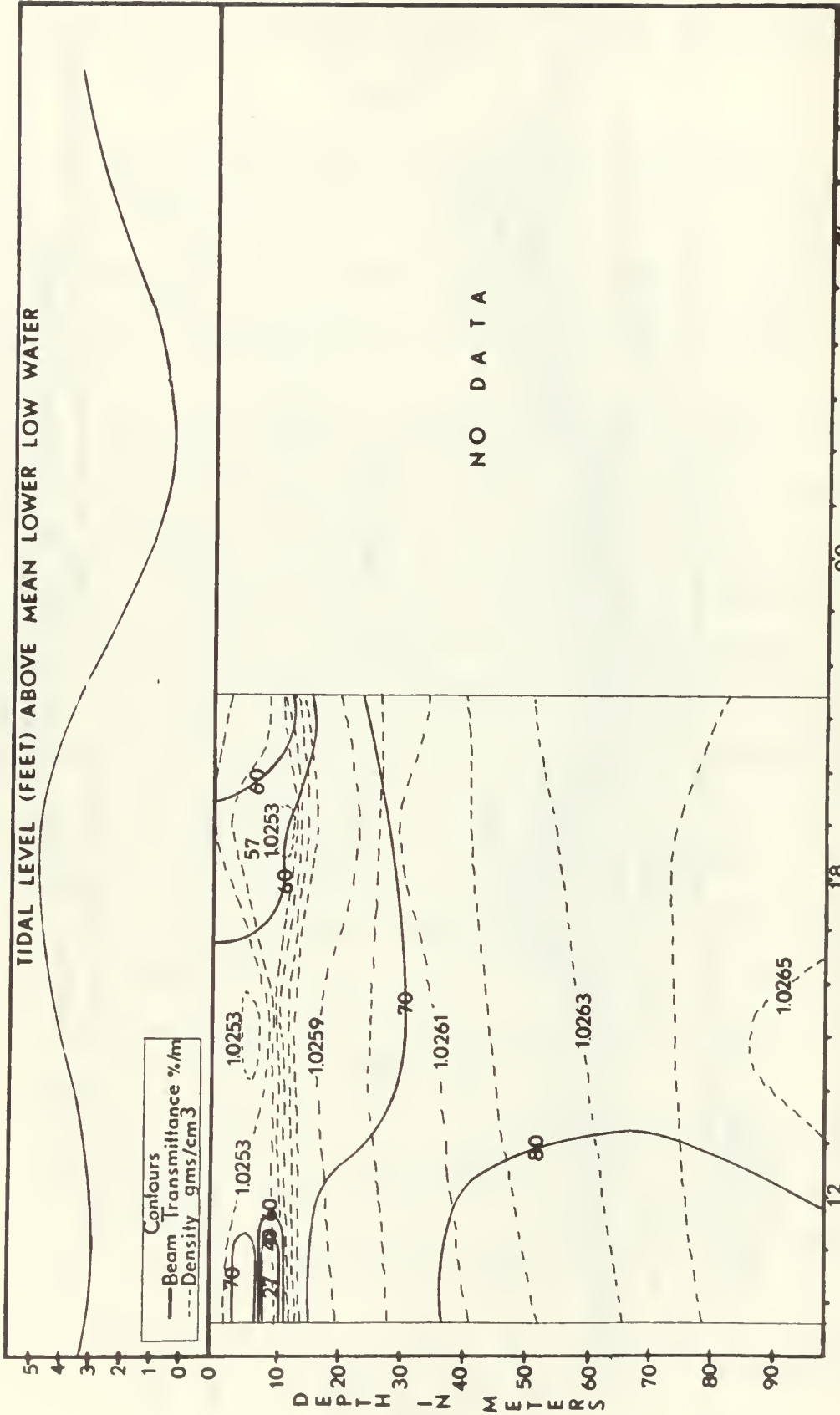
There is an excellent correlation between isolines of beam transmittance and isopycnals (Figs. 33 through 39). The maximum beam transmittance gradient and the pycnocline occur at, or very nearly at, the same depth. Below the pycnocline, transmittance increases markedly. Occasionally, a turbid layer between 50 and 70 m was observed (Figs. 38 and 39) and these layers appeared to oscillate in the same manner as the isopycnals. Some patchiness was noticed in the density structure (Figs. 34 and 38), but far less than that which was observed in the salinity structure.

The average value of density at the bottom of the pycnocline was 1.0258 g/cm^3 . This value remained constant throughout the period of observations at the deeper station, but at the shallow station it ranged from 1.0261 to 1.0256 g/cm^3 .

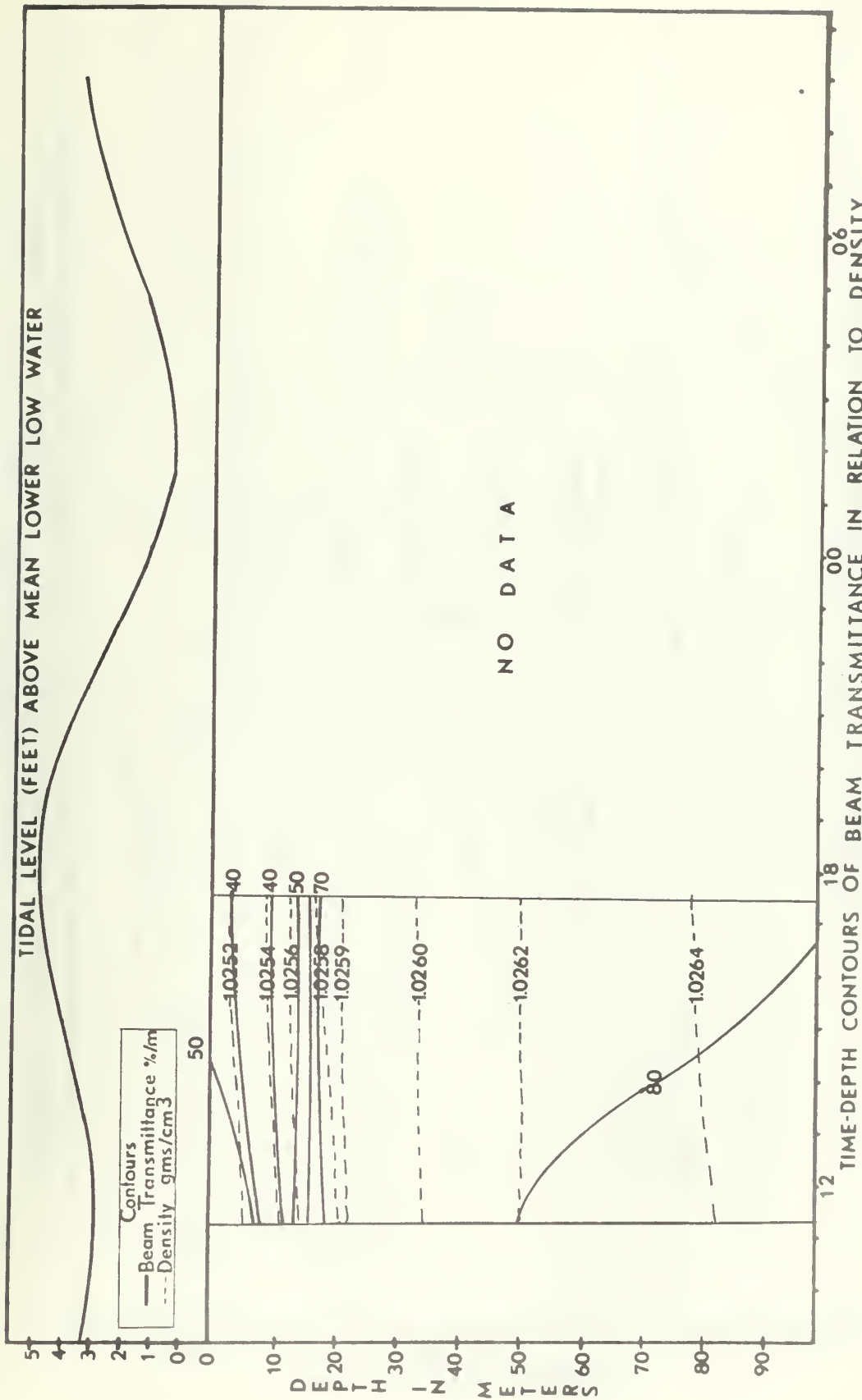
The isopycnals have an oscillatory appearance similar to the isotherms, but no constant relationship with the tidal cycle is apparent. Density ranged from 1.02473 to 1.02676 g/cm^3 during the period of observation.



STATION BRAVO 26-27 JULY 1968
 FIGURE 33



TIME-DEPTH CONTOURS OF BEAM TRANSMITTANCE IN RELATION TO DENSITY
 STATION BRAVO 17 AUGUST 1968
 FIGURE 34



STATION DELTA 17 AUGUST 1968
 FIGURE 35

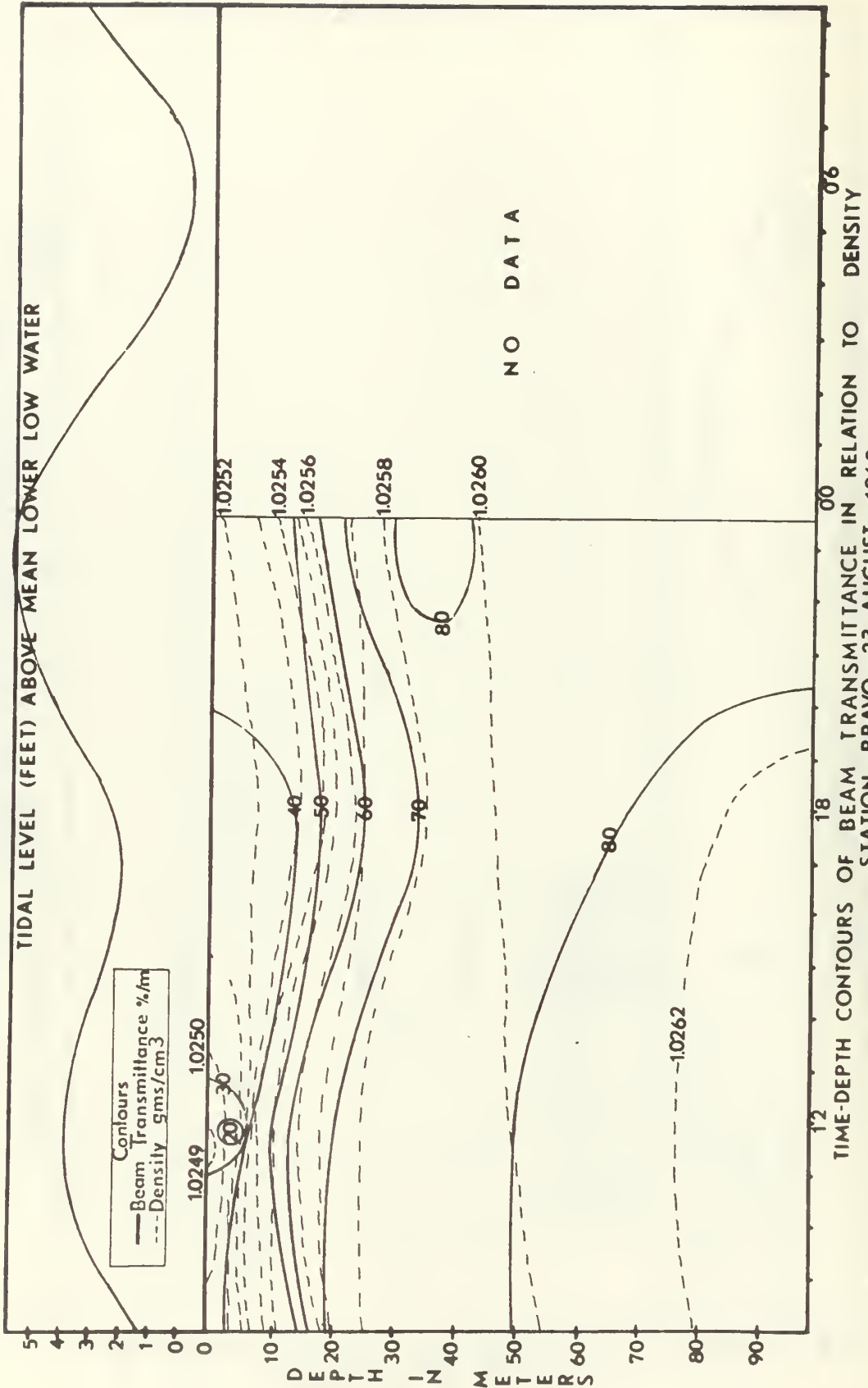
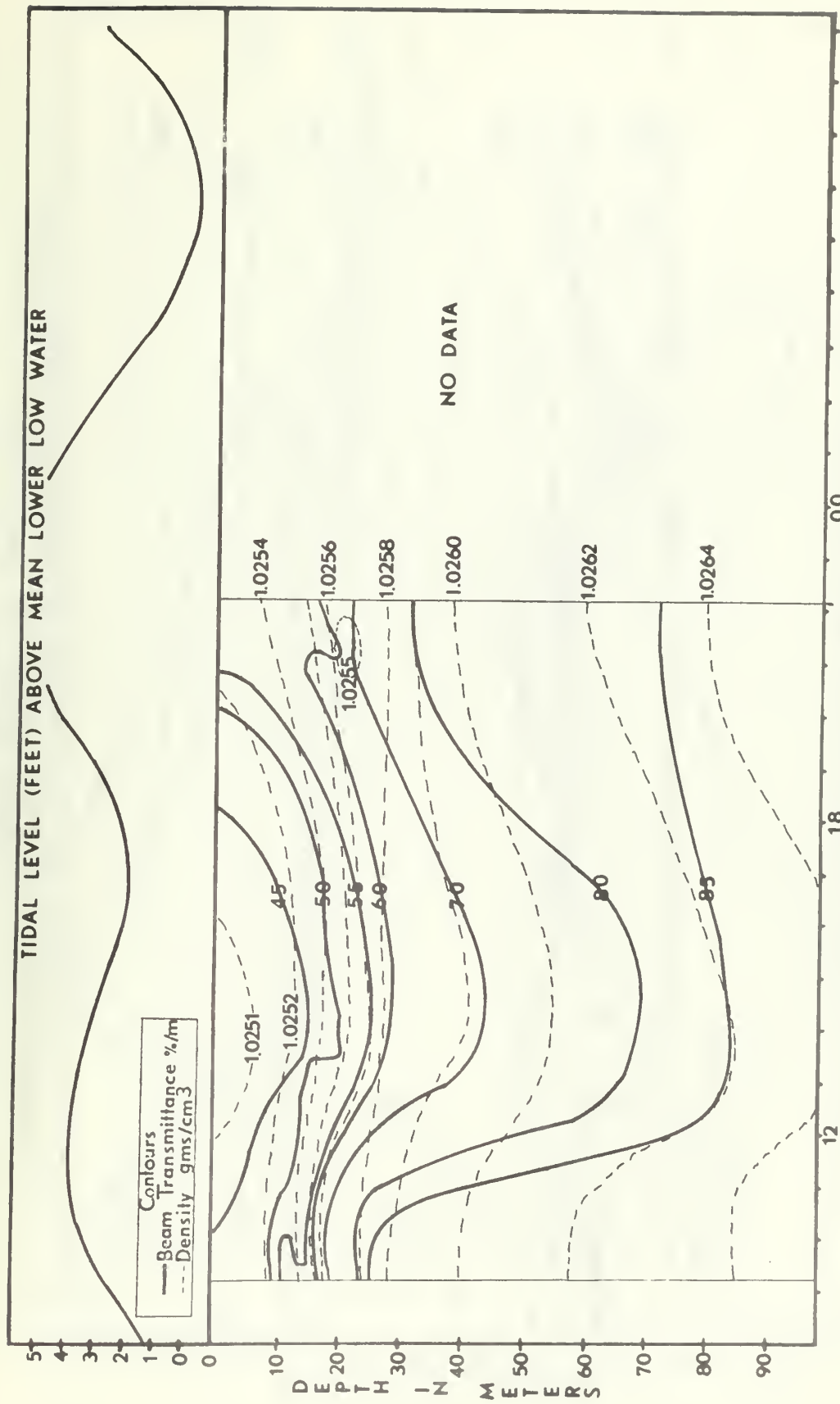


FIGURE 36



TIME-DEPTH CONTOURS OF BEAM TRANSMITTANCE IN RELATION TO DENSITY
 STATION DELTA 23 AUGUST 1968
 FIGURE 37

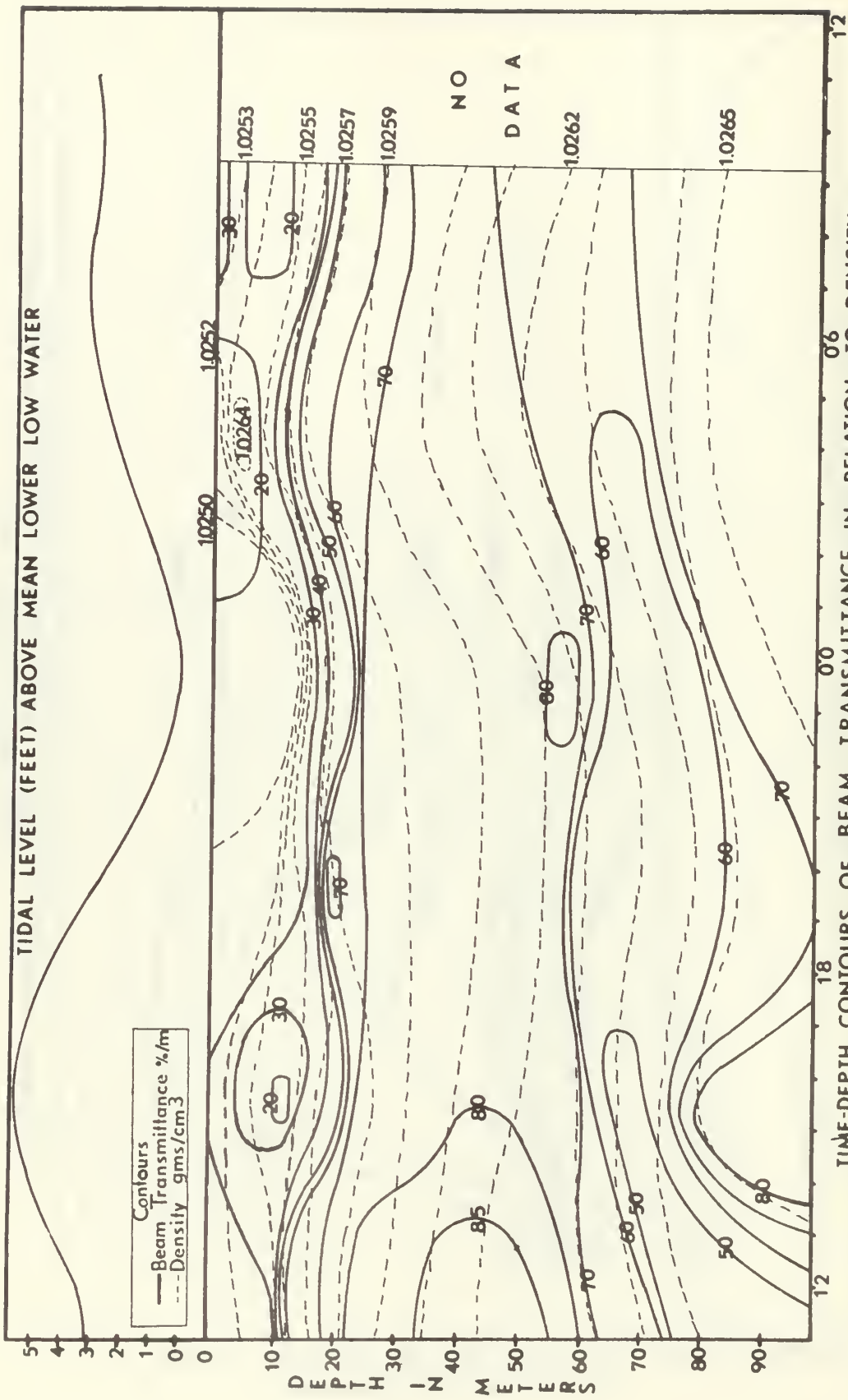


FIGURE 38

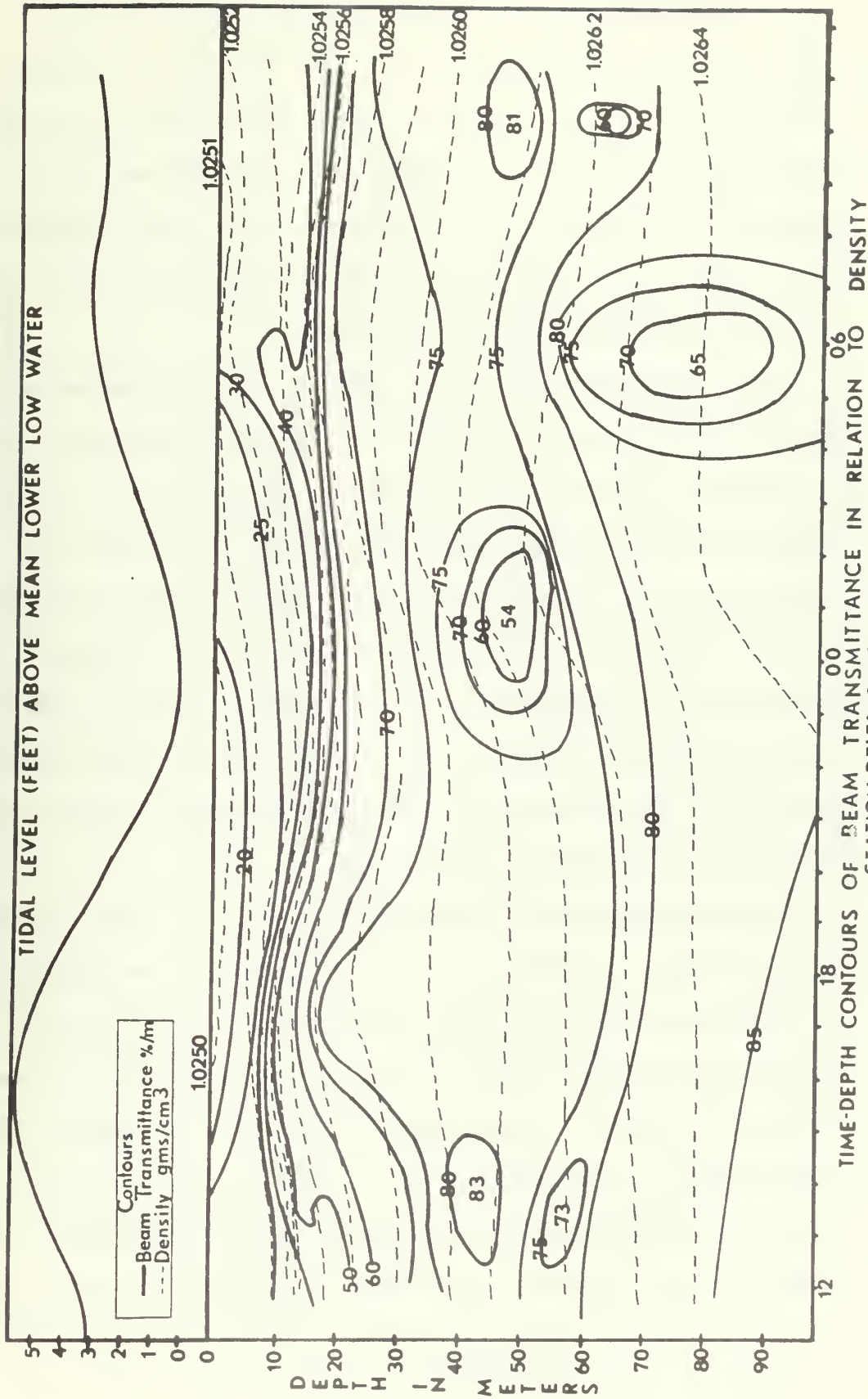


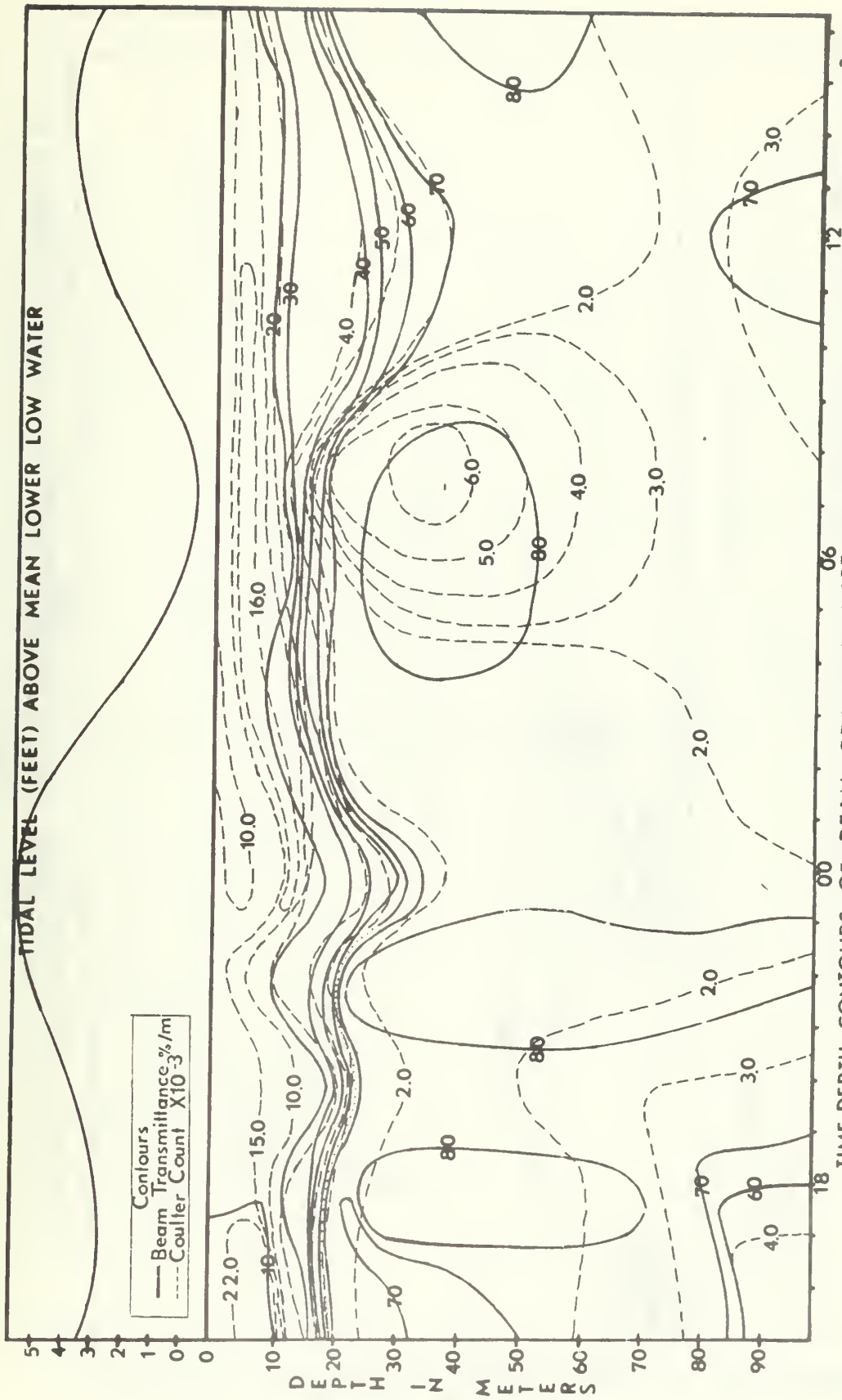
FIGURE 39

4.7 The Correlation of Particulate Matter with Beam Transmittance

An excellent correlation was found to exist between beam transmittance and particulate matter less than 100 μ in diameter (Figs. 40 through 43). Isolines of particulate count vary from smooth undulating contours to random and patchy concentrations. Beam transmittance readings were lowest in the first 8 to 12 m while particle count was highest in this region (Appendix V, Table 2). The larger particles were found closer to the surface.

Beam transmittance values at the surface showed marked variations during the four cruises, ranging from less than 20 percent to a high of 65 percent. These variations were accompanied by equally drastic changes in total particulate count at the surface. While currents, surface waves, and internal waves all have some effect on the distribution of particulate matter, it is evident that biological productivity, specifically of phytoplankton, is a significant factor in reducing light transmission. This was particularly apparent during Cruise 1, when all the surface readings of beam transmittance were less than 20 percent due to a plankton bloom.

Turbidity layers were present during Cruise 4 (Figs. 17 and 18). The upper layer coincides with the concentration of particulates in the thermocline (Fig. 43). The lower layer at station Bravo is perhaps the result of bottom material being placed into suspension by currents, although this does not explain the origin of the corresponding 60 m layer occurring in approximately 950 fathoms of water at station Delta (Fig. 18). Carsola and Dill (6) observed that transmissivity within a turbidity layer increases with distance from shore while layer depth



TIME-DEPTH CONTOURS OF BEAM TRANSMITTANCE IN RELATION TO COULTER COUNT X 10⁻³
 STATION BRAVO 26-27 JULY 1968
 FIGURE 40

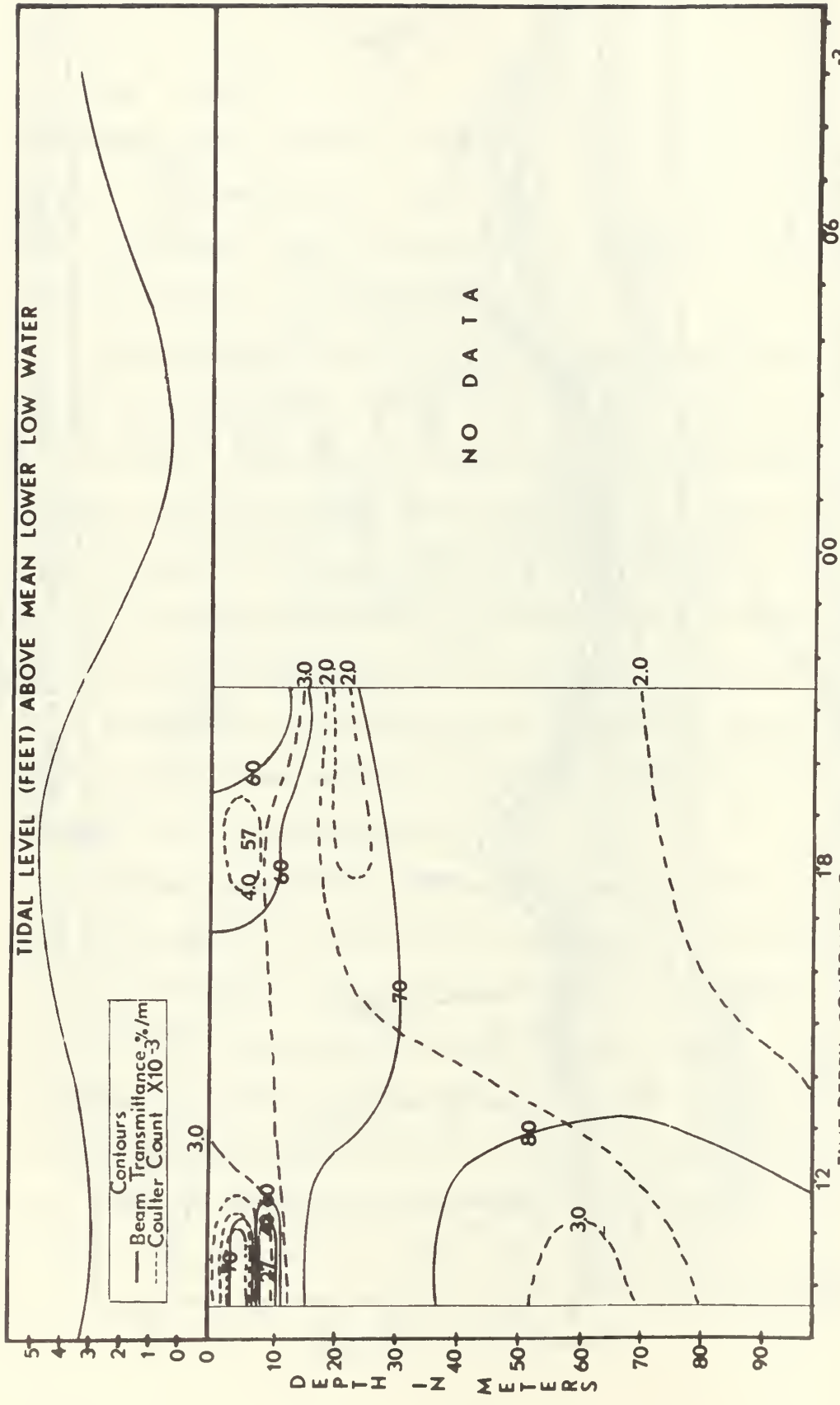


FIGURE 41

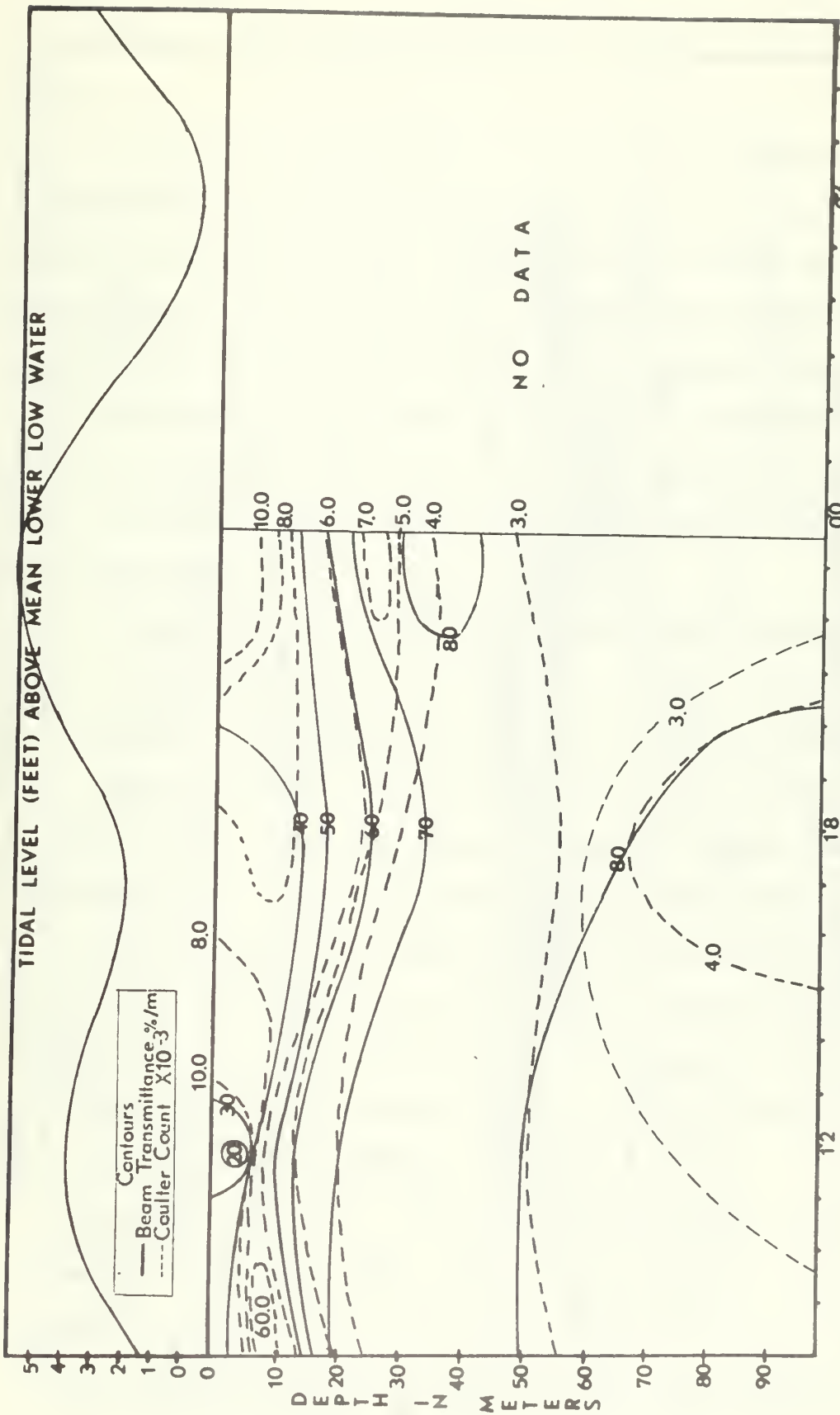
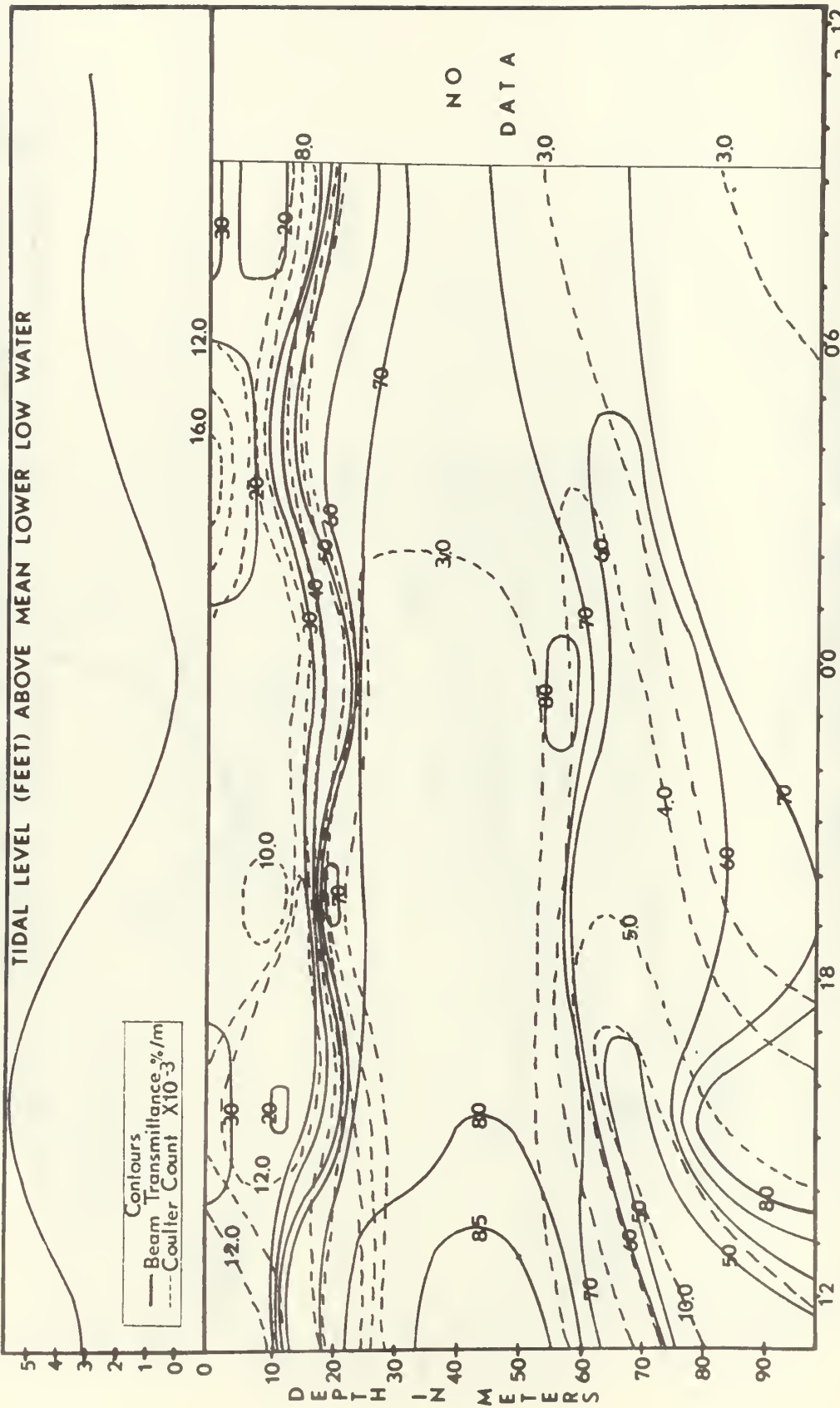


FIGURE 42



STATION BRAVO 30-31 AUGUST 1968
 FIGURE 43

decreases, indicating dilution of the turbidity layer by clear oceanic water. This observation is clearly verified in Figs. 17 and 18.

An attempt was made to identify and classify the different types of organisms found in each sample microscopically, but recognition of specific organisms was difficult except for chain diatoms, specifically Chaetoceros sp., as seen in Fig. 65. This particular species of phytoplankton dominated the samples taken in the upper few meters of water during the first cruise. Figure 65 is not representative of the true particle distribution, since small particles do not appear due to inadequate lighting and the very shallow depth of field for micro-photographs.

A comparison was made between the relative-size distribution histogram for the mixture of 6 to 14 μ latex spheres (Fig. 66) discussed in section 2.2 and individual relative-size distribution histograms for each sample (not shown). An average diameter of 7.22 μ and standard deviation of 2.37 μ were measured by Dow Chemical Company, Midland, Michigan. From Fig. 66, it is seen that the threshold settings corresponding to the mean diameter and one standard deviation to the right of the mean diameter are 17.16 and 31.68, respectively. These results indicate that the particulates corresponding to approximately 68 percent of the total counts are less than 10 μ in diameter, while approximately 96 percent are less than 13 μ .

As noted in section 4.6, the greatest change in transparency occurs in the pycnocline/thermocline. This is also the region where particulate concentrations change the most, since fine detritus and nearly neutrally-buoyant plankton are retarded from further sinking by the presence of

a denser layer beneath the pycnocline. This distribution, however, is easily upset by surface or subsurface turbulence which accounts for some of the radical changes in beam transmittance profiles to be observed in Figs. 44 through 62. Scatter plots of percentage beam transmittance versus particulate count in thousands were made for Coulter threshold settings of 0, 10, 20, and 30. The beam transmittance and particulate count data were then fitted linearly using the least square method (Figs. 63 and 64). The following parameters were determined:

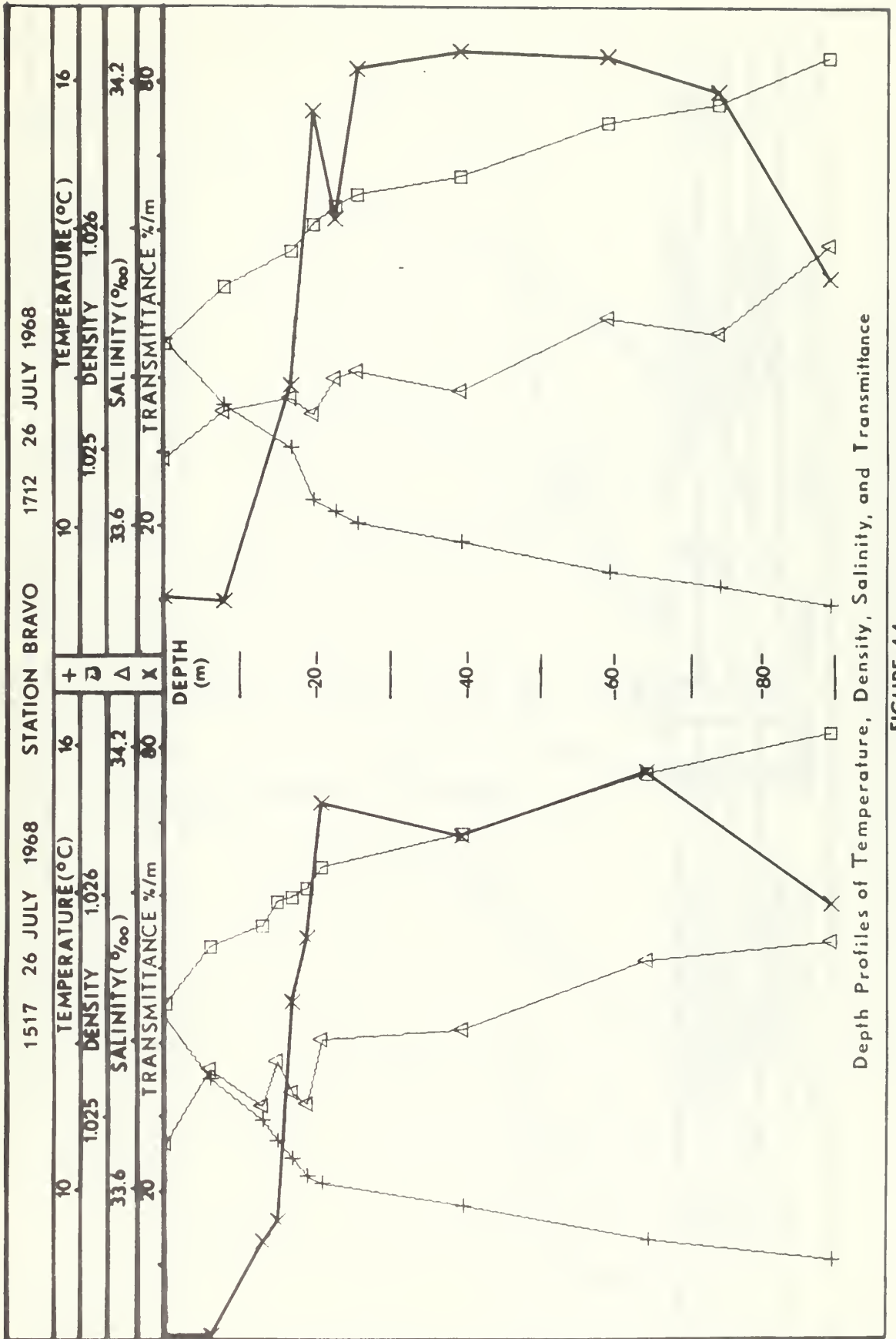
<u>COULTER THRESHOLD</u>	<u>EQUATION</u>	<u>STANDARD DEVIATION</u>
0	$Y = -.156X + 14.49$	2.54
10	$Y = -.088X + 7.34$	1.28
20	$Y = -.058X + 4.74$	0.86
30	$Y = -.042X + 3.42$	0.68

Y = Count in Thousands, X = Transmittance (%/m)

4.8 The Correlation of Lunar Period with Beam Transmittance

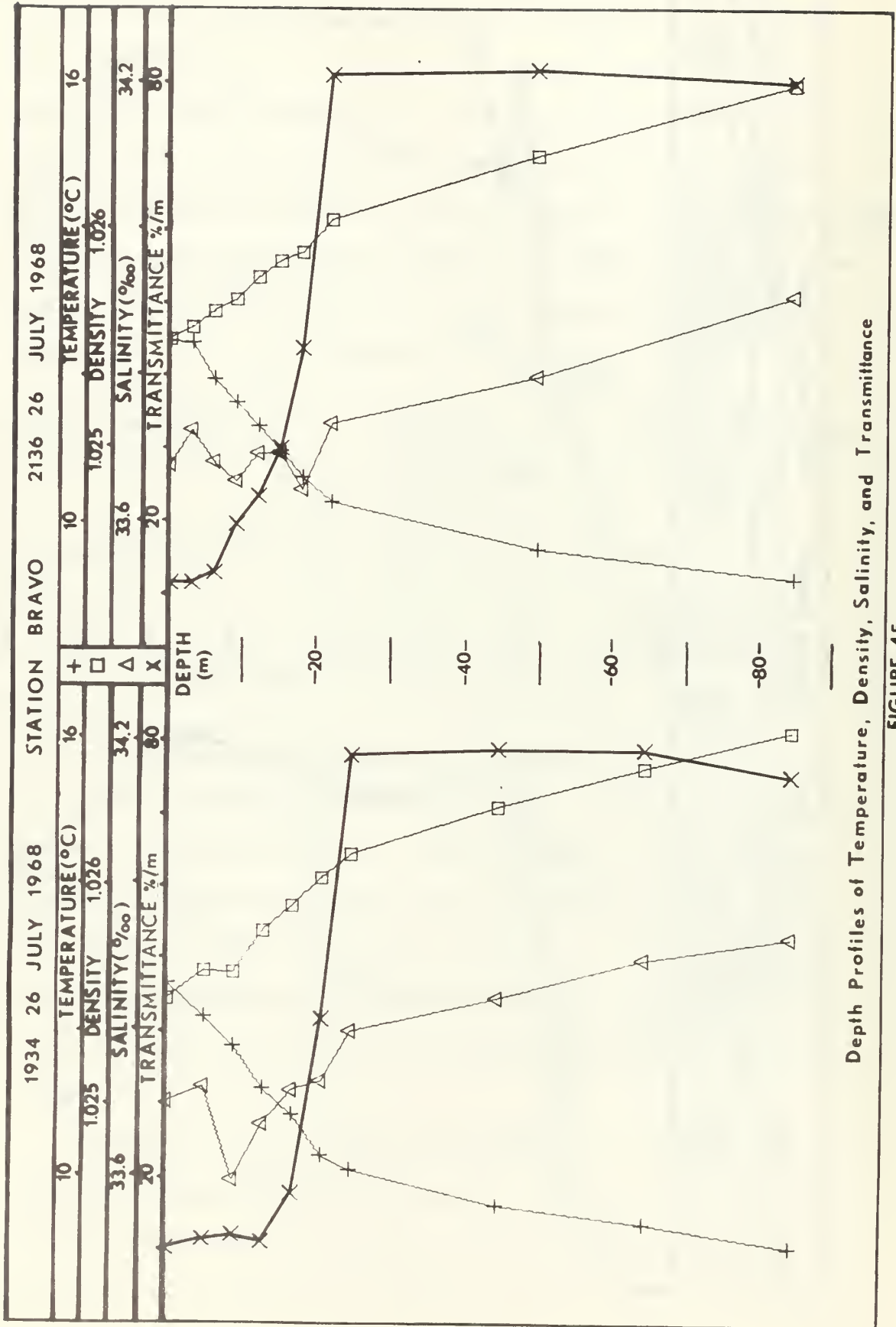
The time relation between lunar phases and sampling periods is shown in Appendix V, Table 3. Although cruises were initially planned to coincide with lunar phases, scheduling difficulties prevented an exact correspondence. The mean times for Cruises 1 and 2 were approximately 47 hours and 44 hours later than their respective lunar phases, whereas Cruises 3 and 4 were nearly coincident.

Figures 13, 14, 17, and 18, corresponding to quarter phases of the moon, show the presence of turbidity layers. Tidal ranges for Cruises 2 and 4 were 4.2 ft and 5.4 ft, respectively.



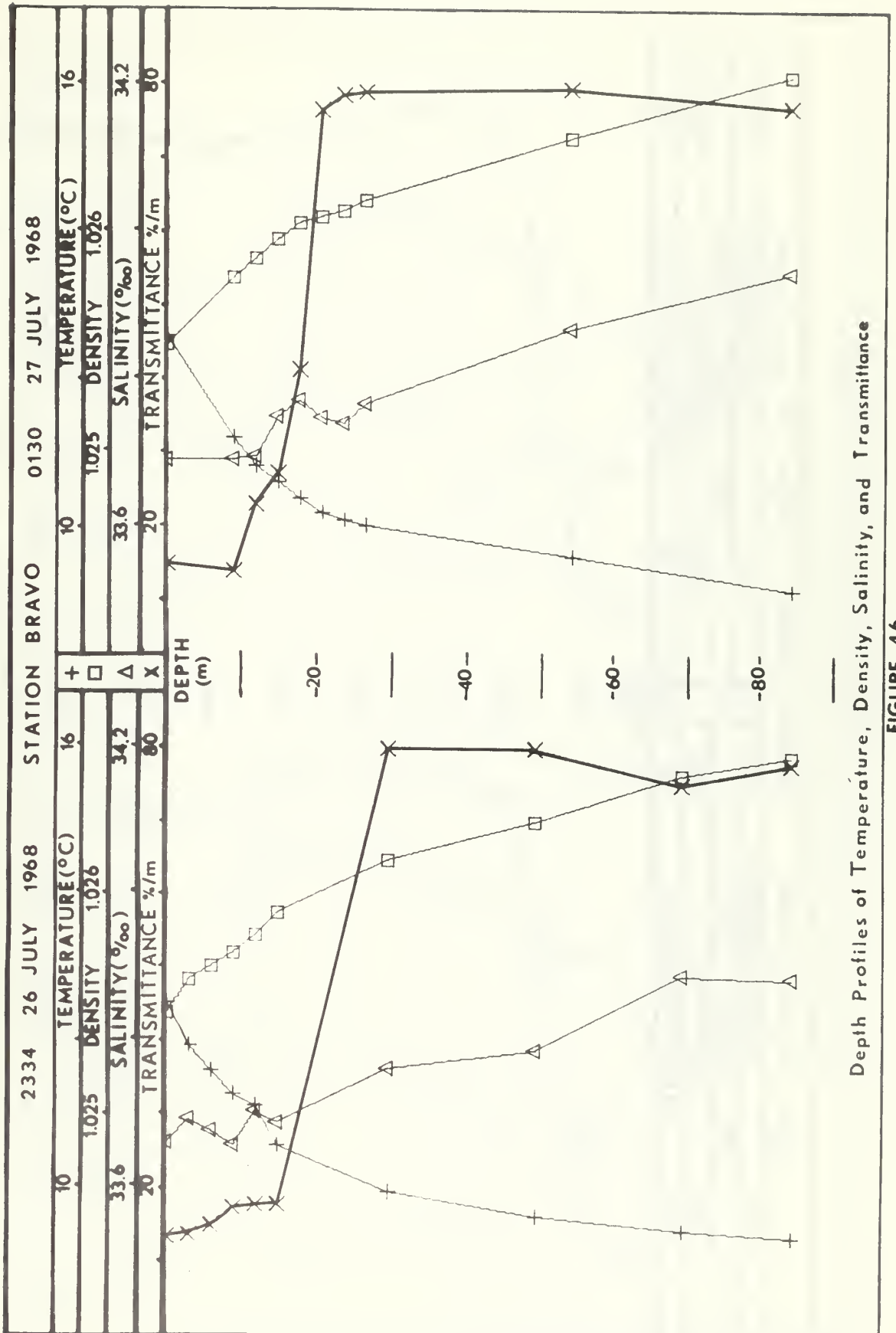
Depth Profiles of Temperature, Density, Salinity, and Transmittance

FIGURE 44

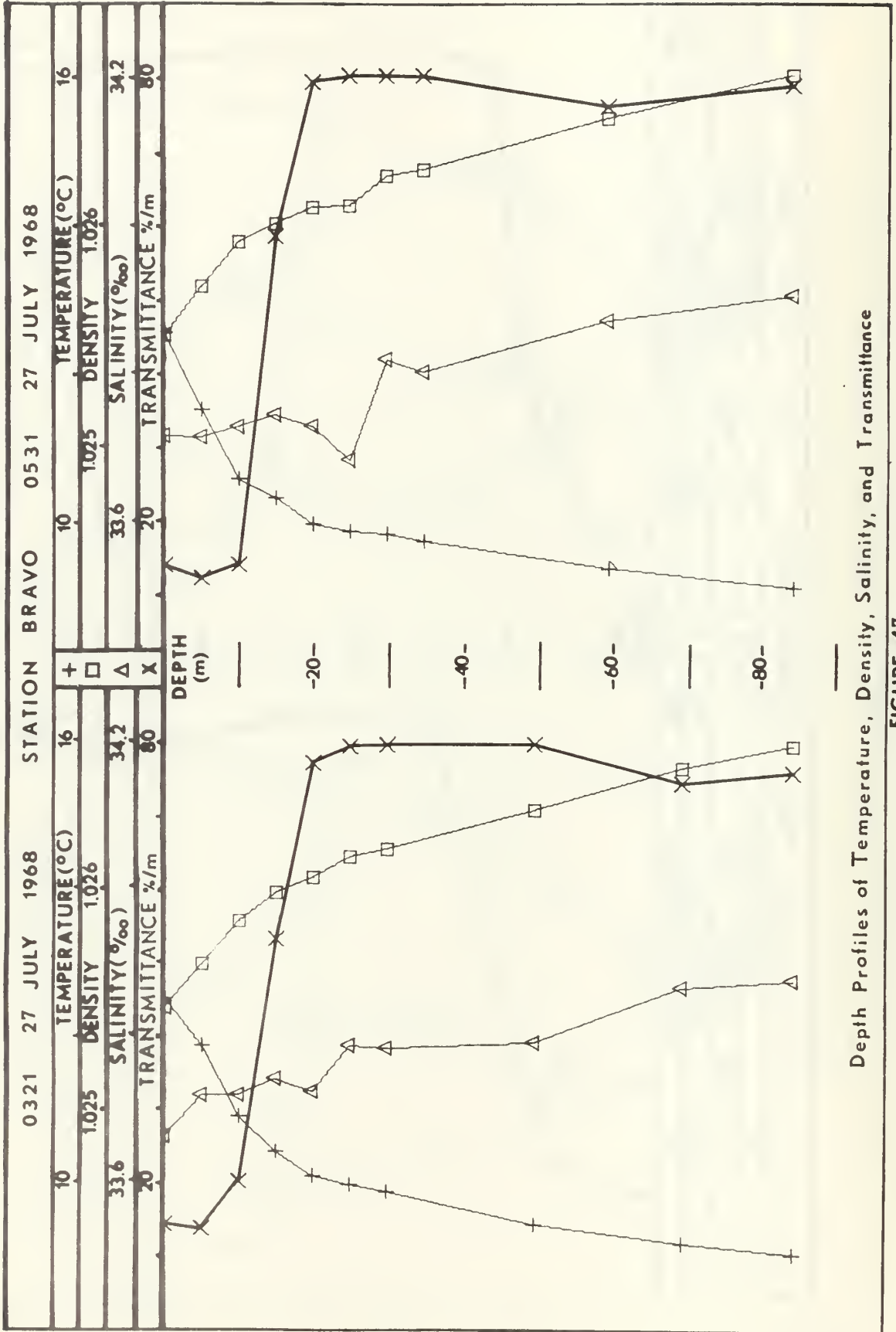


Depth Profiles of Temperature, Density, Salinity, and Transmittance

FIGURE 45

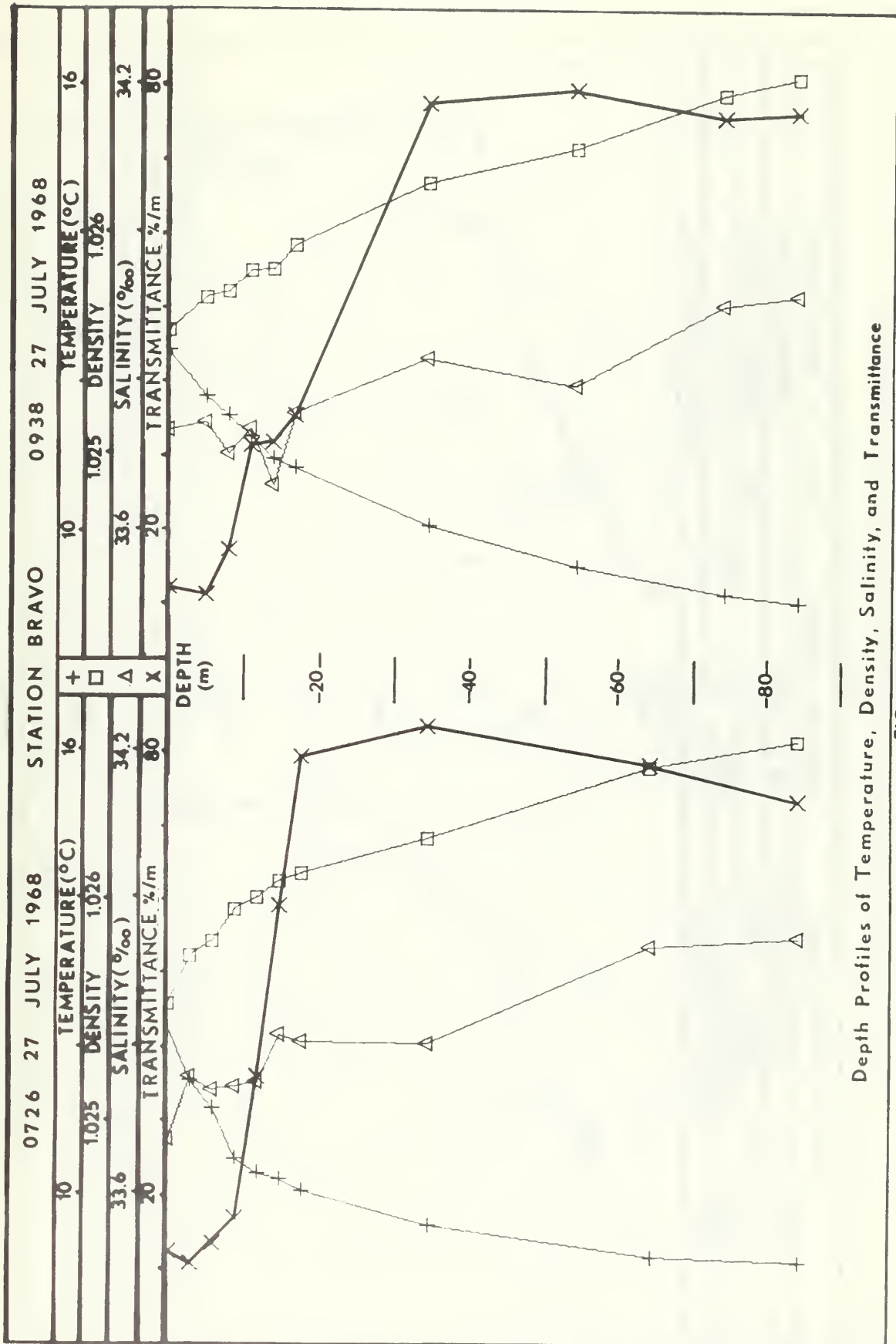


Depth Profiles of Temperature, Density, Salinity, and Transmittance
FIGURE 46



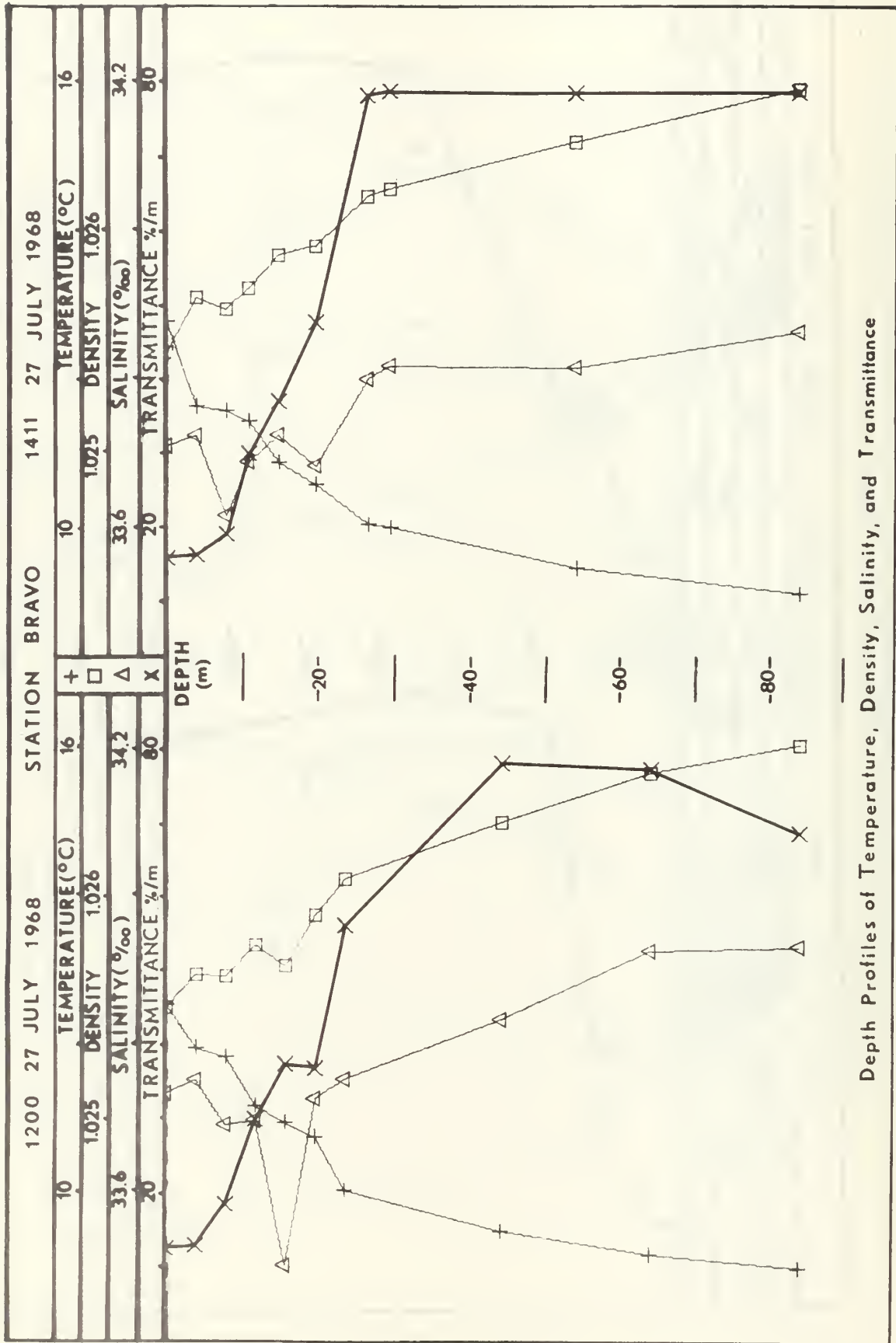
Depth Profiles of Temperature, Density, Salinity, and Transmittance

FIGURE 47



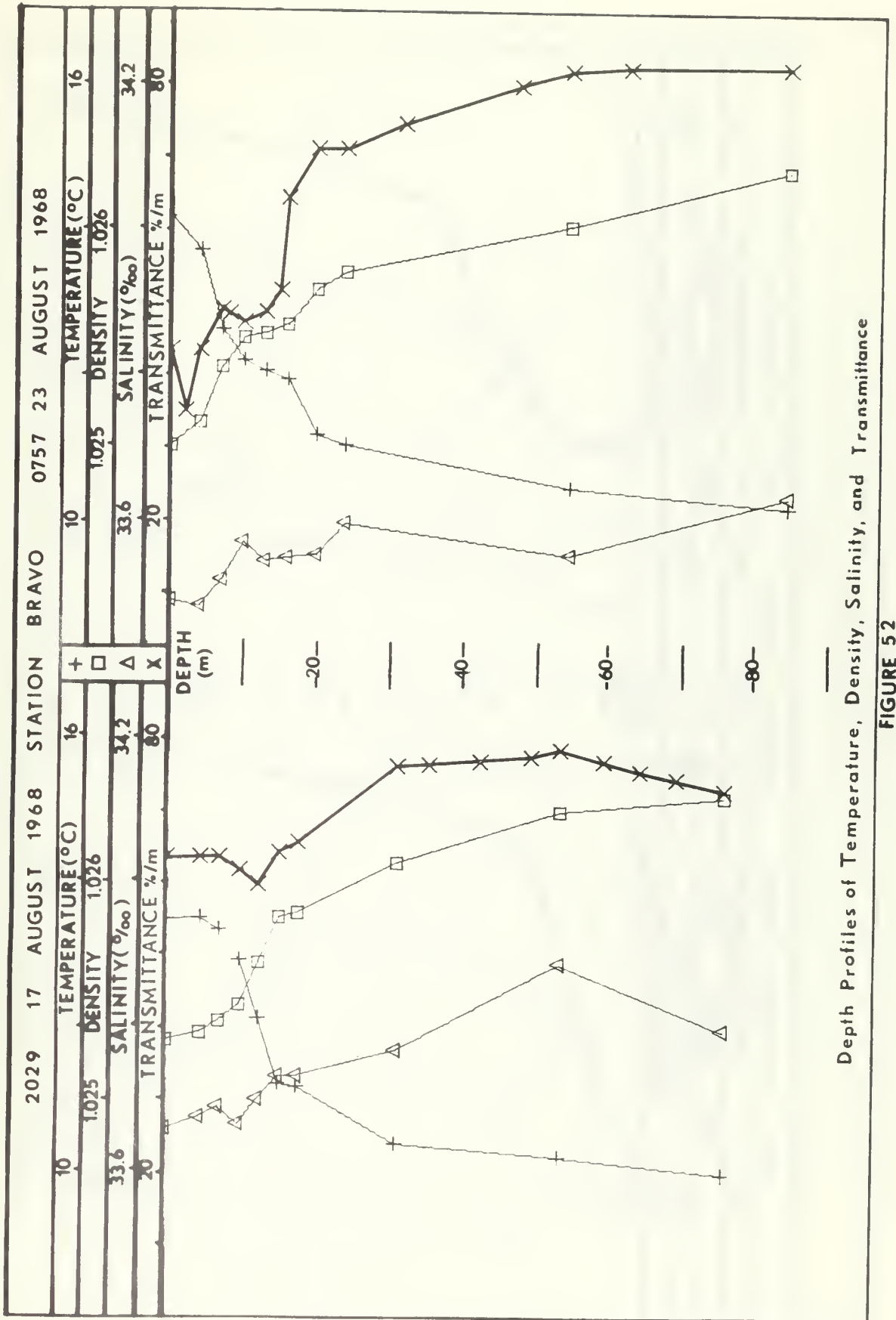
Depth Profiles of Temperature, Density, Salinity, and Transmittance

FIGURE 48



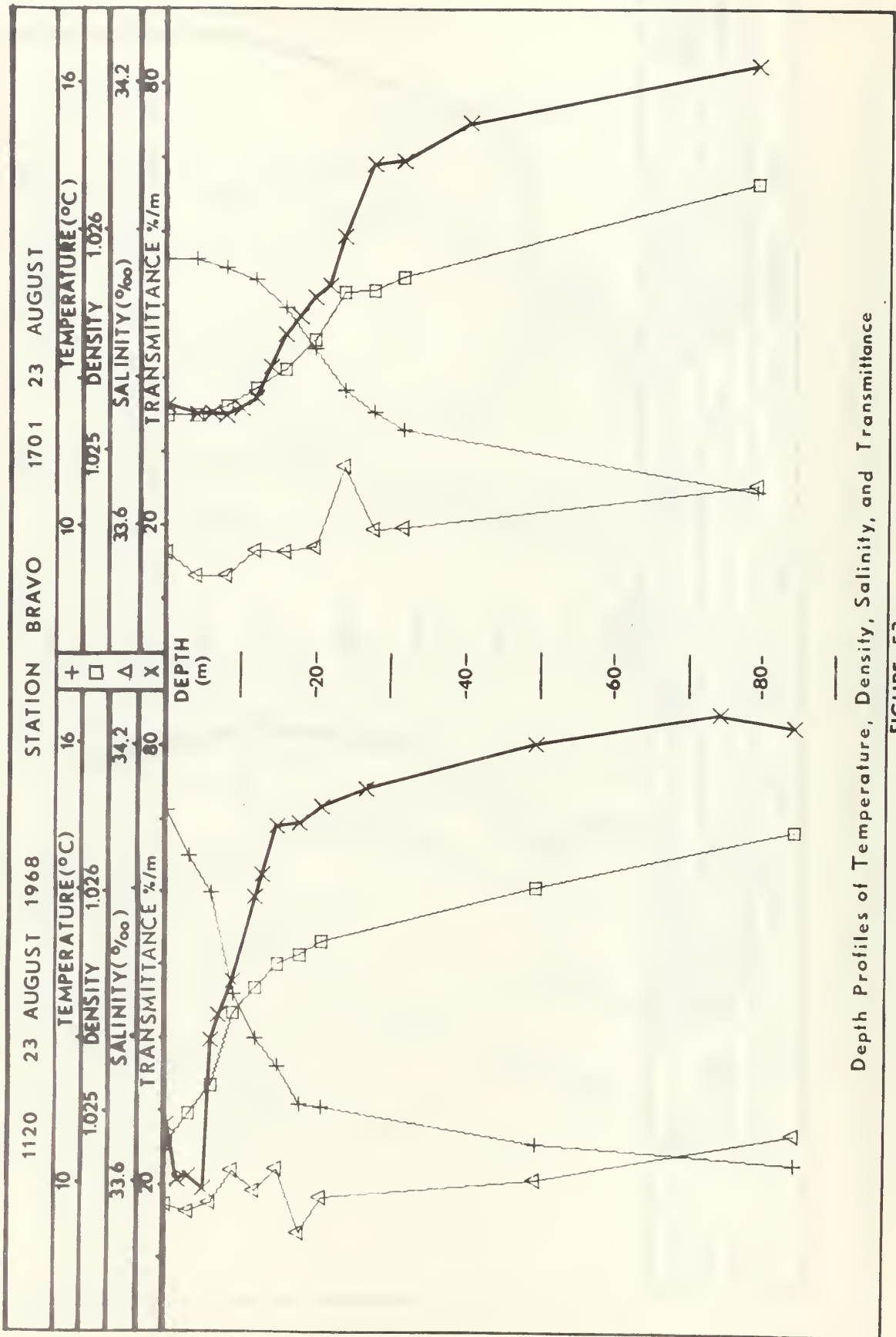
Depth Profiles of Temperature, Density, Salinity, and Transmittance

FIGURE 49

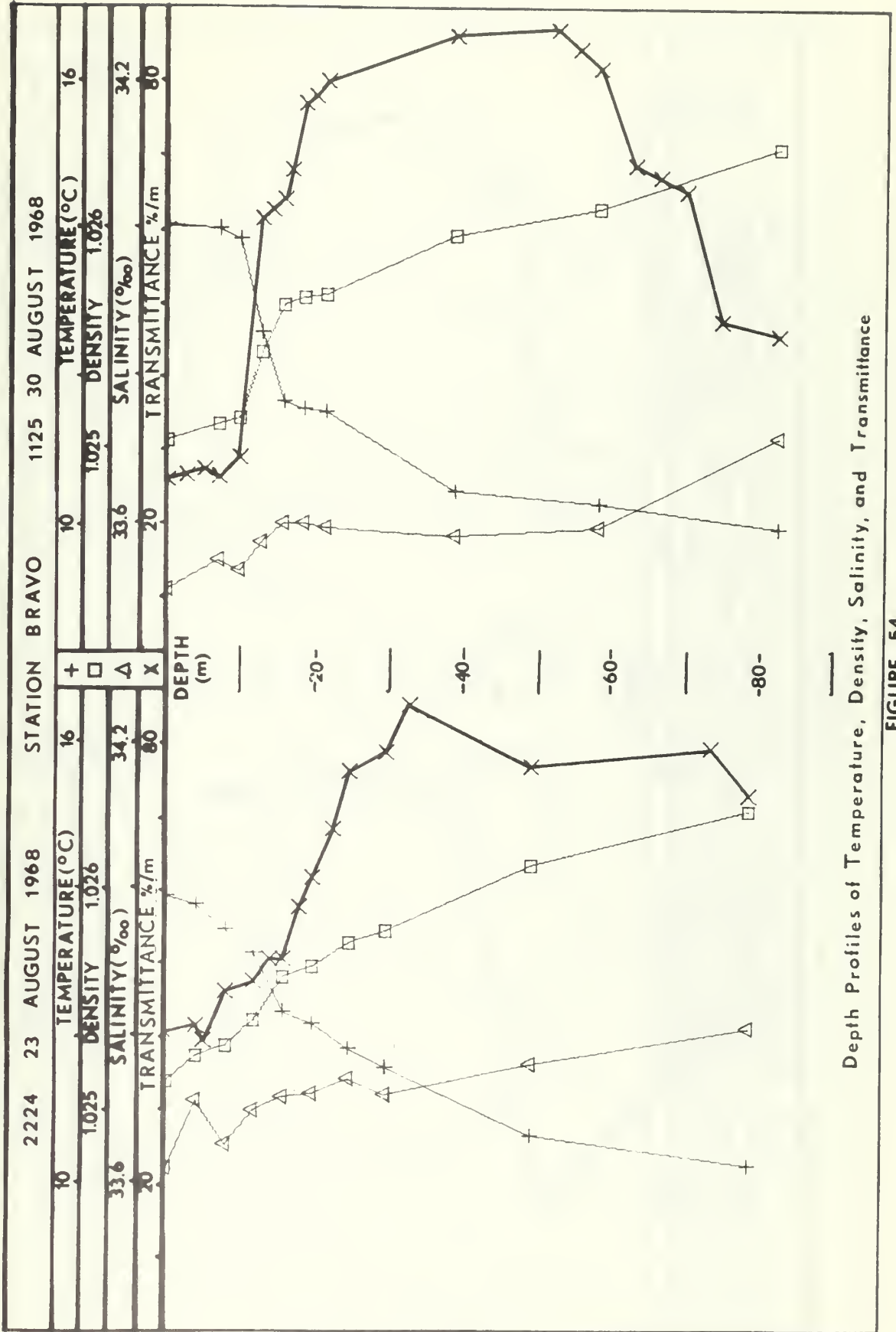


Depth Profiles of Temperature, Density, Salinity, and Transmittance

FIGURE 52

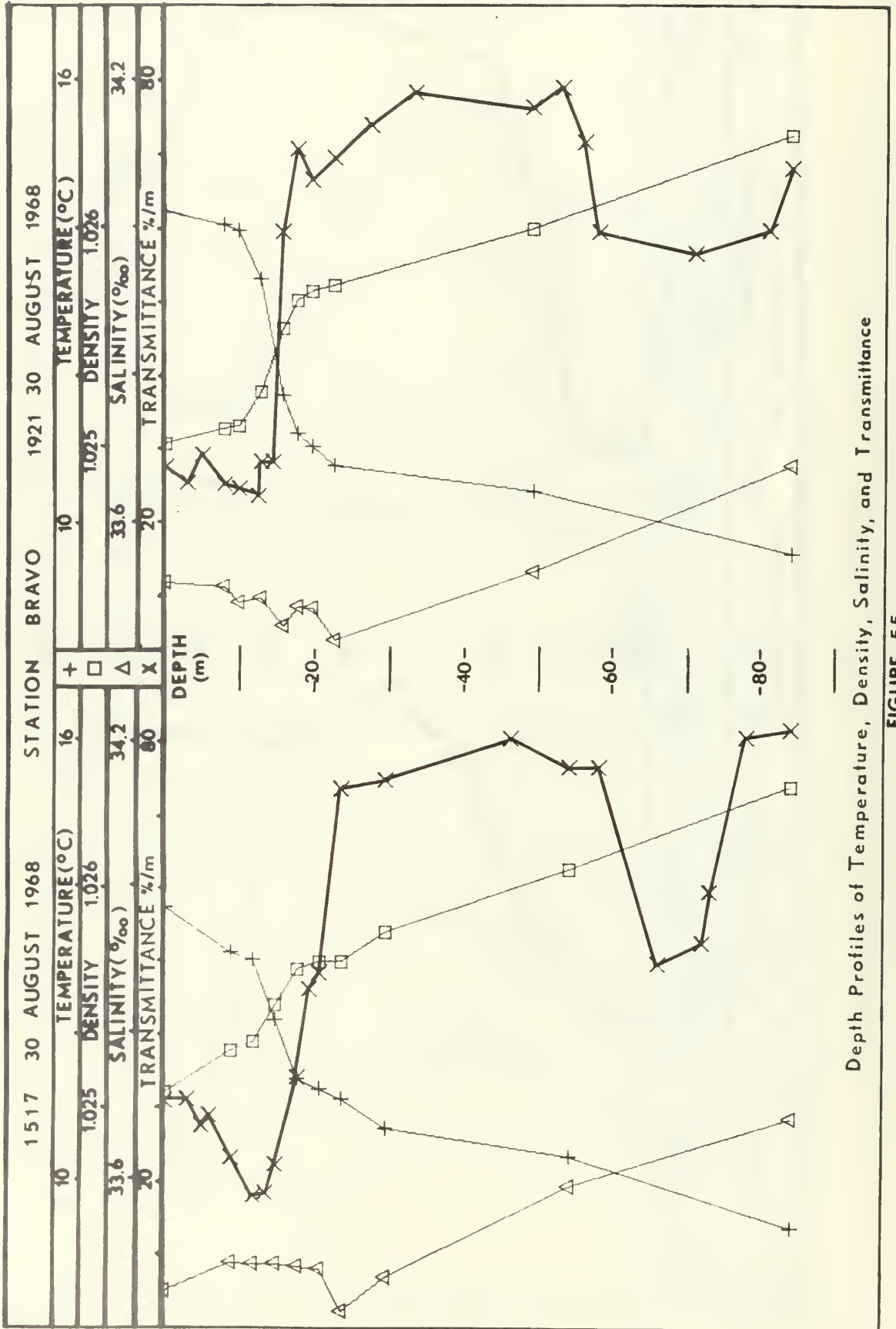


Depth Profiles of Temperature, Density, Salinity, and Transmittance
FIGURE 53



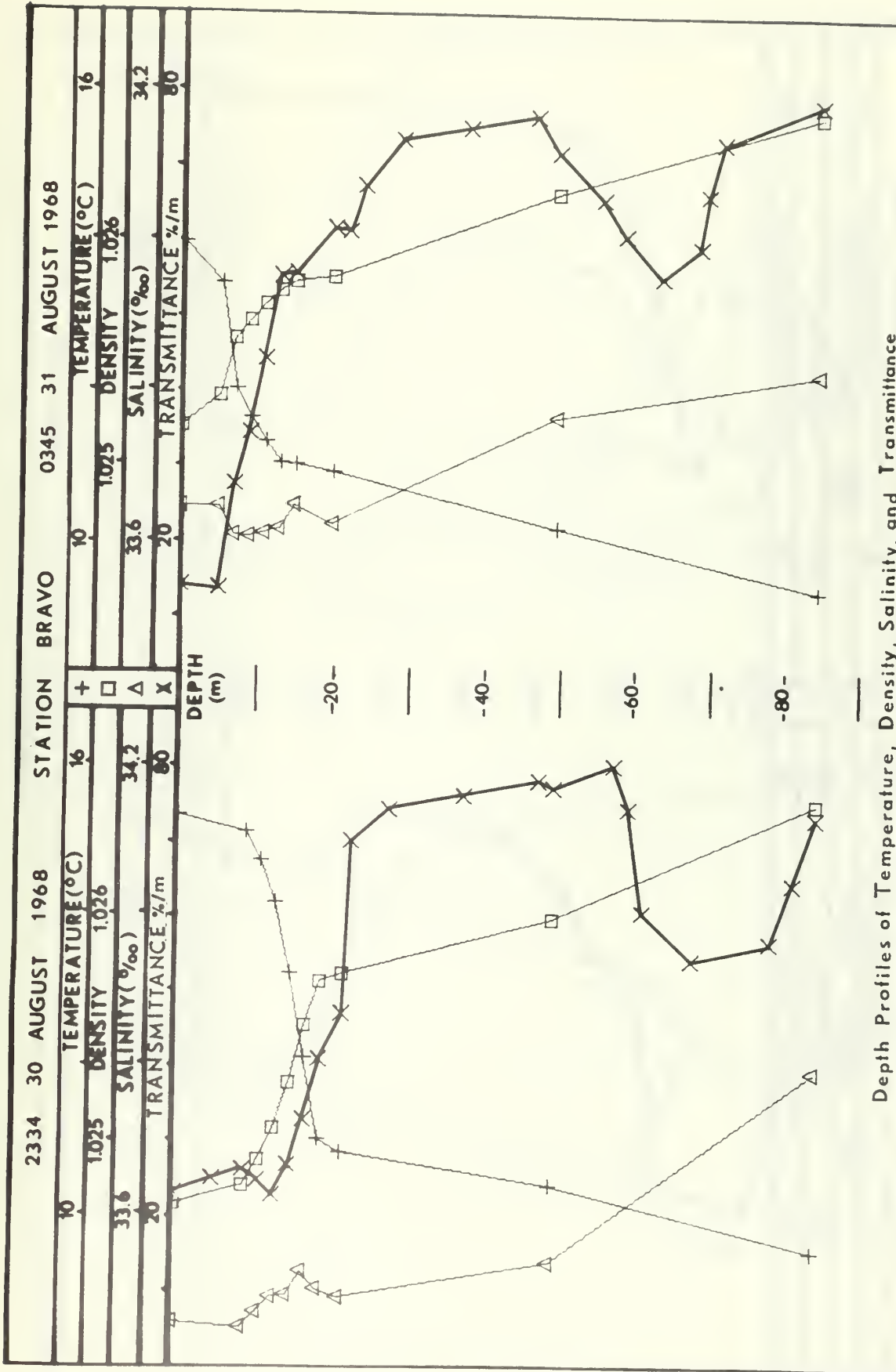
Depth Profiles of Temperature, Density, Salinity, and Transmittance

FIGURE 54



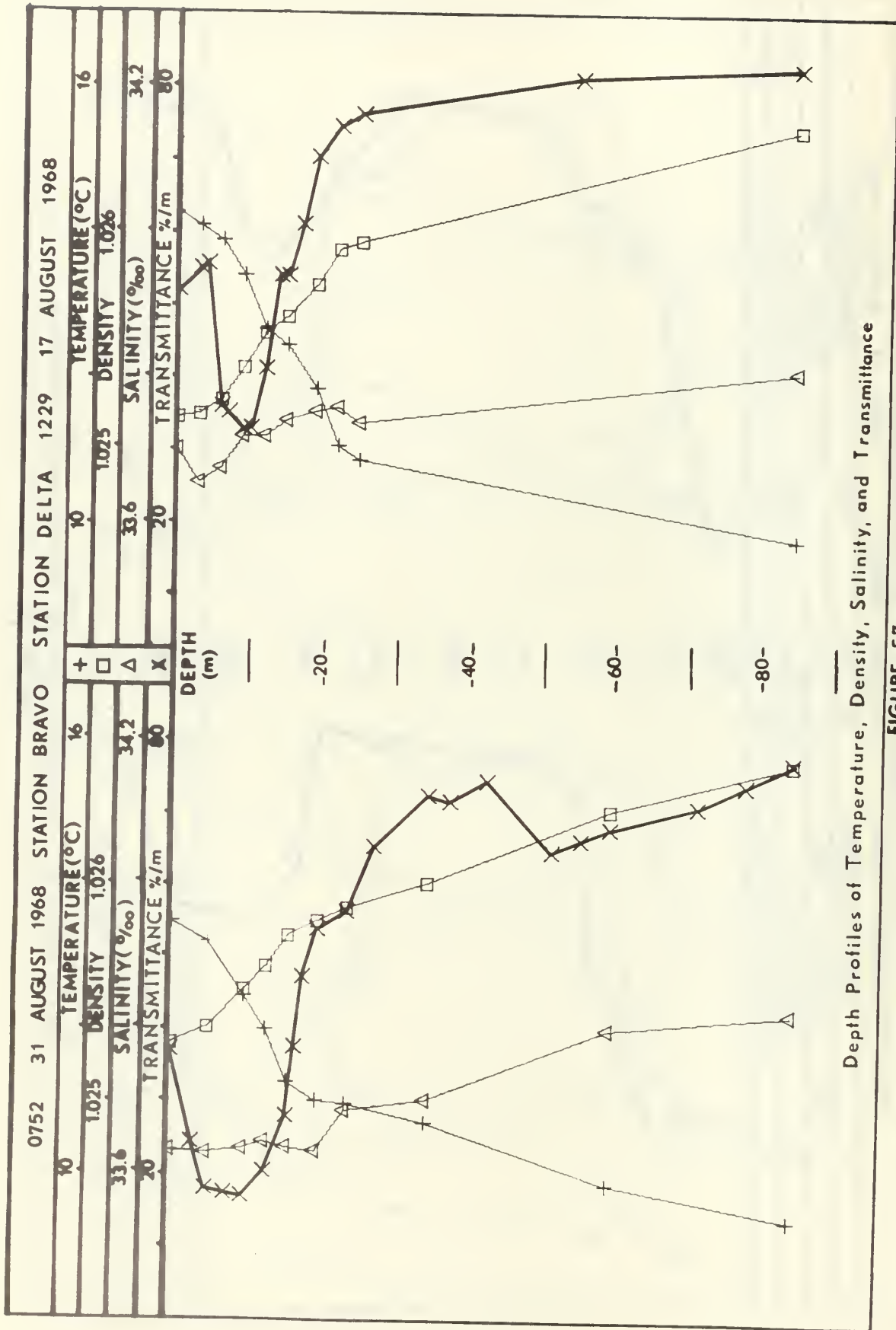
Depth Profiles of Temperature, Density, Salinity, and Transmittance

FIGURE 55



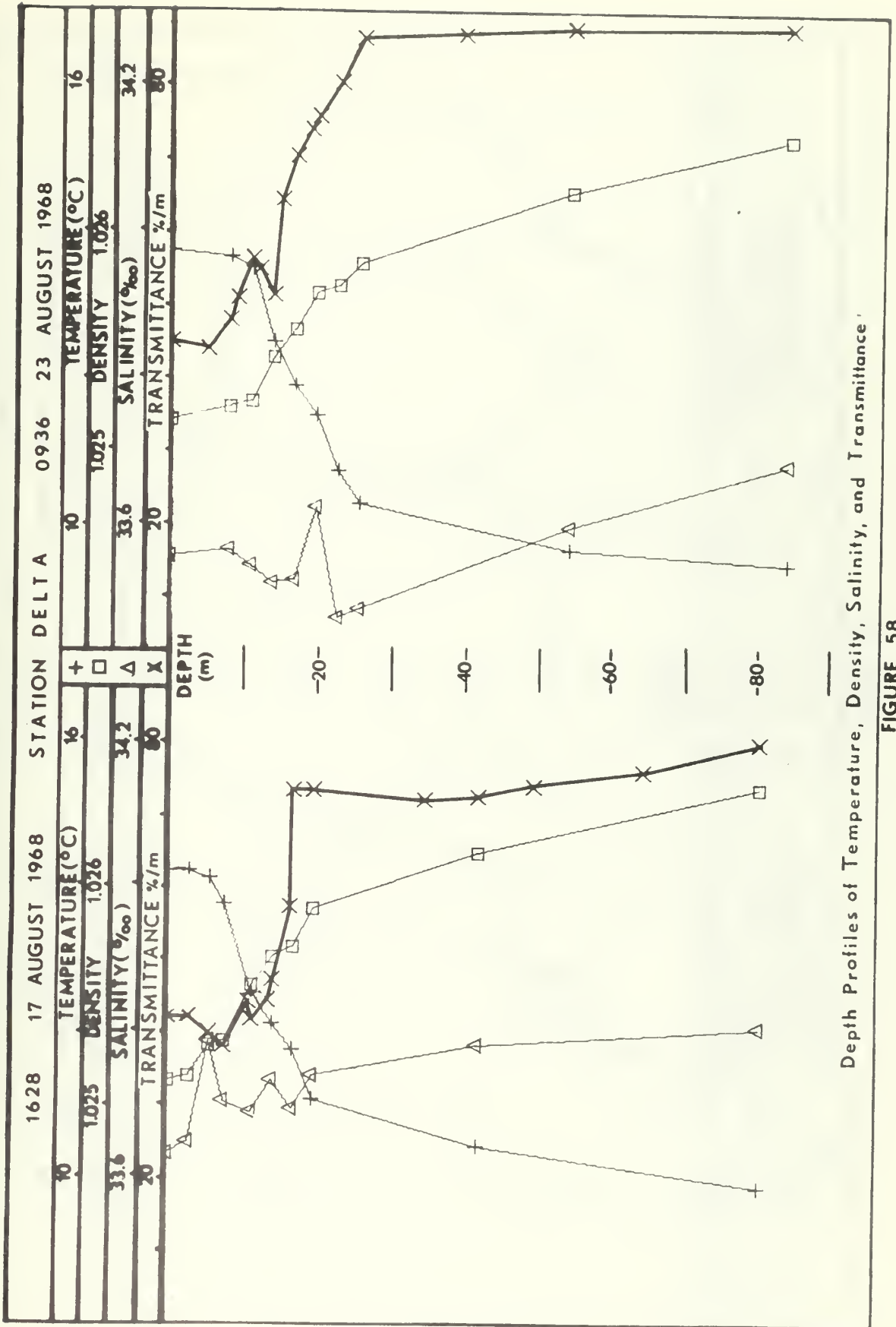
Depth Profiles of Temperature, Density, Salinity, and Transmittance

FIGURE 56



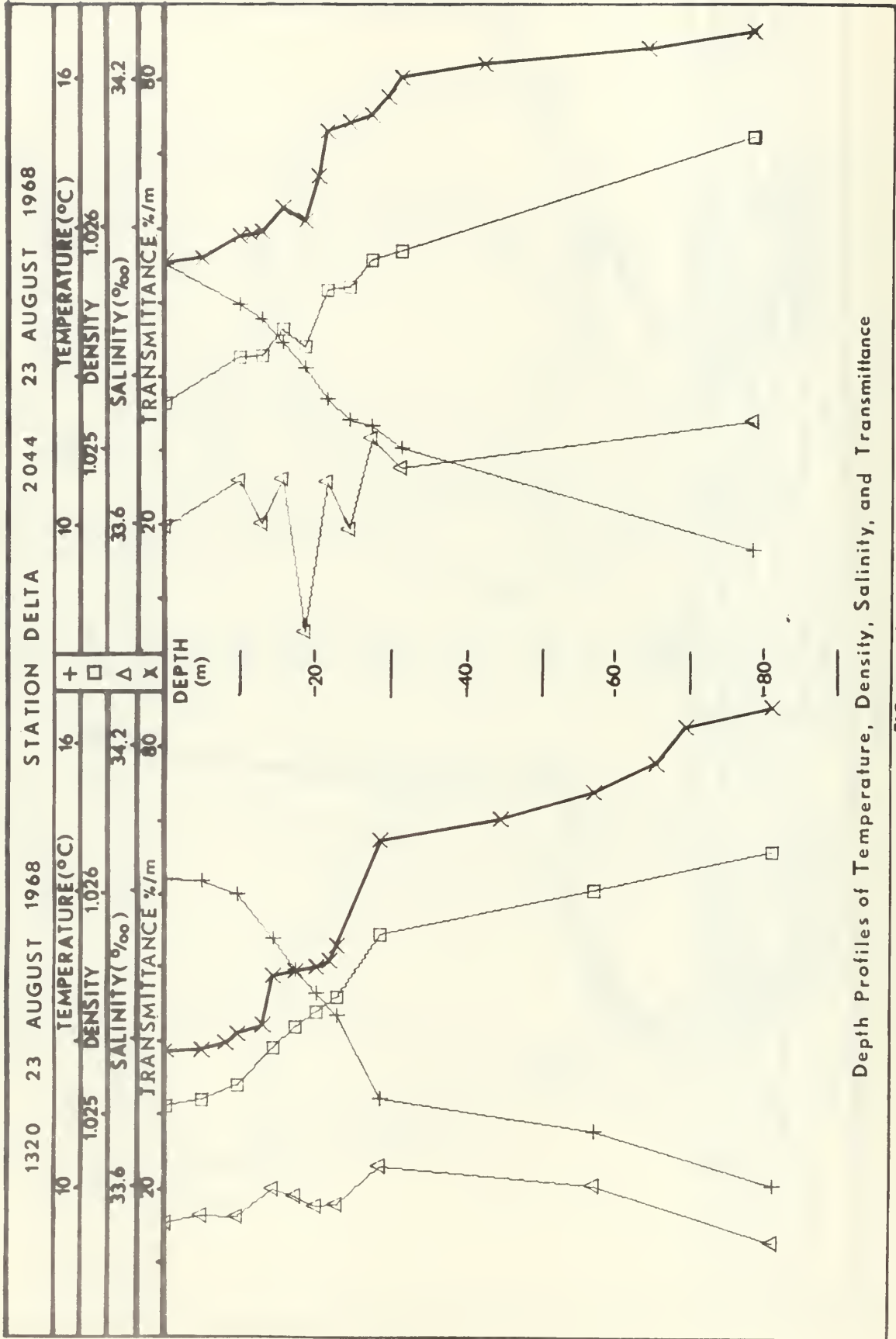
Depth Profiles of Temperature, Density, Salinity, and Transmittance

FIGURE 57



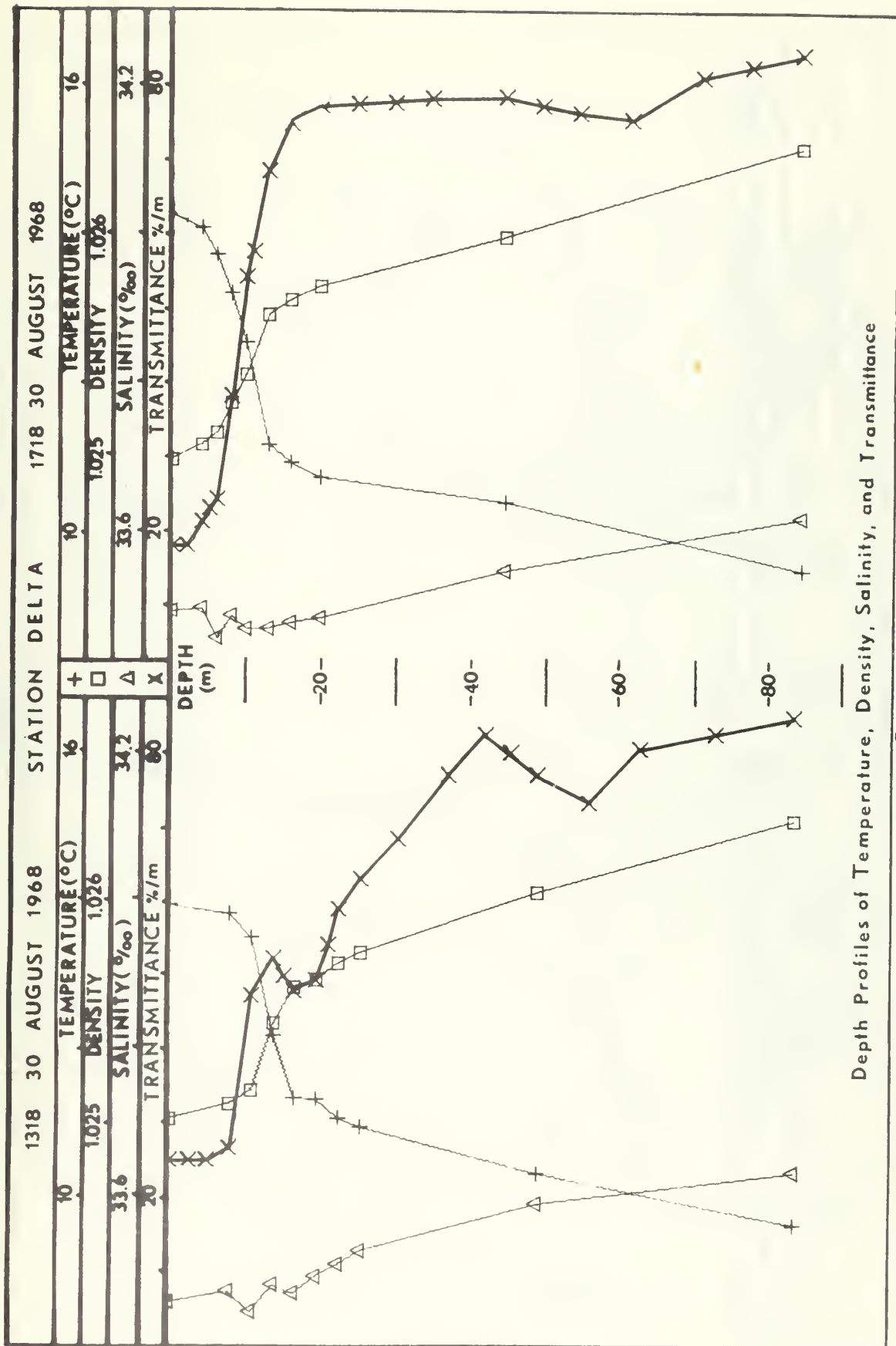
Depth Profiles of Temperature, Density, Salinity, and Transmittance

FIGURE 58



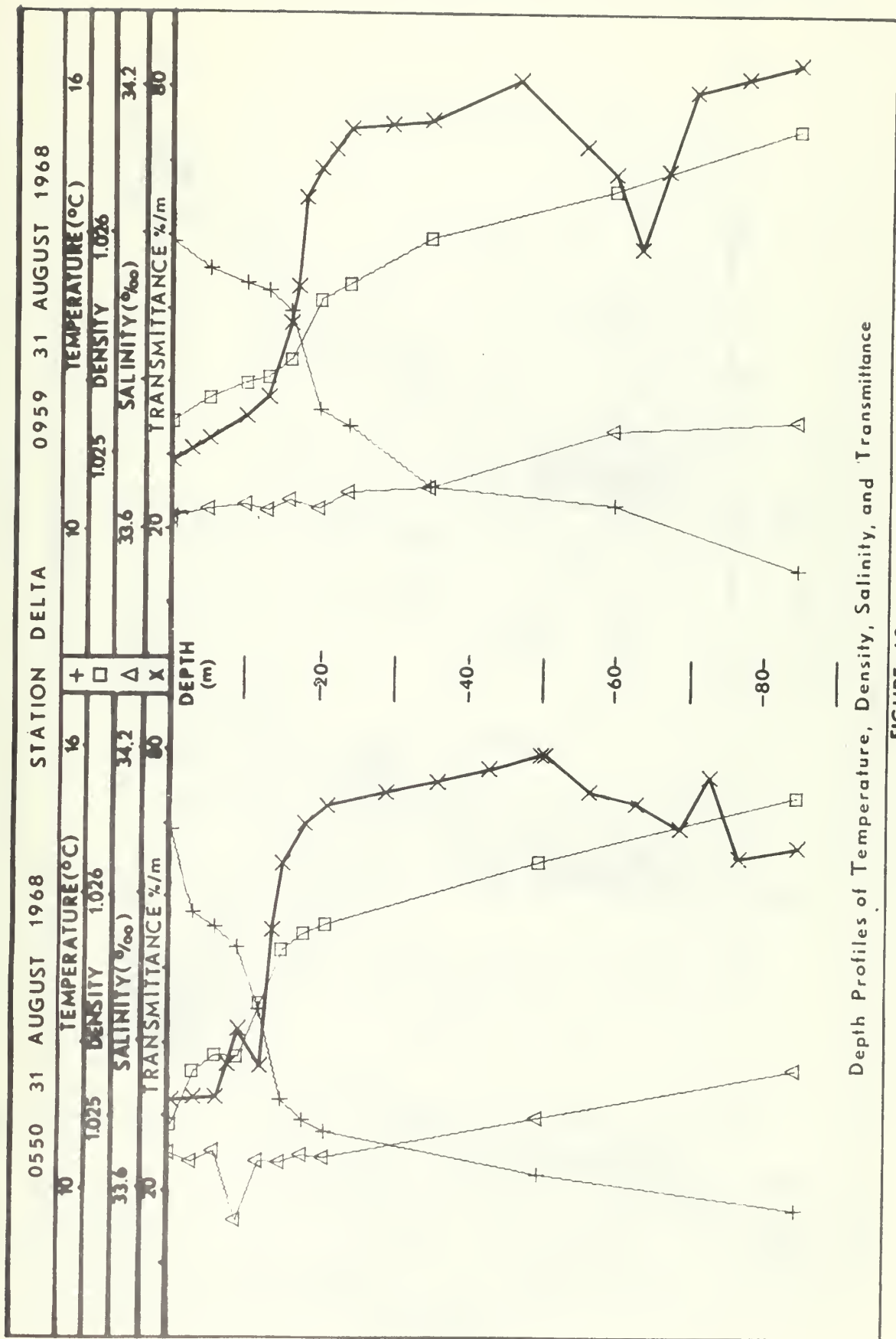
Depth Profiles of Temperature, Density, Salinity, and Transmittance

FIGURE 59



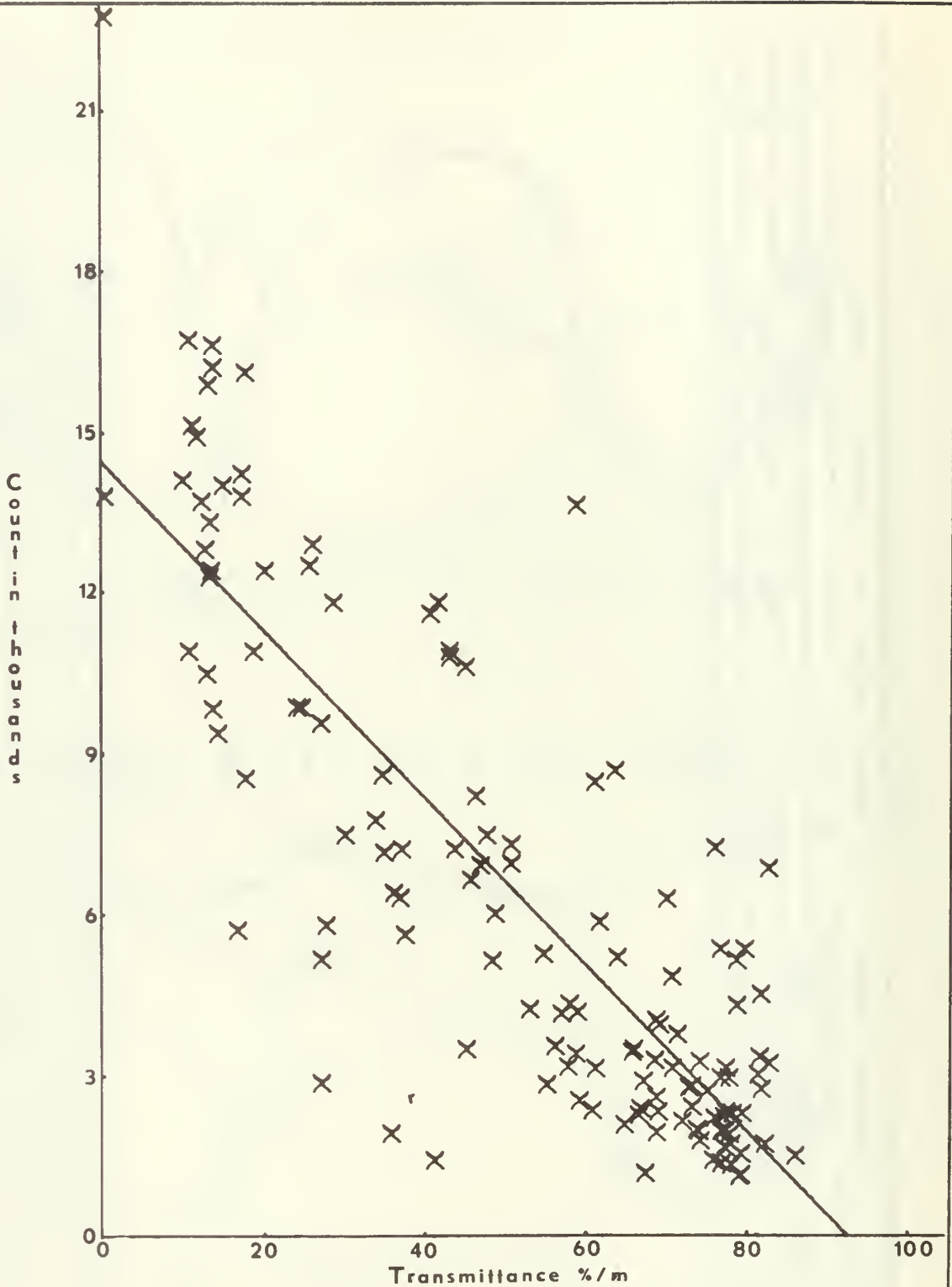
Depth Profiles of Temperature, Density, Salinity, and Transmittance

FIGURE 60



Depth Profiles of Temperature, Density, Salinity, and Transmittance

FIGURE 62



LINEAR LEAST-SQUARES FIT FOR
 BEAM TRANSMITTANCE VS. PARTICLE
 COUNT AT THRESHOLD 0

FIGURE 63

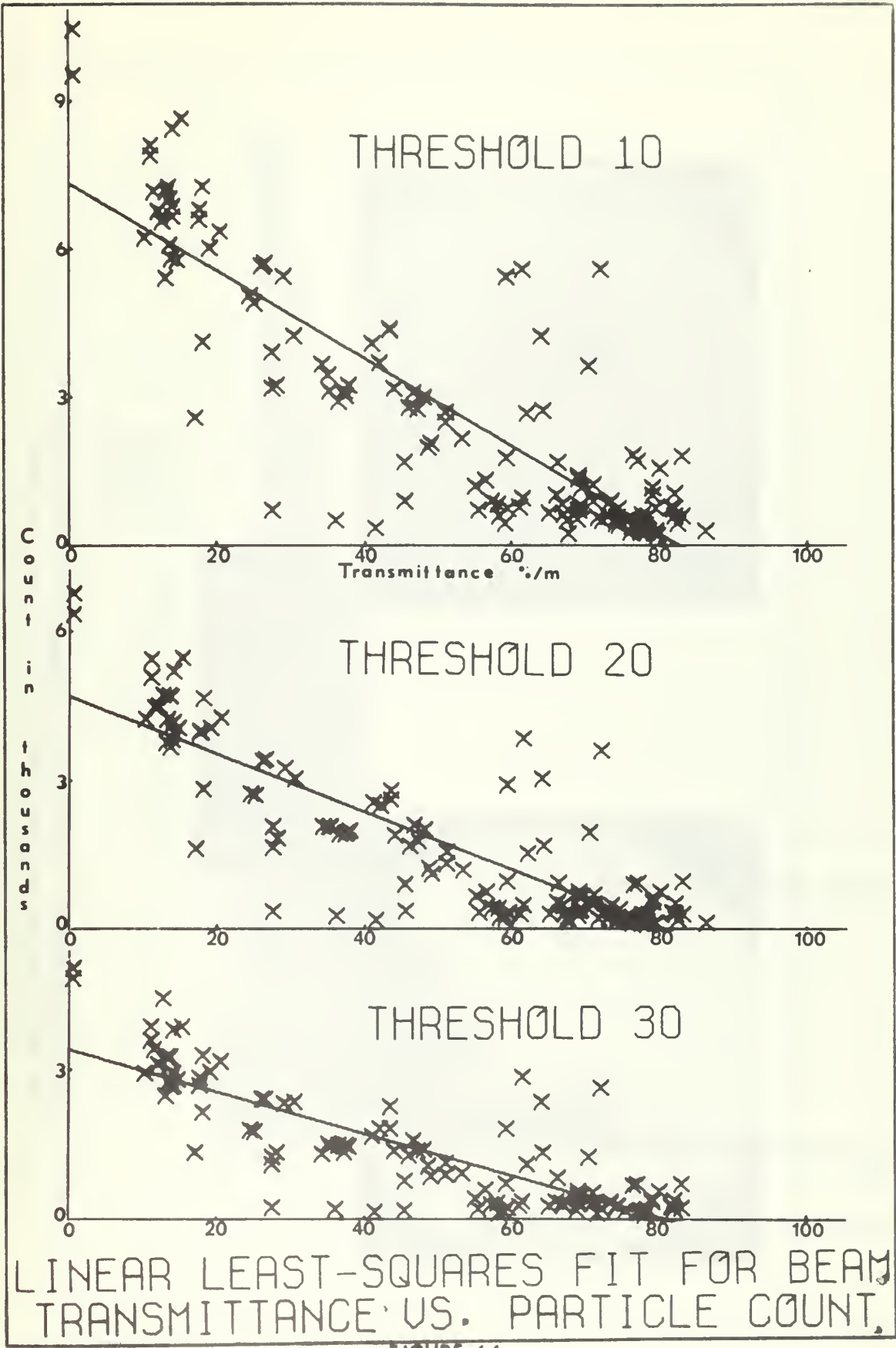
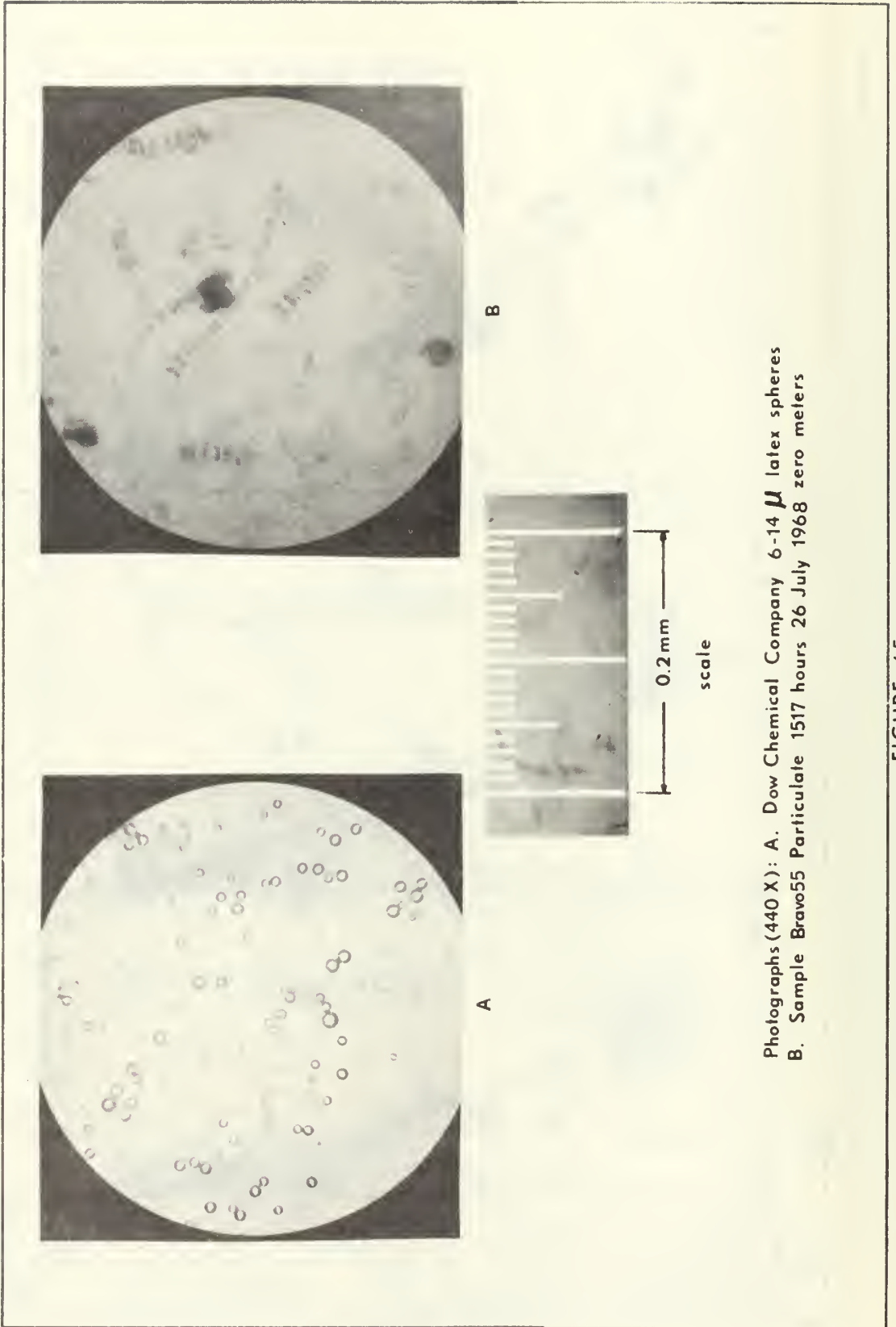
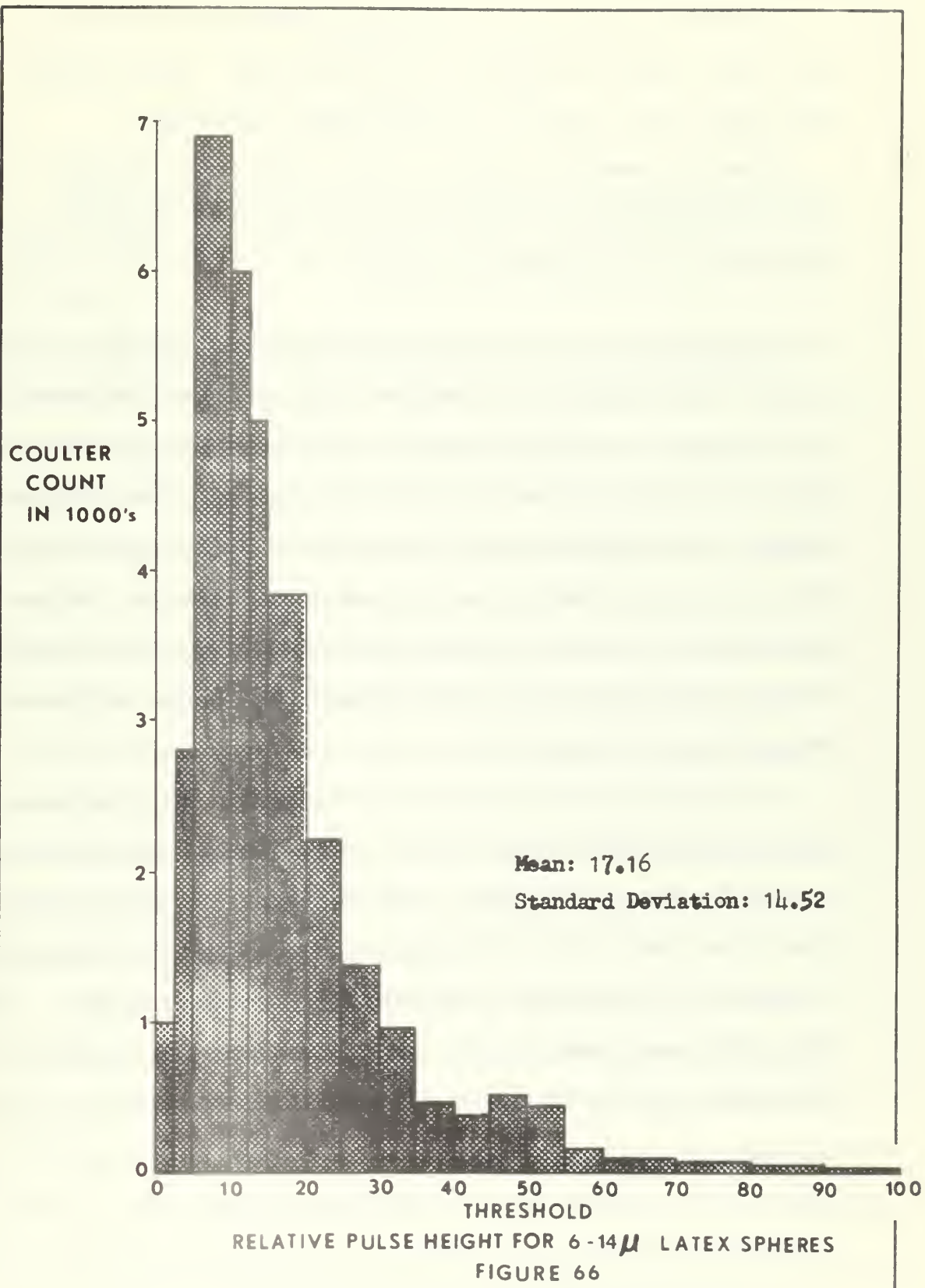


FIGURE 64



Photographs (440 X): A. Dow Chemical Company 6-14 μ latex spheres
B. Sample Bravo55 Particulate 1517 hours 26 July 1968 zero meters

FIGURE 65



In contrast, Figs. 12, 15, and 16, corresponding to new and full moons, reveal an absence of turbidity layers. Tidal ranges for Cruises 1 and 3 were 6.1 ft and 6.0 ft, respectively.

Although a possible turbidity layer, tidal range, and lunar period correlation is indicated, definite conclusions cannot be formed from the limited data available.

4.9 The Correlation of Internal Waves and Seiches with Beam Transmittance

While it is believed that seiches, internal waves, and currents all contribute to the fluctuations in isolines of beam transmittance observed in Figs. 12 through 18, positive proof for these phenomena is lacking. As discussed in section 1.4, seiches in a bay of configuration similar to that of Monterey Bay have amplitudes less than 1 ft and periods up to 70 minutes. Feasibility studies by the Corps of Engineers indicate Monterey Bay shows strong evidence for seiches in the period range of 32 to 36 minutes (17).

The shortest period of oscillation observed in the time-depth plots of beam transmittance was four hours. The shortest interval between successive casts was two hours. Consequently, the intervals between observations made in this study are too large for positive identification of internal wave activity or less-frequently occurring seiches. Similarly, depth measurement uncertainties, probably not exceeding two meters during rough seas, possibly masked the effects of internal waves or seiches.

CHAPTER 5

CONCLUSIONS

Nearly all of the parameters measured or observed during this investigation show correlations of varying degree with beam transmittance.

Beam transmittance isolines usually oscillate with the tidal cycle period, although phase relations are not consistent. Minimum values of beam transmittance frequently occur at or near low tide with the following high tide causing the transmissivity to increase.

Salinity correlations with beam transmittance are not clearly defined. In some observations little or no correlation was seen, whereas in others, beam transmittance contours and isohalines are nearly coincident. Isolated pockets of relatively high or low salinity often appear to be associated with beam transmittance perturbations.

There is a good correlation between temperature and beam transmittance isolines with temperature probably having the greatest correlation with beam transmittance.

Isopycnals and beam transmittance contours also show a clear correlation due to the strong influence of temperature on density.

A good correlation between particulate matter and beam transmittance was also observed. The greatest change in transmissivity occurs in the pycnocline and thermocline since these are the regions of greatest particulate concentration. The dominant phytoplankton found during this study was a chain diatom (Chaetoceros sp.). Approximately 68 percent of the particles affecting beam transmittance

appeared to be less than 10 μ in diameter, while approximately 96 percent appeared to be less than 13 μ . There seems to be a roughly linear relationship between values of particulate count and beam transmittance. Particle sizes were found to decrease with increasing depth.

The lunar period and subsequent tidal range seem to have a correlation with beam transmittance. Results from this investigation suggest that turbidity layers are possibly associated with decreased tidal ranges (quarter phases of the moon).

The effects of internal waves or seiches could not be determined from this study.

CHAPTER 6

SUGGESTIONS FOR FURTHER RESEARCH

For future light attenuation studies, the authors recommend the use of an STD in conjunction with the beam transmissometer to provide continuous measurements of salinity, temperature, and density. This instrument would permit simultaneous measurement of each parameter in depth and time in addition to reducing the interval between successive observations.

A concurrent investigation of internal waves and seiches using isotherm followers or thermistor chains should also be conducted in order to determine their effect in producing oscillations in isolines of beam transmittance.

The use of a larger, more stable research platform would reduce ship motion, thereby eliminating some of the depth uncertainties as well as improving station positioning accuracy.

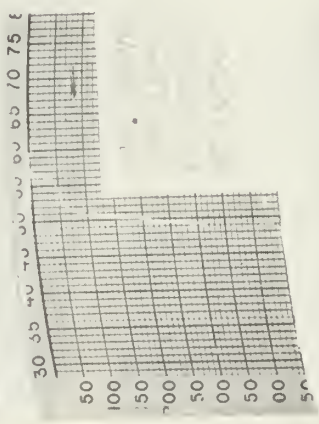
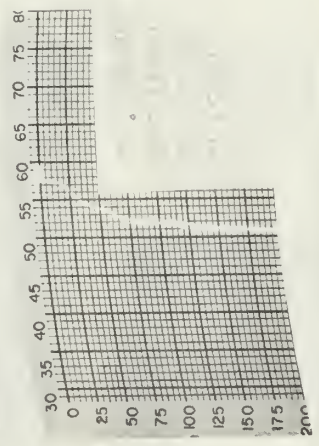
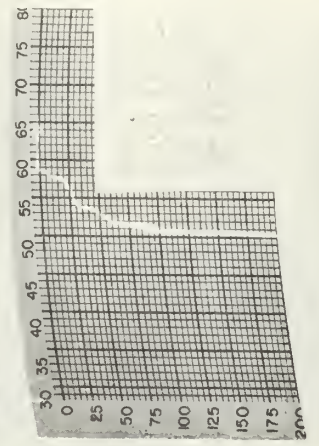
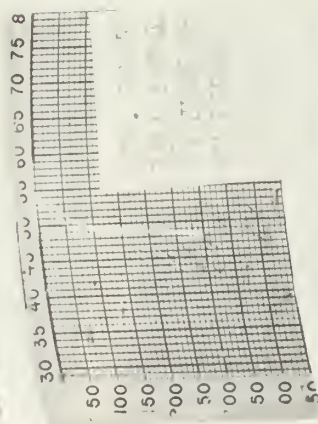
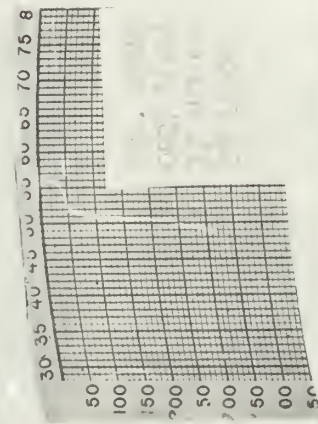
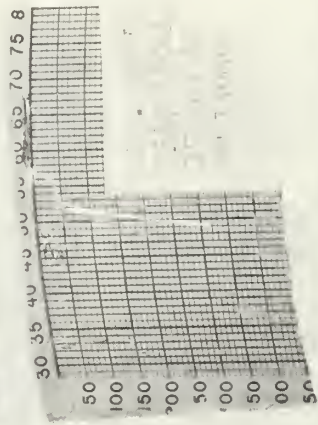
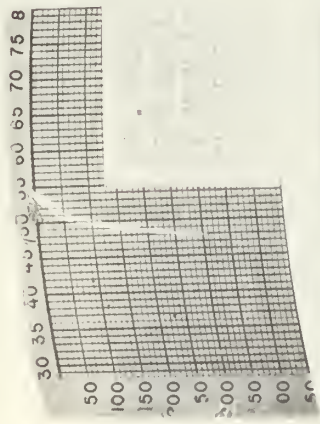
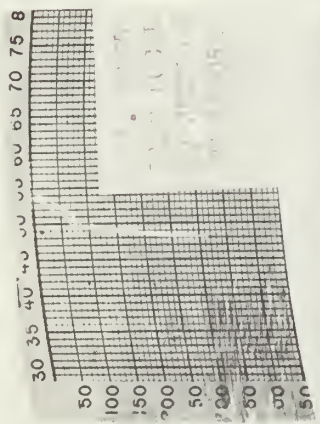
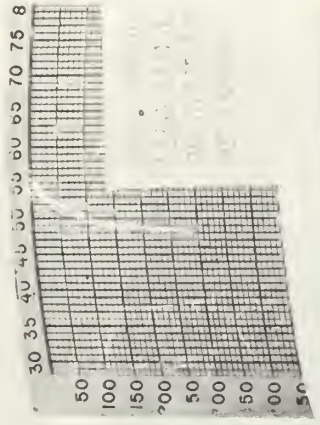
Additional analysis of the particulate samples obtained from this investigation is recommended for the purposes of determining organic carbon content, identifying dominant plankton species, and determining the percentage of detritus in each sample. It is also recommended that scattering measurements be made to determine the contribution of scattering to total light attenuation.

Additional studies are recommended to determine what relationship, if any, exists between turbidity layers and lunar phases. Finally, the possible correlation of beam transmittance gradient changes with salinity gradient changes merits investigation.

BIBLIOGRAPHY

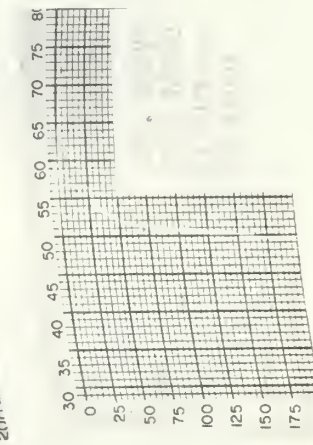
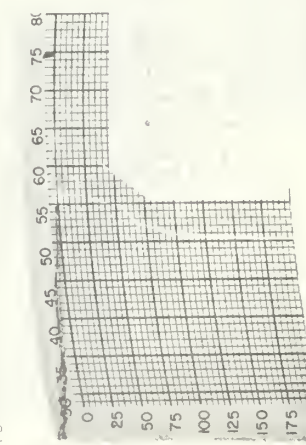
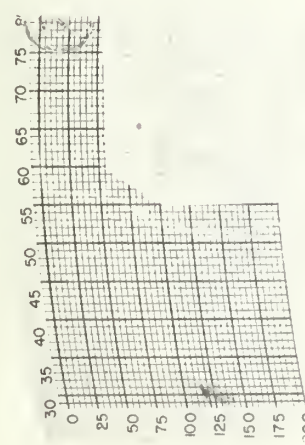
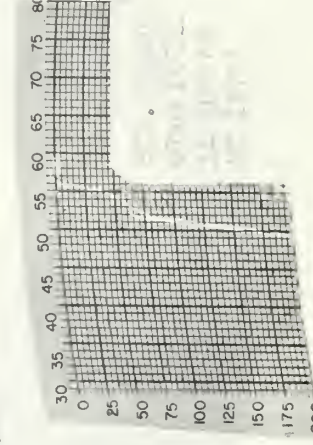
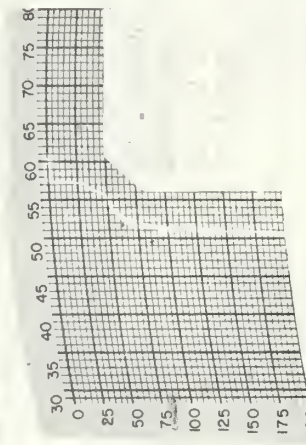
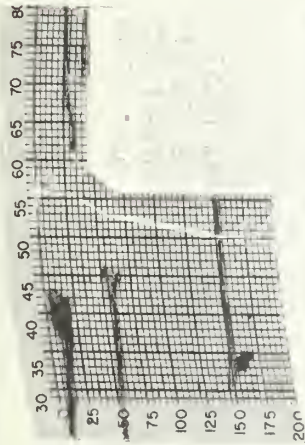
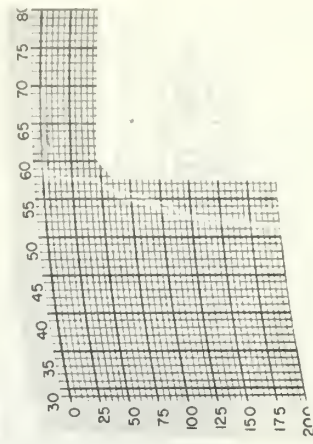
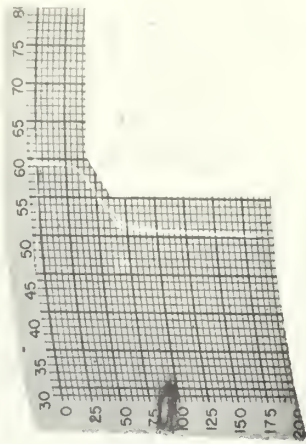
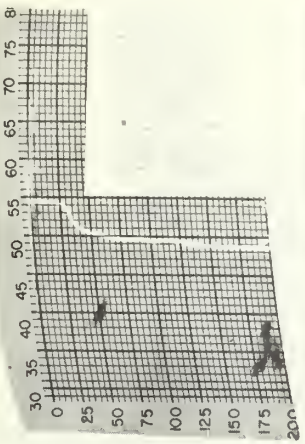
1. Ball, T. F. and E. C. LaFond. Shallow Water Turbidity Studies. U. S. Naval Electronic Laboratory Report, 1129, 1962.
2. Barham, E. G., Wilton, J. W., and M. P. Sullivan. Plankton and Turbidity. U. S. Naval Electronics Laboratory Report, 1386, 1966.
3. Bassett, C. H. and H. C. Furminger. An Investigation of the Vertical Variation of Light Scattering in Monterey Bay, California. Thesis, Naval Postgraduate School, Monterey, 1965.
4. Bumpus, D. F. and A. H. Clarke. Hydrography of the Western Atlantic: Transparency of the Coastal and Oceanic Waters of the Western Atlantic. Woods Hole Oceanographic Institution Technical Report, 10, 1947.
5. Burt, W. V. Distribution of Suspended Materials in Chesapeake Bay. Journal of Marine Research, 14, 47-62, 1955.
6. Carsola, A. J. and R. F. Dill. Spatial Changes in Transparency of the Coastal Waters off San Diego, California. Unpublished, personal correspondence with Dr. E. C. LaFond, U. S. Naval Undersea Warfare Center.
7. Duntley, S. Q. Light in the Sea. Journal of the Optical Society of America, 53, 214-233, 1963.
8. Emery, K. O. Transparency of Water off Southern California. Transactions American Geophysical Union, 35, 217-220, 1954.
9. Jerlov, N. G. Optical Measurements in the Eastern North Atlantic. Meddelanden Från Oceanografiska Institutet I Göteborg, B (8), 1961.
10. Jerlov, N. G. Optical Oceanography. Elsevier, Amsterdam, London, New York, 1968.
11. Joseph, J. Extinction Measurements to Indicate Distribution and Transport of Water Masses. Proceedings of the UNESCO Symposium on Physical Oceanography, Tokyo, 59-75, 1955.
12. Oser, R. K., Berger, J. L., and L. J. Franc. Oceanographic Data Report San Clemente Island Area October to December 1966. U. S. Naval Oceanographic Office Informal Report, 67-77, 1967.
13. Raines, W. A. Sub-Tidal Oscillations in Monterey Harbor. Thesis, Naval Postgraduate School, Monterey, California, 1967.

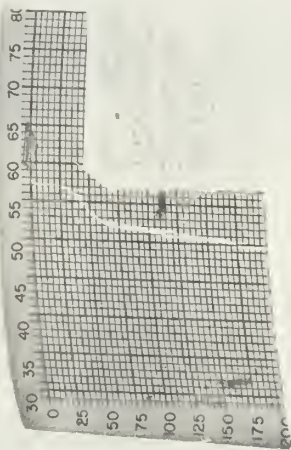
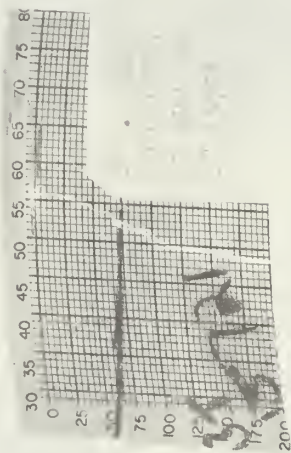
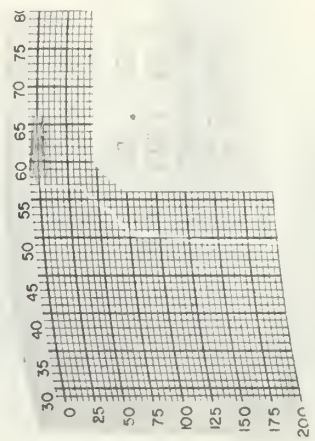
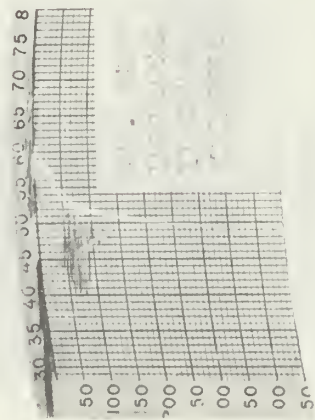
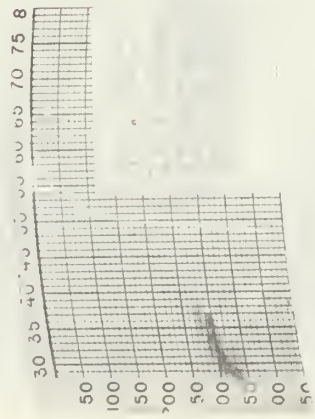
14. Skogsberg, T. Hydrography of Monterey, California: Thermal Conditions 1929-1933. Transactions of the American Philosophical Society, 29, 1936.
15. U. S. Department of Commerce, Coast and Geodetic Survey. Manual of Tide Observations, Publication 30-1, 7-15, 1965.
16. Welch, R. H. A Study of the Stratification of Phytoplankton at Selected Locations in Monterey Bay, California. Thesis, Naval Postgraduate School, Monterey, 1967.
17. Wilson, B. W., Hendrickson, J. A., and R. E. Kilmer. Feasibility Study for a Surge-Action Model of Monterey Harbor, California. U. S. Army Engineer Waterways Experiment Station, Corps of Engineers, 2-136, 1965.
18. Wilson, B. W. Generation of Long-Period Seiches in Table Bay, Cape Town, by Barometrical Oscillations. Transactions American Geophysical Union, 35 (5), 733-746, 1954.
19. Zinsser, H. Textbook of Bacteriology, Appleton, New York, 1927.



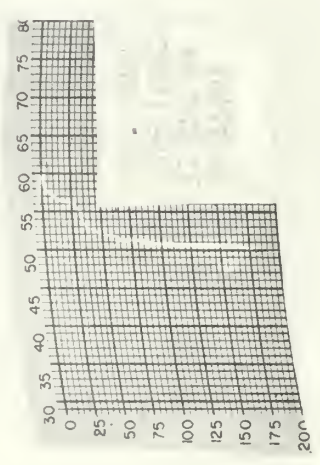
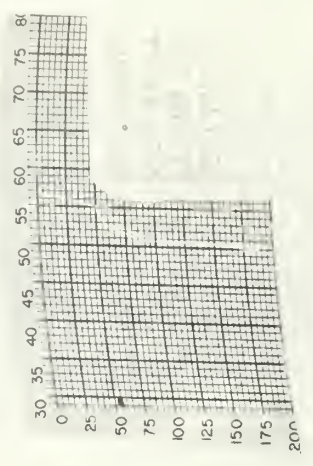
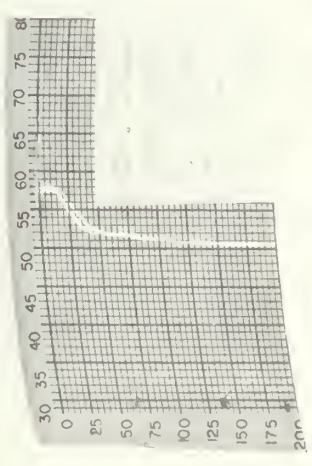
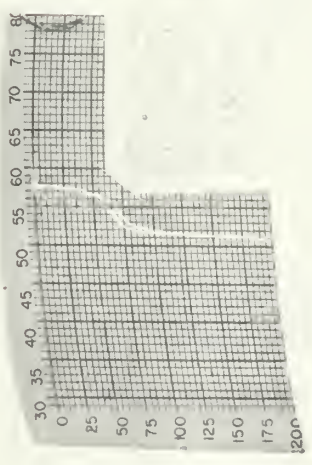
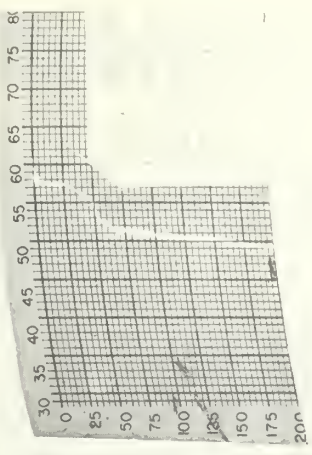
TEMPERATURES IN OF AND DEPTHS IN FLEET

TEMPERATURES IN °F AND DEPTHS IN FEET





TEMPERATURES IN OF AND DEPTHS IN FEET



TEMPERATURES IN °F AND DEPTHS IN FEET


```

SUBROUTINE SGTSVA (T,S,D,SGT,SV,SVA)
ST=-(((T-3.98)**2)/503.57)*((T+283)/(T+67.26))
CL=(S-.030)/1.805
SO=-.069+1.4708*CL-.00157*CL**2+3.98E-5*CL**3
AT=T*(4.7867-.098185*T+.0010843*T**2)*1.E-3
BT=T*(18.030-.8164*T+.01667*T**2)*1.E-6
SGT=ST+(SO+.1324)*(1.-AT+BT*(SO-.1324))
AFST=1./(1.+SGT*1.E-3)
A=D*AFST*1.E-9
B=4886./(1.+1.83E-5*D)
C=227.+28.33*T-.551*T**2+.004*T**3
E=D*1.E-4
G=(SO-28.)/10.
H=147.3-2.72*T+.04*T**2
U=105.5+9.5*T-.158*T**2
V=1.5*D**2*T*1.E-8
W=32.4-.87*T+.02*T**2
X=4.5-.1*T
Y=1.8-.06*T
SV=AFST-A*(B-C+E*U-V-G*(H-E*W)+G**2*(X-E*Y))
AZ=.972643
YA=-227.+0.01055*D
YB=.0126*(147.3-.00324*D)
AP=AZ-D*AZ*(B+YA-YB)*1.E-9
SVA=SV-AP
RETURN
END

```


Appendix IV

```

C      FORTRAN PROGRAM TO DETERMINE THE LEAST SQUARE LINEAR
C      FIT FOR THE BEAM TRANSMITTANCE MEASUREMENTS AS A
C      FUNCTION OF COULTER PARTICLE COUNTS AT VARIOUS
C      COULTER THRESHOLDS
C
REAL*8 LABEL/8H          /,ITITLE(12)
REAL*8 MABEL/4H        /
REAL*8 TRANS,CCOUNT,Y,B,T,C,A
REAL*4 SIGMA,DELY,SB,ST,SC,W
REAL*4 XX(900),YY(900),XXX(136),YYY(136)
C      UP TO ONE HUNDRED THIRTY-SIX POINTS ARE USED.
C      XXX CORRESPONDS TO BEAM TRANSMITTANCE AND
C      THE ABSCISSA. YYY CORRESPONDS TO PARTICLE
C      COUNT AND THE ORDINATE.
DIMENSION TRANS(136),COUNT(136),W(136),Y(136),DELY(136),
* B(6),SB(6),T(6),ST(6),C(6),SC(6),A(30,30)
READ(5,4) (ITITLE(I),I=1,12)
4  FORMAT(6A8)
READ(5,1) (COUNT(I),TRANS(I),I=1,135)
C      COUNT IS PARTICLE COUNT IN THOUSANDS.
C      TRANS IS BEAM TRANSMITTANCE IN PERCENT.
1  FORMAT(2F10.5)
WRITE(6,20)
20  FORMAT(20X,'COUNT',T52,'TRANS',///)
WRITE(6,2) (COUNT(I),TRANS(I),I=1,135)
2  FORMAT(18X,F10.5,T50,F10.5,///)
DO 3 M=1,5
JKL=30
IF(M.EQ.5)JKL=15
C      JKL IN THE ABOVE STATEMENT MUST BE ADJUSTED WHEN
C      THE NUMBER OF DATA POINTS IS CHANGED.
DO 68 I=1,JKL
J=I
IF(M.EQ.2)J=I+30
IF(M.EQ.3)J=I+60
IF(M.EQ.4)J=I+90
IF(M.EQ.5)J=I+120
XXX(I)=TRANS(J)
YYY(I)=COUNT(J)
68  CONTINUE
JJ=2
IF(M.EQ.1)JJ=1
CALL DRAW(JKL,XXX,YYY,JJ,1,LABEL,ITITLE,15.0,3.0,0.0,
* 2,2,6,8,0,L)
3  CONTINUE
CALL LSQPQL(135,1,0,0,0,SIGMA,TRANS,COUNT,W,Y,DELY,
* B,SB,T,ST,C,SC,A)
DY=100.0/900.0
RR=0.0
DO 6 I=1,900
XX(I)=RR
YY(I)=B(1)+B(2)*RR
6  RR=RR+DY
CALL DRAW(900,XX,YY,3,0,MABEL,ITITLE,15.0,3.0,0.0,2,
* 2,6,8,0,L)
RETURN
END

```

Appendix V

DATA TABLES

TABLE 1A

DEPTH, DATE, TIME, TEMPERATURE, SALINITY, DENSITY,
TRANSMITTANCE, AND TOTAL COULTER COUNT DATA

STATION BRAVO

DEPTH (m)	DATE/TIME (1968)	TEMPERATURE (°C)	SALINITY (0/00)	DENSITY (g/cm ³)	TRANSMITTANCE (%/m)	TOTAL Coulter Count
0	261600 Jul	12.34	33.666	1.02551	0.78	13800
6	261559 Jul	11.54	33.765	1.02576	0.78	22700
13	261558 Jul	10.98	33.715	1.02586	13.3	10500
15	261556 Jul	10.69	33.776	1.02597	16.0	
17	261555 Jul	10.45	33.733	1.02598	45.5	3500
19	261552 Jul	10.21	33.718	1.02602	54.0	
21	261550 Jul	10.12	33.803	1.02611	72.3	2152
40	261548 Jul	9.79	33.815	1.02626	67.7	1197
65	261545 Jul	9.32	33.907	1.02653	76.4	2205
90	261543 Jul	9.02	33.931	1.02671	58.4	4333
0	261744 Jul	12.53	33.691	1.02549	10.7	
8	261735 Jul	11.65	33.755	1.02574	10.0	
17	261732 Jul	11.07	33.773	1.02590	39.0	
20	261731 Jul	10.37	33.750	1.02602	76.0	
23	261728 Jul	10.22	33.800	1.02610	61.5	
26	261727 Jul	10.05	33.809	1.02615	81.8	
40	261724 Jul	9.80	33.780	1.02624	84.2	
60	261721 Jul	9.38	33.880	1.02647	83.4	
75	261718 Jul	9.18	33.858	1.02656	78.6	
90	261715 Jul	8.91	33.974	1.02676	53.0	

TABLE 1A (Continued)

DEPTH (m)	DATE/TIME (1968)	TEMPERATURE (°C)	SALINITY (0/00)	DENSITY (g/cm ³)	TRANSMITTANCE (%/m)	TOTAL COULTER COUNT
0	262000 Jul	12.65	33.702	1.02548	10.4	14100
5	261957 Jul	12.20	33.723	1.02560	11.6	15100
9	261955 Jul	11.80	33.595	1.02560	12.2	14900
13	261953 Jul	11.21	33.670	1.02578	11.0	10900
17	261952 Jul	10.86	33.718	1.02590	17.8	13800
21	261948 Jul	10.30	33.729	1.02602	41.5	1428
25	261946 Jul	10.09	33.797	1.02613	77.6	2228
45	261943 Jul	9.60	33.841	1.02634	78.4	1725
65	261941 Jul	9.33	33.892	1.02651	78.1	2955
85	261936 Jul	9.01	33.922	1.02668	74.5	3254
0	262200 Jul	12.47	33.678	1.02549	11.8	
3	262159 Jul	12.45	33.725	1.02555	11.8	
6	262157 Jul	11.95	33.681	1.02562	13.2	
9	262155 Jul	11.63	33.655	1.02567	19.7	
12	262154 Jul	11.32	33.694	1.02578	23.5	
15	262153 Jul	10.98	33.693	1.02585	30.1	
18	262151 Jul	10.62	33.643	1.02589	43.7	
22	262148 Jul	10.27	33.732	1.02604	80.9	
50	262146 Jul	9.61	33.796	1.02633	81.6	
85	262140 Jul	9.20	33.903	1.02664	79.6	
0	262355 Jul	12.55	33.666	1.02547	13.9	12400
3	262354 Jul	11.98	33.696	1.02561	14.0	9831
6	262353 Jul	11.64	33.681	1.02568	15.4	14000
9	262351 Jul	11.31	33.661	1.02574	17.7	14200
12	262349 Jul	11.16	33.707	1.02582	18.1	16100
15	262348 Jul	10.61	33.691	1.02591	18.1	8547
30	262346 Jul	9.98	33.763	1.02615	79.8	2290
50	262343 Jul	9.61	33.784	1.02632	79.6	1558
70	262340 Jul	9.39	33.886	1.02652	74.5	1792
85	262337 Jul	9.27	33.880	1.02661	77.1	1966

TABLE 1A (Continued)

DEPTH (m)	DATE/TIME (1968)	TEMPERATURE (°C)	SALINITY (‰)	DENSITY (g/cm ³)	TRANSMITTANCE (%/m)	TOTAL COULTER COUNT
0	270152 Jul	12.57	33.690	1.02548	14.9	
9	270148 Jul	11.19	33.690	1.02578	13.9	
12	270147 Jul	10.81	33.693	1.02587	22.9	
15	270146 Jul	10.60	33.748	1.02596	27.0	
18	270145 Jul	10.37	33.770	1.02603	41.0	
21	270143 Jul	10.18	33.745	1.02606	76.4	
24	270142 Jul	10.08	33.738	1.02608	78.3	
27	270140 Jul	9.99	33.763	1.02613	78.7	
55	270137 Jul	9.55	33.862	1.02641	79.0	
85	270132 Jul	9.08	33.937	1.02668	76.4	
0	270339 Jul	12.54	33.665	1.02547	14.8	9373
5	270337 Jul	11.89	33.722	1.02566	14.1	16200
10	270336 Jul	10.94	33.721	1.02586	20.5	12400
15	270335 Jul	10.45	33.743	1.02598	53.3	4241
20	270334 Jul	10.11	33.724	1.02605	77.2	1361
25	270333 Jul	9.99	33.786	1.02614	79.4	1135
30	270332 Jul	9.90	33.782	1.02617	79.5	1169
50	270330 Jul	9.43	33.790	1.02635	79.5	1539
70	270327 Jul	9.18	33.862	1.02654	74.1	1990
85	270323 Jul	9.04	33.873	1.02664	75.5	2722
0	270547 Jul	12.56	33.715	1.02550	14.2	
5	270545 Jul	11.50	33.713	1.02573	12.4	
10	270544 Jul	10.57	33.726	1.02592	14.1	
15	270542 Jul	10.32	33.744	1.02600	58.5	
20	270541 Jul	9.95	33.726	1.02608	79.4	
25	270539 Jul	9.85	33.682	1.02608	80.0	
30	270537 Jul	9.81	33.816	1.02622	80.1	
35	270535 Jul	9.72	33.799	1.02624	80.0	
60	270532 Jul	9.34	33.866	1.02647	75.8	
85	270528 Jul	9.05	33.898	1.02666	78.3	

TABLE 1A (Continued)

DEPTH (m)	DATE/TIME (1968)	TEMPERATURE (°C)	SALINITY (0/00)	DENSITY (g/cm ³)	TRANSMITTANCE (%/m)	TOTAL COULTER COUNT
0	270747 Jul	12.27	33.676	1.02553	12.8	13700
3	270746 Jul	11.57	33.760	1.02574	11.0	16700
6	270743 Jul	11.19	33.743	1.02581	13.8	13300
9	270742 Jul	10.51	33.748	1.02595	17.2	5718
12	270741 Jul	10.31	33.752	1.02600	36.0	1921
15	270740 Jul	10.23	33.817	1.02608	59.0	3392
18	270736 Jul	10.07	33.807	1.02611	79.2	5159
35	270734 Jul	9.60	33.803	1.02626	83.0	6860
65	270732 Jul	9.14	33.931	1.02658	77.7	3143
85	270727 Jul	-	-	1.02669	72.8	-
0	270958 Jul	12.40	33.730	1.02555	12.0	
5	270956 Jul	11.77	33.742	1.02570	11.0	
8	270955 Jul	11.51	33.698	1.02573	17.0	
11	270953 Jul	11.24	33.732	1.02582	31.2	
14	270951 Jul	10.94	33.657	1.02582	31.6	
17	270949 Jul	10.82	33.752	1.02593	35.0	
35	270947 Jul	10.04	33.828	1.02621	77.0	
55	270944 Jul	9.48	33.788	1.02636	78.9	
75	270941 Jul	9.09	33.896	1.02660	75.0	
85	270939 Jul	8.97	33.910	1.02668	75.7	
0	271218 Jul	12.59	33.740	1.02552	13.0	12800
4	271216 Jul	12.01	33.757	1.02566	13.5	15866
8	271215 Jul	11.89	33.696	1.02565	19.0	10900
12	271212 Jul	11.24	33.702	1.02580	30.5	7497
16	271211 Jul	11.00	33.506	1.02571	37.9	5626
20	271210 Jul	10.82	33.731	1.02593	37.4	6306
24	271209 Jul	10.10	33.756	1.02609	56.5	3558
45	271207 Jul	9.54	33.836	1.02635	78.3	1326
65	271205 Jul	9.22	33.930	1.02656	77.6	1960
85	271201 Jul	9.04	33.935	1.02669	68.9	3275

TABLE 1A (Continued)

DEPTH (m)	DATE/TIME (1968)	TEMPERATURE (°C)	SALINITY (0/00)	DENSITY (g/cm ³)	TRANSMITTANCE (%/m)	TOTAL COULTER COUNT
0	271430 Jul	12.79	33.712	1.02546	16.0	
4	271428 Jul	11.66	33.725	1.02570	16.6	
8	271427 Jul	11.60	33.617	1.02565	19.3	
11	271426 Jul	11.45	33.690	1.02574	30.0	
15	271424 Jul	10.89	33.725	1.02589	37.1	
20	271422 Jul	10.60	33.684	1.02593	47.8	
27	271420 Jul	10.05	33.799	1.02615	78.0	
30	271419 Jul	10.00	33.817	1.02619	78.8	
55	271416 Jul	9.45	33.813	1.02639	78.4	
85	271412 Jul	9.10	33.859	1.02662	78.0	
0	271625 Jul	12.43	33.761	1.02557	15.0	
3	271624 Jul	12.06	33.727	1.02562	15.0	
6	271622 Jul	11.70	33.671	1.02566	22.0	
9	271620 Jul	11.17	33.529	1.02566	34.0	
12	271617 Jul	10.86	33.680	1.02585	39.5	
15	271616 Jul	10.36	33.649	1.02592	57.2	
18	271615 Jul	10.11	33.840	1.02613	78.0	
45	271612 Jul	9.46	33.858	1.02638	82.0	
75	271608 Jul	9.26	33.881	1.02656	79.0	
85	271606 Jul	9.06	33.749	1.02654	79.5	
0	171041 Aug	13.59	33.660	1.02526	65.2	2094
5	171039 Aug	13.51	33.696	1.02532	72.1	27970
7	171038 Aug	-	-	-	70.0	-
8	171036 Aug	13.22	33.671	1.02538	27.5	2878
9	171035 Aug	-	-	-	40.1	-
10	171034 Aug	12.28	33.683	1.02558	66.0	3424
11	171033 Aug	-	-	-	67.1	-
12	171033 Aug	11.40	33.712	1.02577	69.0	2597
14	171032 Aug	11.17	33.733	1.02584	73.5	2423
16	171032 Aug	11.11	33.754	1.02588	73.5	2793
20	171032 Aug	-	-	-	74.3	-

TABLE 1A (Continued)

DEPTH (m)	DATE/TIME (1968)	TEMPERATURE (°C)	SALINITY (0/00)	DENSITY (g/cm ³)	TRANSMITTANCE (%/m)	TOTAL COULTER COUNT
25	171030 Aug	-	-	-	78.3	-
30	171028 Aug	10.73	33.769	1.02602	78.6	2292
45	171027 Aug	-	-	-	82.0	-
60	171025 Aug	10.22	33.795	1.02627	83.2	3226
85	171021 Aug	9.82	33.822	1.02647	82.5	1721
0	171459 Aug	14.02	33.671	1.02518	61.6	
3	171459 Aug	14.03	33.786	1.02528	63.6	
6	171458 Aug	13.88	33.776	1.02531	63.6	
9	171457 Aug	13.57	33.645	1.02529	67.0	
11	171456 Aug	11.91	33.723	1.02568	64.8	
13	171455 Aug	11.40	33.815	1.02586	66.0	
15	171454 Aug	11.30	33.717	1.02581	69.0	
17	171453 Aug	11.19	33.806	1.02591	69.0	
29	171452 Aug	-	-	-	69.6	
35	171451 Aug	-	-	-	75.1	
50	171449 Aug	10.48	33.879	1.02624	77.5	
65	171448 Aug	-	-	-	78.9	
85	171447 Aug	9.73	33.836	1.02650	76.5	
0	171847 Aug	13.57	33.700	1.02529	58.0	3178
4.7	171846 Aug	13.58	33.889	1.02546	57.3	4162
8.5	171845 Aug	13.55	33.886	1.02548	59.5	2529
11.3	171845 Aug	13.51	33.727	1.02537	61.0	2364
14.1	171844 Aug	12.58	33.810	1.02564	67.0	2385
16.9	171843 Aug	11.34	33.823	1.02589	69.0	1923
19.7	171842 Aug	11.23	33.703	1.02583	66.9	2265
28.0	171841 Aug	-	-	-	70.5	-
32.9	171839 Aug	10.62	33.884	1.02614	74.4	1953
58.4	171837 Aug	10.32	33.888	1.02632	77.5	1651
80.9	171833 Aug	10.07	33.886	1.02646	77.8	2322

TABLE 1A (Continued)

DEPTH (m)	DATE/TIME (1968)	TEMPERATURE (°C)	SALINITY (0/00)	DENSITY (g/cm ³)	TRANSMITTANCE (%/m)	TOTAL COULTER COUNT
0	172044 Aug	13.49	33.662	1.02528	63.5	
4.5	172043 Aug	13.50	33.678	1.02531	63.5	
7.2	172042 Aug	13.35	33.692	1.02536	63.5	
9.9	172042 Aug	12.93	33.667	1.02544	61.7	
12.6	172041 Aug	12.14	33.700	1.02563	59.8	
15.3	172040 Aug	11.24	33.733	1.02584	64.0	
18.0	172039 Aug	11.19	33.733	1.02586	65.5	
20.9	172037 Aug	-	-	-	69.0	
31.5	172036 Aug	10.40	33.768	1.02609	75.9	
54.0	172034 Aug	10.19	33.885	1.02632	78.2	
76.5	172030 Aug	9.96	33.793	1.02638	72.5	
0	230814 Aug	14.17	33.492	1.02501	43.5	10900
2	230814 Aug	-	-	-	35.1	-
4	230813 Aug	13.71	33.484	1.02511	43.6	10800
7	230812 Aug	12.64	33.519	1.02537	49.0	6016
10	230811 Aug	12.21	33.572	1.02550	47.4	6902
13	230810 Aug	12.08	33.545	1.02552	48.7	5144
15	230809 Aug	-	-	-	51.8	-
16	230809 Aug	11.96	33.550	1.02556	64.4	5215
20	230808 Aug	11.20	33.553	1.02572	71.1	4831
24	230808 Aug	11.06	33.597	1.02580	71.2	3124
32	230807 Aug	-	-	-	74.6	-
48	230806 Aug	-	-	-	79.8	-
55	230803 Aug	10.46	33.551	1.02601	81.7	3012
63	230800 Aug	-	-	-	82.0	-
85	230759 Aug	10.17	33.632	1.02626	82.0	2744
0	231138 Aug	15.14	33.578	1.02486	28.7	
1.5	231137 Aug	-	-	-	21.0	
3	231136 Aug	14.52	33.567	1.02500	21.7	

TABLE 1A (Continued)

DEPTH (m)	DATE/TIME (1968)	TEMPERATURE (°C)	SALINITY (0/00)	DENSITY (g/cm ³)	TRANSMITTANCE (%/m)	TOTAL COULTER COUNT
5	231136 Aug	-	-	-	19.9	
6	231135 Aug	14.02	33.579	1.02513	40.0	
7	231134 Aug	-	-	-	43.5	
9	231133 Aug	12.63	33.622	1.02546	48.0	
12	231132 Aug	12.03	33.595	1.02557	59.6	
13	231132 Aug	-	-	-	62.5	
15	231131 Aug	11.65	33.625	1.02567	69.1	
18	231131 Aug	11.13	33.537	1.02571	69.5	
21	231130 Aug	11.09	33.585	1.02577	71.7	
27	231129 Aug	-	-	-	74.1	
33	231128 Aug	-	-	-	78.0	
50	231127 Aug	10.57	33.608	1.02601	80.0	
75	231125 Aug	-	-	-	84.0	
85	231122 Aug	10.30	33.668	1.02627	82.3	
0	231715 Aug	13.64	33.564	1.02517	36.5	6404
4	231714 Aug	13.63	33.532	1.02517	35.4	7154
6	231714 Aug	-	-	-	35.5	-
8	231713 Aug	13.52	33.532	1.02521	35.0	8587
10	231713 Aug	-	-	-	36.0	-
12	231712 Aug	13.35	33.567	1.02529	37.6	7216
16	231711 Aug	12.97	33.565	1.02538	46.0	6651
20	231710 Aug	12.42	33.572	1.02551	51.1	7315
22	231710 Aug	-	-	-	52.8	-
24	231709 Aug	11.86	33.582	1.02572	59.4	4190
28	231708 Aug	11.55	33.595	1.02573	69.0	4048
32	231707 Aug	11.31	33.598	1.02579	69.6	3958
41	231705 Aug	-	-	-	74.7	-
80	231702 Aug	10.46	33.654	1.02620	82.2	4507
0	232244 Aug	13.98	33.628	1.02515	41.0	11600

TABLE 1A (Continued)

DEPTH (m)	DATE/TIME (1968)	TEMPERATURE (°C)	SALINITY (0/00)	DENSITY (g/cm ³)	TRANSMITTANCE (%/m)	TOTAL COULTER COUNT
3.9	232243 Aug	13.85	33.719	1.02527	42.0	11800
5.0	232242 Aug	-	-	-	40.0	-
7.9	232241 Aug	13.51	33.659	1.02531	46.7	8220
11.8	232240 Aug	13.20	33.706	1.02542	48.0	7490
14.0	232239 Aug	-	-	-	51.0	-
15.8	232238 Aug	12.39	33.723	1.02561	51.0	6957
18.0	232237 Aug	-	-	-	58.0	-
19.8	232236 Aug	12.24	33.727	1.02566	62.0	5869
24.8	232235 Aug	11.89	33.747	1.02577	76.5	7253
29.7	232235 Aug	11.63	33.724	1.02582	79.0	4304
33.0	232233 Aug	-	-	-	85.5	-
49.5	232231 Aug	10.70	33.766	1.02611	77.0	2966
74.0	232229 Aug	-	-	-	79.5	-
79.2	232226 Aug	10.27	33.813	1.02636	73.0	2781
10.0	301140 Aug	14.06	33.512	1.02504	26.0	12500
4.9	301140 Aug	-	-	-	27.5	-
6.9	301139 Aug	14.00	33.551	1.02512	26.6	12900
9.8	301138 Aug	13.88	33.536	1.02514	29.0	11800
12.7	301137 Aug	12.62	33.576	1.02544	61.5	8467
15.7	301136 Aug	11.67	33.602	1.02566	64.0	8673
16.7	301136 Aug	-	-	-	68.0	-
18.6	301136 Aug	11.57	33.601	1.02569	77.0	5344
21.6	301135 Aug	11.54	33.595	1.02570	80.0	5368
39.2	301133 Aug	10.45	33.583	1.02597	86.4	1524
52.5	301132 Aug	-	-	-	87.0	-
58.7	301131 Aug	10.28	33.592	1.02609	81.9	3337
63.6	301130 Aug	-	-	-	68.8	-
70.5	301129 Aug	-	-	-	65.0	-
75.4	301128 Aug	-	-	-	47.5	-
83.2	301127 Aug	9.93	33.716	1.02636	45.5	10600

TABLE 1A (Continued)

DEPTH (m)	DATE/TIME (1968)	TEMPERATURE (°C)	SALINITY (0/00)	DENSITY (g/cm ³)	TRANSMITTANCE (%/m)	TOTAL COULTER COUNT
0	301537 Aug	13.73	33.451	1.02507	31.0	
3	301536 Aug	-	-	-	31.4	
5	301535 Aug	-	-	-	27.7	
6	301534 Aug	-	-	-	29.0	
9	301533 Aug	13.12	33.489	1.02526	23.4	
12	301532 Aug	13.00	33.488	1.02529	18.2	
13.5	301531 Aug	-	-	-	18.6	
15	301530 Aug	12.20	33.487	1.02546	22.4	
18	301529 Aug	11.40	33.482	1.02562	34.0	
19.5	301529 Aug	-	-	-	46.0	
21	301529 Aug	11.26	33.478	1.02566	48.4	
24	301528 Aug	11.12	33.421	1.02565	73.4	
30	301527 Aug	10.72	33.467	1.02579	74.5	
47	301527 Aug	-	-	-	80.0	
55	301524 Aug	10.31	33.588	1.02607	76.1	
59	301524 Aug	-	-	-	76.0	
67	301523 Aug	-	-	-	49.4	
73	301522 Aug	-	-	-	52.1	
74	301521 Aug	-	-	-	59.0	
79	301520 Aug	-	-	-	80.0	
85	301518 Aug	9.33	33.681	1.02644	81.2	
0	301938 Aug	14.22	33.517	1.02502	27.5	5178
3	301937 Aug	-	-	-	25.3	-
5	301937 Aug	-	-	-	29.2	-
8	301936 Aug	14.03	33.510	1.02508	25.0	9866
10	301936 Aug	13.96	33.489	1.02509	24.5	9854
12.5	301935 Aug	-	-	-	23.5	-
13	301934 Aug	13.30	33.496	1.02525	28.0	5807
14.5	301934 Aug	-	-	-	28.0	-
16	301933 Aug	11.71	33.457	1.02554	59.4	13600

TABLE 1A (Continued)

DEPTH (m)	DATE/TIME (1968)	TEMPERATURE (°C)	SALINITY (0/00)	DENSITY (g/cm ³)	TRANSMITTANCE (%/m)	TOTAL COULTER COUNT
18	301933 Aug	11.20	33.482	1.02566	70.5	6283
20	301932 Aug	11.02	33.480	1.02570	66.4	3500
23	301931 Aug	10.76	33.437	1.02573	69.3	2320
28	301930 Aug	-	-	-	73.8	-
34	301929 Aug	-	-	-	78.2	-
50	301928 Aug	10.40	33.528	1.02598	76.0	1416
54	301927 Aug	-	-	-	78.7	-
57	301927 Aug	-	-	-	71.3	-
59	301926 Aug	-	-	-	59.0	-
72	301925 Aug	-	-	-	56.0	-
82	301924 Aug	-	-	-	59.0	-
85	301922 Aug	9.54	33.670	1.02640	67.6	2900
0	302349 Aug	15.36	33.464	1.02473	23.5	
5	302349 Aug	-	-	-	25.0	
9	302348 Aug	15.14	33.455	1.02481	26.5	
11	302348 Aug	14.75	33.475	1.02492	25.0	
13	302347 Aug	14.20	33.495	1.02506	23.0	
15	302347 Aug	13.25	33.497	1.02527	27.0	
17	302346 Aug	12.14	33.528	1.02552	33.1	
19	302346 Aug	11.06	33.504	1.02571	41.0	
22	302345 Aug	10.87	33.493	1.02574	47.0	
23	302344 Aug	-	-	-	70.0	
28	302343 Aug	-	-	-	74.3	
50	302342 Aug	10.42	33.536	1.02598	77.0	
58	302341 Aug	-	-	-	80.0	
60	302340 Aug	-	-	-	74.3	
62	302339 Aug	-	-	-	60.5	
68.5	302338 Aug	-	-	-	54.0	
79	302337 Aug	-	-	-	56.6	

TABLE IA (Continued)

DEPTH (m)	DATE/TIME (1968)	TEMPERATURE (°C)	SALINITY (0/00)	DENSITY g/cm ³	TRANSMITTANCE (%/m)	TOTAL COULTER COUNT
82	302336 Aug	-	-	-	64.3	
85	302335 Aug	9.53	33.791	1.02649	73.2	
0	310401 Aug	13.95	33.645	1.02517	14.0	16600
2	310400 Aug	-	-	-	13.7	-
5	310400 Aug	13.41	33.645	1.02645	13.7	12300
7	310359 Aug	12.02	33.608	1.02556	27.5	9551
9	310359 Aug	11.64	33.606	1.02563	34.4	7760
11	310358 Aug	11.31	33.609	1.02571	44.0	7213
13	310357 Aug	11.04	33.615	1.02577	55.0	5258
15	310357 Aug	11.01	33.646	1.02581	55.5	2822
20	310356 Aug	10.92	33.621	1.02583	61.5	3123
22	310355 Aug	-	-	-	61.2	-
24	310354 Aug	-	-	-	67.0	-
29	310353 Aug	-	-	-	73.3	-
47	310353 Aug	-	-	-	76.5	-
50	310353 Aug	10.18	33.763	1.02620	71.7	3754
56	310352 Aug	-	-	-	65.6	-
59	310351 Aug	-	-	-	60.8	-
64	310350 Aug	-	-	-	55.0	-
69	310350 Aug	-	-	-	59.0	-
70	310349 Aug	-	-	-	66.0	-
72	310348 Aug	-	-	-	73.0	-
85	310346 Aug	9.33	33.822	1.02655	78.0	1892
0	310807 Aug	13.47	33.633	1.02526	37.0	
3	310806 Aug	-	-	-	24.5	
5	310806 Aug	13.19	33.629	1.02534	18.0	
10	310805 Aug	12.46	33.635	1.02551	17.0	
13	310805 Aug	11.99	33.644	1.02562	20.5	

TABLE 1A (Continued)

DEPTH (m)	DATE/TIME (1968)	TEMPERATURE (°C)	SALINITY (0/00)	DENSITY (g/cm ³)	TRANSMITTANCE (%/m)	TOTAL COULTER COUNT
16	310803 Aug	11.27	33.637	1.02576	28.0	
18	310802 Aug	-	-	-	47.0	
20	310802 Aug	11.00	33.631	1.02582	53.7	
24	310801 Aug	10.98	33.687	1.02589	56.0	
27.5	310800 Aug	-	-	-	65.0	
35	310800 Aug	10.71	33.701	1.02599	72.0	
38	310759 Aug	-	-	-	71.4	
43	310758 Aug	-	-	-	74.1	
52	310757 Aug	-	-	-	64.3	
60	310757 Aug	9.85	33.797	1.02633	67.5	
72	310755 Aug	-	-	-	70.5	
85	310753 Aug	9.37	33.819	1.02654	76.8	

TABLE 1B STATION DELTA

DEPTH (m)	DATE/TIME (1968)	TEMPERATURE (°C)	SALINITY (0/00)	DENSITY (g/cm ³)	TRANSMITTANCE (%/m)
0	171250 Aug	14.27	33.700	1.02515	52.0
3	171249 Aug	14.09	33.656	1.02516	55.2
4	171248 Aug	-	-	-	55.7
6	171248 Aug	13.89	33.674	1.02523	36.1
7	171247 Aug	-	-	-	35.3
9	171247 Aug	13.42	33.719	1.02538	33.0
10	171246 Aug	-	-	-	33.0
12	171244 Aug	12.68	33.720	1.02554	41.4
14	171243 Aug	-	-	-	54.0
15	171243 Aug	12.45	33.741	1.02561	54.0
17	171242 Aug	-	-	-	61.0
19	171241 Aug	11.86	33.753	1.02575	70.4
22	171240 Aug	11.08	33.759	1.02591	74.6
25	171239 Aug	10.88	33.737	1.02595	76.0
55	171238 Aug	-	-	-	81.0
85	171231 Aug	9.78	33.807	1.02646	82.3
0	171646 Aug	14.21	33.634	1.02511	42.0
2.8	171645 Aug	14.22	33.649	1.02513	42.0
5.6	171644 Aug	14.12	33.787	1.02527	39.9
7.5	171643 Aug	13.75	33.704	1.02529	38.1
11	171643 Aug	-	-	-	44.0
11.3	171642 Aug	12.51	33.690	1.02554	41.8
13.5	171641 Aug	-	-	-	44.3
14.1	171640 Aug	12.11	33.734	1.02567	47.0
16.5	171639 Aug	-	-	-	57.0
16.9	171639 Aug	11.75	33.694	1.02572	73.0
19.7	171639 Aug	11.07	33.740	1.02589	73.1
35	171636 Aug	-	-	-	71.7
42.3	171635 Aug	10.42	33.779	1.02614	72.0
80.9	171630 Aug	9.83	33.801	1.02643	79.3

TABLE 1B (Continued)

DEPTH (m)	DATE/TIME (1968)	TEMPERATURE (°C)	SALINITY (0/00)	DENSITY (g/cm ³)	TRANSMITTANCE (%/m)
0	230952 Aug	13.75	33.557	1.02514	45.0
5	230951 Aug	-	-	-	44.1
8	230950 Aug	13.67	33.566	1.02520	48.1
11	230949 Aug	13.53	33.546	1.02523	56.5
14	230948 Aug	12.51	33.522	1.02543	51.5
15	230947 Aug	-	-	-	64.5
17	230947 Aug	11.91	33.526	1.02556	70.5
20	230946 Aug	11.50	33.626	1.02572	75.9
23	230945 Aug	10.76	33.473	1.02575	80.5
26	230944 Aug	10.32	33.485	1.02585	86.5
55	230942 Aug	9.68	33.597	1.02618	87.9
85	230937 Aug	9.47	33.684	1.02642	87.9
0	231335 Aug	14.21	33.556	1.02505	39.2
4.8	231335 Aug	14.20	33.566	1.02508	39.2
9.6	231334 Aug	14.00	33.565	1.02514	41.4
13	231333 Aug	-	-	-	42.5
14.4	231333 Aug	13.42	33.604	1.02531	49.0
17.3	231332 Aug	12.99	33.593	1.02540	49.7
20.2	231332 Aug	12.68	33.580	1.02547	50.3
23	231331 Aug	12.38	33.582	1.02554	53.0
28.8	231328 Aug	11.26	33.634	1.02581	67.3
57.6	231326 Aug	10.80	33.606	1.02601	73.7
66	231325 Aug	-	-	-	77.5
70	231324 Aug	-	-	-	82.5
81.6	231322 Aug	10.05	33.527	1.02618	85.0
0	232058 Aug	13.54	33.599	1.02522	55.8
5	232058 Aug	-	-	-	56.0
9.9	232057 Aug	12.99	33.661	1.02542	59.1

TABLE 1B (Continued)

DEPTH (m)	DATE/TIME (1968)	TEMPERATURE (°C)	SALINITY (0/00)	DENSITY (g/cm ³)	TRANSMITTANCE (%/m)
12.9	232056 Aug	12.80	33.603	1.02543	59.7
15.8	232055 Aug	12.48	33.664	1.02555	62.9
18.8	232055 Aug	12.14	33.458	1.02547	61.0
21.8	232054 Aug	11.72	33.660	1.02572	73.0
24.8	232054 Aug	11.43	33.596	1.02574	74.4
27.8	232053 Aug	11.36	33.718	1.02586	75.3
31.7	232052 Aug	11.06	33.677	1.02590	80.4
43	232050 Aug	-	-	-	82.0
79.2	232045 Aug	9.67	33.739	1.02640	86.3
0	301332 Aug	13.97	33.463	1.02503	25.5
4.9	301332 Aug	-	-	-	25.5
7.9	301331 Aug	13.86	33.476	1.02509	27.0
10.9	301330 Aug	13.53	33.449	1.02515	47.6
13.9	301330 Aug	12.22	33.486	1.02546	52.5
16.8	301329 Aug	11.38	33.473	1.02561	48.0
19.8	301329 Aug	11.36	33.496	1.02565	49.5
22.8	301328 Aug	11.09	33.510	1.02572	59.1
25.8	301327 Aug	10.97	33.529	1.02577	63.0
30.7	301326 Aug	-	-	-	68.6
37.6	301325 Aug	-	-	-	77.0
42.6	301324 Aug	-	-	-	82.6
49.5	301324 Aug	10.34	33.591	1.02604	77.0
56.5	301323 Aug	-	-	-	73.4
63.4	301322 Aug	-	-	-	80.5
84.2	301319 Aug	9.61	33.632	1.02635	84.7
0	301731 Aug	14.28	33.491	1.02498	18.0
2	301731 Aug	-	-	-	18.0
4	301731 Aug	14.08	33.496	1.02505	21.4

TABLE 1B (Continued)

DEPTH (m)	DATE/TIME (1968)	TEMPERATURE (°C)	SALINITY (0/00)	DENSITY (g/cm ³)	TRANSMITTANCE (%/m)
5	301730 Aug	-	-	-	23.0
6	301730 Aug	13.71	33.455	1.02510	24.4
8	301729 Aug	13.19	33.485	1.02524	38.0
10	301729 Aug	12.54	33.468	1.02536	54.1
11	301729 Aug	-	-	-	57.5
13	301728 Aug	11.16	33.467	1.02563	68.4
16	301728 Aug	10.91	33.474	1.02570	74.7
20	301727 Aug	10.72	33.481	1.02575	77.0
45	301725 Aug	10.38	33.543	1.02597	78.4
62	301724 Aug	-	-	-	75.0
71.5	301723 Aug	-	-	-	80.7
85	301719 Aug	9.43	33.612	1.02637	83.7
0	302145 Aug	14.41	33.504	1.02496	24.0
5	302145 Aug	-	-	-	20.0
8	302144 Aug	13.85	33.500	1.02512	23.0
9	302144 Aug	-	-	-	23.5
12	302143 Aug	13.52	33.487	1.02519	25.5
14	302143 Aug	-	-	-	37.5
16	302142 Aug	13.01	33.478	1.02530	41.5
19	302142 Aug	-	-	-	49.5
20	302141 Aug	11.64	33.502	1.02560	59.0
22	302140 Aug	11.22	33.502	1.02569	64.3
24	302140 Aug	11.04	33.498	1.02573	66.5
26	302139 Aug	10.94	33.504	1.02576	70.0
45	302138 Aug	10.62	33.610	1.02598	76.2
55	302138 Aug	-	-	-	76.2
71.5	302137 Aug	-	-	-	80.5
85	302137 Aug	9.45	33.602	1.02636	83.1

TABLE 1B (Continued)

DEPTH (m)	DATE/TIME (1968)	TEMPERATURE (°C)	SALINITY (0/00)	DENSITY (g/cm ³)	TRANSMITTANCE (%/m)
0	310154 Aug	14.32	33.619	1.02507	26.0
5	310154 Aug	-	-	-	28.3
8	310153 Aug	14.01	33.608	1.02516	25.0
10	310152 Aug	13.83	33.618	1.02522	25.6
12	310152 Aug	13.43	33.628	1.02532	26.6
14	310151 Aug	13.24	33.614	1.02535	30.1
16	310151 Aug	12.94	33.582	1.02540	40.0
18	310150 Aug	11.82	33.622	1.02565	51.0
21	310149 Aug	-	-	-	64.0
25	310148 Aug	10.74	33.628	1.02589	69.9
37	310147 Aug	-	-	-	76.4
42	310146 Aug	-	-	-	63.5
45	310146 Aug	10.20	33.766	1.02618	55.1
49	310145 Aug	-	-	-	53.0
54	310144 Aug	-	-	-	73.4
62	310143 Aug	-	-	-	79.0
85	310140 Aug	9.32	33.679	1.02644	82.2
0	310606 Aug	14.92	33.653	1.02497	32.5
3	310605 Aug	13.80	33.640	1.02521	32.9
6	310604 Aug	13.59	33.656	1.02528	32.9
9	310603 Aug	13.31	33.560	1.02528	42.0
12	310602 Aug	12.48	33.640	1.02552	37.0
13.5	310602 Aug	-	-	-	55.5
15	310602 Aug	11.25	33.639	1.02576	64.5
18	310601 Aug	10.97	33.649	1.02583	69.9
21	310600 Aug	10.81	33.644	1.02587	72.3
29	310559 Aug	-	-	-	74.2
50	310558 Aug	10.21	33.696	1.02615	79.0
63	310557 Aug	-	-	-	72.5

TABLE 1B (Continued)

DEPTH (m)	DATE/TIME (1968)	TEMPERATURE (°C)	SALINITY (0/00)	DENSITY (g/cm ³)	TRANSMITTANCE (%/m)
69	310556 Aug	-	-	-	69.2
77	310555 Aug	-	-	-	65.0
85	310552 Aug	9.71	33.762	1.02644	66.5
0	311016 Aug	13.92	33.617	1.02516	29.5
5	311015 Aug	13.56	33.630	1.02526	32.6
10	311014 Aug	13.36	33.635	1.02533	35.5
13	311014 Aug	13.25	33.627	1.02536	38.0
16	311013 Aug	12.98	33.640	1.02544	48.0
17	311012 Aug	-	-	-	53.0
18	311012 Aug	-	-	-	65.1
20	311011 Aug	11.63	33.629	1.02570	69.0
24	311011 Aug	11.42	33.651	1.02578	74.5
35	311010 Aug	10.59	33.657	1.02598	75.7
47	311009 Aug	-	-	-	81.0
56	311009 Aug	-	-	-	72.1
60	311008 Aug	10.33	33.733	1.02620	68.3
63.5	311007 Aug	-	-	-	58.0
71	311006 Aug	-	-	-	79.5
85	311000 Aug	9.46	33.746	1.02647	83.2

COULTER PARTICLE COUNT
(2 ml sample)

STATION BRAVO

DATE TIME	SAMPLE DEPTH	TOTAL COUNT AT THRESHOLD ZERO	RELATIVE PULSE HEIGHT									
			0-10	10-20	20-30	30-40	40-50	50-60	60-70	70-80	80-90	90-100
26 July 1517	0	13800	4318	3100	1545	1330	1007	292	494	362	251	146
	6	22700	12000	3892	1747	1449	675	440	418	555	352	265
	13	10500	3330	2907	988	512	500	99	319	249	277	176
	17	3500	1816	724	186	129	77	26	76	103	33	
	21	2152	1634	186	116							
	40	1197	937	67								
	65	2205	1799	231								
	90	4333	3714	338	144							
26 July 1935	0	14100	7867	1958	1310	540	375	346	525	325	157	193
	5	15100	7950	2622	1105	854	600	405	261	273	272	124
	9	14900	8141	2206	1415	909	533	168	175	321	153	191
	13	10900	3024	2770	1497	110	1455	372	298	268	295	163
	17	13800	7204	2574	1295	687	376	403	257	225	221	157
	21	1428	1045	171	53							
	25	2228	1718	259	76							
	45	1725	1442	141								
	65	2955	1587	194								
85	3254	2483	348	148	93							

TABLE 2 (Continued)

DATE TIME	SAMPLE DEPTH	TOTAL COUNT AT THRESHOLD ZERO	0-10	10-20	20-30	30-40	40-50	50-60	60-70	70-80	80-90	90-100	
26 July 2335	0	12400	6593	1961	1152	866	372	316	182	290	125	101	
	3	9831	3188	2423	1252	755	510	407	163	239	144	144	
	6	14000	5360	3130	1629	1027	542	447	373	345	195	96	
	9	14200	7400	2787	1154	670	582	586	95	230	209	90	
	12	16100	8850	2562	1360	862	563	418	364	188	160	158	
	15	8547	4425	1266	677	501	184	310	35	299	204	82	
	30	2290	2077										
	50	1558	1240	166									
	70	1792	1342	204									
	85	1966	1501	213	71								
27 July 0321	0	9373	3589	1700	1250	699	598	257	302	281	142	121	
	5	16200	7775	3194	1400	1112	638	413	246	200	288	166	
	10	12400	6050	2043	1121	676	456	335	428	234	247	109	
	15	4241	2054	927	310	209	97	48	102	62	127	32	
	20	1361	974	172	52								
	25	1135	854	110									
	30	1169	897	115									
	50	1539	773	602									
	70	1990	1522	274									
	85	2722	2189	254	77								
27 July 0726	0	13700	7142	1791	298	1826	705	505	92	200	283	197	
	3	16700	8603	2620	1604	1058	590	540	397	101	361	174	
	6	13300	6291	2291	1428	1171	85	578	327	266	221	155	
	9	5718	3126	940	297	268	61	211	89	92	178	114	
	12	1921	1401	201	80								
	15	3392	2945	177	121								
	18	5159	4136	435	203	100							
	35	6860	3034	715	290	200	129	69	60				
	65	3143	2494	310	140								

TABLE 2 (Continued)

DATE TIME	SAMPLE DEPTH	TOTAL COUNT AT THRESHOLD ZERO	RELATIVE PULSE HEIGHT									
			0-10	10-20	20-30	30-40	40-50	50-60	60-70	70-80	80-90	90-100
27 July 1200	0	12800	7379	1625	1291	684	439	304	87	263	83	113
	4	15866	8615	2481	1522	1063	636	195	132	248	187	178
	8	10900	4882	1912	1112	970	498	298	212	234	164	70
	12	7497	3251	1179	678	269	315	274	46	65	409	190
	16	5626	2375	1215	545	316	196	134	169	239	64	64
	20	6306	3168	1158	612	177	218	151	188	72	149	77
	24	3558	2214	557	173	107	88	107	49	34	54	
	45	1326	982	138	25							
	65	1960	1669	138								
	85	3275	2731	232	102	62						
17 Aug 1018	0	2094	1432	325	53							
	5	27970	22378	1940	965	418	316	206				
	8	2878	2138	327	147							
	10	3424	2391	440	204	77	57					
	12	2597	1238	653	211	127						
	14	2423	1508	376	206	81						
	16	2793	1868	409	147	108						
	30	2292	1663	287	102							
	60	3226	2622	250	93							
	85	1721	1253	233								
17 Aug 1831	0	3178	2319	380	147	84						
	4.7	4162	3243	458	133	47						
	8.5	2529	1764	392	6							
	11.3	2364	1587	429	86							
	14.1	2385	1739	296	77							
	16.9	1923	1180	334	100	36						
	19.7	2265	1424	306	184	59						
	32.9	1953	1368	302	10							
	58.4	1651	1350	82								
	80.9	2322	1804	214	117							

TABLE 2 (Continued)

DATE TIME	SAMPLE DEPTH	TOTAL COUNT AT THRESHOLD ZERO	0-10	10-20	20-30	30-40	40-50	50-60	60-70	70-80	80-90	90-100
23 Aug 0757	0	10900	6502	1757	783	328	174	287	120	163	147	41
	4	10800	6430	1522	559	646	356	213	158	151	160	41
	7	6016	3941	910	292	137	163	65	85	85	54	88
	10	6902	4114	962	444	363	86	177	143	41	173	67
	13	5144	3156	700	205	354	128	100	60	123	5	50
	16	5215	2472	1018	362	385	195	54	89	58	66	92
	20	4831	3576	528	174	149	50	83	84			
	24	3124	2212	369	187	73						
	55	3012	2224	405	111	82						
	85	2744	2143	263	116							
23 Aug 1701	0	6404	3469	983	450	234	197	198	97	169	50	57
	4	7154	4021	1011	633	240	142	298	91	62	165	42
	8	8587	5111	1372	548	342	243	155	84	214	46	150
	12	7216	4161	1063	482	362	15	276	78	171	87	67
	16	6651	3831	1103	400	217	170	57	174	148	120	43
	20	7315	4801	1139	463	219	130	52	73	58	102	
	24	4190	2418	758	275	165	113	42	98			
	28	4048	2624	633	197	125	122					
	32	3958	2771	489	214	135	7					
	80	4507	3436	504	160	149						
23 Aug 2224	0	11600	7512	1481	912	532	283	235	138	121	69	43
	3.9	11800	8106	1171	674	465	275	330	119	103	159	76
	7.9	8220	5128	958	524	386	239	84	148	162	138	9
	11.8	7490	4463	963	626	168	251	177	185	121	81	103
	15.8	6957	4230	1127	431	216	129	149	79	78	103	37
	19.8	5869	3193	1097	440	298	89	146	145	104	109	
	24.8	7253	5404	897	255	248	54	50				
	29.7	4304	3122	499	261	109						
	49.5	2966	2493	232								
	79.2	2781	2152	356								

TABLE 2 (Continued)

DATE TIME	SAMPLE DEPTH	TOTAL COUNT AT THRESHOLD ZERO	0-10	10-20	20-30	30-40	40-50	50-60	60-70	70-80	80-90	90-100	
30 Aug 1125	0	12500	6852	2225	973	635	365	177	199	176	132	91	
	6.9	12900	7189	2234	1027	509	339	289	250	209	188	179	
	9.8	11800	6342	2165	945	552	306	211	309	168	113	81	
	12.7	8467	2863	1731	977	318	517	292	186	157	249	123	
	15.7	8673	4434	1155	701	445	398	160	374	204	107	78	
	18.6	5344	3631	749	220	143	97	131	47	56	29	47	
	21.6	5368	3806	778	197	150	90						
	39.2	1524	1218	139									
	58.7	3337	2560	405	91								
	83.2	10600	9775	505	217								
30 Aug 1921	0	5178	1985	1511	564	332	189	95	146	83	79		
	8	9866	4970	2146	969	454	268	347	129	152	64	75	
	10	9854	4793	2271	976	449	329	202	214	163	95	80	
	13	5807	2565	1375	514	301	191	95	162	173	48	66	
	16	13600	8163	2482	1118	653	350	191	57	199	84	80	
	18	6283	2637	1660	721	416	220	176	101	85			
	20	3500	1816	699	119	277	127	98					
	23	2320	1504	373	92	134							
	50	1416	1139										
	85	2900	2372	277									
31 Aug	0	16600	9759	2833	1297	912	481	304	211	310	62	139	
	5	12300	6229	2357	912	581	354	455	232	372	94	123	
	7	9551	5641	1781	855	389	255	141	96	116	51		
	9	7760	4086	1553	799	281	258	226	129	92	98		
	11	7213	4014	1250	558	289	168	312	177	65	146		
	13	5258	4032	515	287	94	92	39					
	15	2822	2094	365	130								
	20	3123	2153	446	134	94							
	50	3754	3171	332	113								
	85	1892	1445	239	98								

TABLE 3

RELATION BETWEEN LUNAR PHASES AND SAMPLING PERIODS

DATE	TIME (PST)	MOON PHASE	SAMPLING PERIOD
25 July 1968	0449	New	1511/26 July 1968 to 1559/27 July 1968
1 August 1968	1134	First Quarter	
8 August 1968	0432	Full	
15 August 1968	1913	Last Quarter	1012-2023 17 August 1968
23 August 1968	1657	New	0757-2218 23 August 1968
30 August 1968	1635	First Quarter	1125/30 Aug 1968 to 0959/31 Aug 1968

INITIAL DISTRIBUTION LIST

	No. Copies
1. Defense Documentation Center Cameron Station Alexandria, Virginia 22314	20
2. Library Naval Postgraduate School Monterey, California 93940	2
3. Department of Oceanography Naval Postgraduate School Monterey, California 93940	10
4. Naval Weather Service Command Washington Navy Yard Washington, D. C. 20390	1
5. Officer in Charge Fleet Numerical Weather Facility Naval Postgraduate School Monterey, California 93940	1
6. Commanding Officer and Director U. S. Naval Undersea Warfare Center Attn: Code 2230 San Diego, California 92152	1
7. Director, Naval Research Laboratory Attn: Tech. Services Info. Officer Washington, D. C. 20390	1
8. Office of Naval Research Department of the Navy Washington, D. C. 20360	1
9. Commander, Air Weather Service Military Airlift Command U. S. Air Force Scott Air Force Base, Illinois 62226	2
10. Department of Commerce, ESSA Weather Bureau Washington, D. C. 20235	2
11. Oceanographer of the Navy The Madison Building 732 N. Washington Street Alexandria, Virginia 22314	1
12. Naval Oceanographic Office Attn: Library Washington, D. C. 20390	1

13. National Oceanographic Data Center 1
Washington, D. C. 20390
14. Mission Bay Research Foundation 1
7730 Herschel Avenue
La Jolla, California 92038
15. Director, Maury Center for Ocean Sciences 1
Naval Research Laboratory
Washington, D. C. 20390
16. Dr. George F. Beardsley 1
Department of Oceanography
Oregon State University
Corvallis, Oregon 97331
17. Dr. Bob Dresnack 1
Department of Civil Engineering
323 High Street
Newark, New Jersey 07102
18. Dr. Seibert Q. Duntley 1
Visibility Laboratory
Scripps Institution of Oceanography
La Jolla, California 92037
19. CDR J. E. Geary, USN 1
Department of Oceanography
Naval Postgraduate School
Monterey, California 93940
20. Dr. Eugene C. Haderlie 1
Department of Oceanography
Naval Postgraduate School
Monterey, California 93940
21. Professor Alexandre Ivanoff 1
Laboratoire d'Océanographie Physique de la
Faculté des Sciences de Paris
9, Quai Saint-Bernard
Paris (V⁰), France
22. Dr. G. Kullenberg 1
Institute for Physical Oceanography
Solvgade 83K
Copenhagen, K, Denmark
23. Mr. Kenneth V. Mackenzie 1
U. S. Naval Undersea Warfare Center
Ocean Sciences Department - Code D503
San Diego Division
San Diego, California 92152

24. Dr. Robert E. Morrison 1
Tracor, Inc.
1735 I Street, N. W.
Washington, D. C. 20006
25. Dr. John H. Phillips 1
Director
Hopkins Marine Station
Stanford University
Pacific Grove, California 93950
26. Professor Stevens P. Tucker 5
Department of Oceanography
Naval Postgraduate School
Monterey, California 93940
27. Mr. John E. Tyler 1
Visibility Laboratory
Scripps Institution of Oceanography
La Jolla, California 92037
28. LT Richard D. Waer 2
USS HALFBEAK (SS-352)
Fleet Post Office
New York, New York 09501
29. LT Lanny A. Yeske 2
USS BAYA (AGSS-318)
Fleet Post Office
San Francisco, California 96601

DOCUMENT CONTROL DATA - R & D

(Security classification of title, body of abstract and indexing annotation must be entered when the overall report is classified)

1. ORIGINATING ACTIVITY (Corporate author) Naval Postgraduate School Monterey, California 93940		2a. REPORT SECURITY CLASSIFICATION Unclassified	
		2b. GROUP	
3. REPORT TITLE The Correlation of Oceanic Parameters with Light Attenuation in Monterey Bay, California.			
4. DESCRIPTIVE NOTES (Type of report and inclusive dates) Master's thesis, December 1968			
5. AUTHOR(S) (First name, middle initial, last name) Lanny A. Yeske Richard D. Waer			
6. REPORT DATE December 1968		7a. TOTAL NO. OF PAGES 143	7b. NO. OF REFS 19
8a. CONTRACT OR GRANT NO. N/A		9a. ORIGINATOR'S REPORT NUMBER(S) N/A	
b. PROJECT NO. N/A			
c.		9b. OTHER REPORT NO(S) (Any other numbers that may be assigned this report)	
d. N/A		N/A	
10. DISTRIBUTION STATEMENT This document has been approved for public release and sale; its distribution is unlimited.			
11. SUPPLEMENTARY NOTES N/A		12. SPONSORING MILITARY ACTIVITY Naval Postgraduate School Monterey, California 93940	

13. ABSTRACT An investigation of the correlation of oceanic parameters with light attenuation in Monterey Bay, California, was conducted during July and August 1968. Measurements of beam transmittance, salinity, temperature, density, and particulate matter, related in time and depth, were obtained during four cruises. Nearly 400 water samples were taken from two stations at depths between 0 and 85 m. Temperature showed the greatest correlation with beam transmittance. Isopycnals and beam transmittance contours showed a similar good correlation. Although salinity correlations were not clearly defined, isolated salinity pockets often appeared to be associated with transmissivity perturbations. A nearly linear relationship between values of particulate count and beam transmittance was observed. Particle sizes were found to decrease with increased depths. Approximately 96 percent of the particles affecting beam transmittance were less than 13 μ in diameter. Beam transmittance isolines generally oscillate with a tidal cycle period, the minimum values usually occurring at low tide. A possible correlation between lunar period, tidal ranges, and turbidity layers were indicated.	
--	--

KEY WORDS

LINK A

LINK B

LINK C

ROLE

WT

ROLE

WT

ROLE

WT

Light attenuation
Turbidity
Beam transmittance
Transparency
Suspended material
Particulate matter
Plankton
Salinity
Temperature
Density
Tidal Cycle
Lunar Period
Monterey Bay, California

thesY43

The correlation of oceanic parameters wi



3 2768 001 90516 9

DUDLEY KNOX LIBRARY